Late Holocene environmental change across the Canadian Arctic

Thesis submitted in partial fulfillment of the requirements for the degree of Master of Science in Geography

Camille Tamo

Supervisor:
Konrad Gajewski

Department of Geography, Environment, and Geomatics
Faculty of Arts
University of Ottawa

Acknowledgements

I'd like to thank Dr. Konrad Gajewski, my dedicated and encouraging supervisor, for teaching me and guiding me through the difficulties of working with samples from the Arctic. It has been an honour learning from you and I look forward to our freeze-dried meal test in 2040.

Thanks to all my fellow sub-basement dwellers – Michelle Briere, Michelle Chaput, Amanda Lagacé, Mercedes Lietke, and Karen Neil – for your support and encouragement when my samples failed over and over again. Your friendship has made these two years much brighter. Special shout out to Karen Neil for spending hours in the lab helping me process my biogenic silica samples. Thank you to Dr. Marie-Claude Fortin for taking the time to teach me the processing technique for biogenic silica and responding to all my questions over the subsequent months. Jean Bjornson, thank you for all the quick fixes when everything in the lab broke as soon as I wanted to use it.

I'd like to thank both Amarualik Uluriak and Ross Pudluk for their help during our field seasons. You were both a joy to work with and I hope we meet again in the future! Thank you also to our helicopter pilot, Steve Lodge, for taking the chance to get us into the field despite our freezing rain weather curse and to the Twin Otter pilots who rescued us from being stranded on "fog-island" (Prince of Wales).

I'd also like to thank my committee members, Dr. Antoni Lewkowicz and Dr. Denis Lacelle, and the funding agencies that supported my research (NSERC, NSTP, PCSP).

Finally, thank you to my family and friends who supported me throughout my research. Mid-week patio nights, potlucks, and movie nights were a perfect contrast to 12-hour days processing samples.

Abstract

Lake sediment cores spanning the last 2000 years from four sites across the Canadian Arctic Archipelago (CAA) document the responses of terrestrial and freshwater ecosystems to regional climate variability. Biogenic silica (BSi) records in cores from Banks Island, NWT (Lake B503; 72.3245, -123.4036, 84 masl), Bathurst Island, Nunavut (PR01; 75.6497, -99.1144, 30 masl), Prince of Wales Island, Nunavut (SW08; 72.3177, -97.2678, 104 masl), and Ellesmere Island, Nunavut (CV03; 79.9211, -82.9348, 363 masl) were used to examine the relationship between diatom production and climate. A pollen record from Prince of Wales Island provided the first high-resolution July temperature reconstruction for the last 1000 years for the central CAA.

Dissolution was evident in three out of the four lakes; core SW08 contained no BSi above detection and cores CV03 and PR01 only contained values above detection in the uppermost sediments, suggesting that the preservation of biogenic silica (BSi) in the sediment is likely influenced by sedimentary carbonates. A BSi sequence from core B503 showed that diatom production was affected by climate changes such as the Medieval Climate Anomaly and the Little Ice Age.

The vegetation on southern Prince of Wales Island underwent marked transitions during the Little Ice Age and Medieval Climate Anomaly, which was mainly observed in the proportion of Cyperaceae and Poaceae. The mean July temperature reconstruction showed a long-term cooling from 1080-1915 CE with a sustained cold period from 1800-1915 CE prior to 20th-century warming. A synthesis of paleoclimate records from across the Arctic demonstrated that pollen-based reconstructions record both high and low frequency climate variability, when sampling resolution is sufficient, and can improve regional climate reconstructions.

Table of Contents

List of Figures

List of Tables

CHAPTER ONE

Introduction and Literature Review

1.1 Objectives

This thesis examines climate variability over the last 2000 years across the Canadian Arctic Archipelago (CAA) and the impacts on terrestrial and freshwater ecosystems. Using a multiproxy paleoenvironmental approach, new records of environmental change were obtained from several lake sediment cores collected from across the CAA. A detailed analysis of pollen, including a July temperature reconstruction, was obtained for eastern Prince of Wales Island, Nunavut, which will aid in understanding regional climate variability in the Canadian Arctic. A biogenic silica record was also obtained from eastern Prince of Wales Island, as well as from three other cores from Banks Island, Bathurst Island, and Ellesmere Island, to analyze aquatic productivity and evaluate the impact of climate variability on lacustrine aquatic production. These new data were analyzed in the context of published work on the climates of the past 2000 years across the circumpolar Arctic to examine spatial and temporal variability across multiple timescales.

1.2 Paleoenvironmental Approach

This study uses the paleoenvironmental approach to quantify past climate variability. Since the instrumental temperature record does not extend far enough back in time to permit the analysis of multiple scales of climate variability, so-called "proxy data" are needed to reconstruct past conditions. The term proxy data is used for some component preserved in an archive (commonly lake or ocean sediment, ice core or tree ring records) that can be interpreted to provide information about past climates.

Lake sediments provide an ideal environment for the preservation of many physical and biotic proxies including diatoms, chironomids, varves, plant macrofossils, and pollen. For example, pollen may be used to estimate past summer temperatures since the distribution of plant communities has been associated with mean July isotherms across the Arctic (Edlund & Alt, 1989; Gajewski, 1995). Due to the limitations of different proxies, a multi-proxy approach is preferred to minimize potential error in climate reconstructions (Birks & Birks, 2006). In aquatic communities, separating climate factors from non-climate factors that cause changes in the lake environment create added uncertainty. For example, studies that analyzed chironomid assemblages found that thermal stratification in lakes may influence chironomid populations because cold and warm indicator taxa could survive at the same time in different sections of the lake (Kaufman, 2009; Porinchu et al., 2009). As another example, some studies have found diatom-free zones in Holocene sediment cores where diatoms were either not present or else changing characteristics in the lake caused their dissolution (Paull et al., 2017; Podritske & Gajewski, 2007; Ryves et al., 2006). In the case of dissolution, the availability of another proxy climate indicator in the core can help identify different factors that affected the lake ecosystem.

In the Arctic, palynology has historically been considered of limited use in paleoclimate reconstructions due to low pollen concentrations, long-distance transport of subarctic and temperate pollen grains to lakes in the Arctic, and low taxonomic resolution of traditional pollen analysis (Birks & Birks, 2000; Gajewski, 2006; Gajewski et al., 1995). As with any proxy indicator of past environments, it has strengths and limitations (discussed below) but recent studies have demonstrated the importance of pollen analysis in robust paleoenvironmental studies (Birks & Birks, 2006; Gajewski, 2006, 2015a, 2015b). Pollen assemblages extracted from lake sediment cores are a reliable proxy to determine past environmental changes based on the vegetation

response in a given area. When analysing a sequence in a sediment core, changes in pollen composition represent vegetation changes over time (Bennett & Willis, 2001). Pollen are also directly associated with climate when transfer functions are computed that relate modern pollen to modern climate (Overpeck et al., 1985; Sawada, 2006) or to plant production using pollen influx to the sediments (Gajewski, 2015b). As a consequence of the extensive literature on plant-climate interactions, it is frequently assumed that changes in pollen abundance are primarily due to changes in climate (Delcourt & Delcourt, 1991; Gajewski, 2015a). In the Canadian Arctic, most plants are near their physiological limits (Edlund & Alt, 1989) and that makes them particularly sensitive to short and long-term temperature changes (Gajewski, 2015a).

When interpreting climatic information from pollen data, non-climatic factors, such as changes in the abundance of certain taxa due to ecological succession or human activity, must be distinguished from climatic causes (Faegri & Iversen, 1989). This problem is less important in the Arctic because plants are more sensitive to changes in temperature than soil conditions or time (Gajewski, 2015a) and the impact of human activity is extremely localized. Moreover, Gajewski (2015a) suggests that the common concepts of plant succession do not apply in the Arctic where the growing season is so short and the environment is in a state of constant disturbance. As with any fossil analysis, the differential preservation of fossils may distort the record. Preservation is typically not an issue in lake sediments. The walls of pollen grains are made of sporopollenin, which is resistant to most forms of degradation except oxidization (Bennett & Willis, 2001; Faegri & Iversen, 1989) allowing them to be preserved for millions of years in anaerobic conditions (Bennett & Willis, 2001).

1.3 Climate of the Arctic during the Common Era

The climate of the last 2000 years is characterized by a long-term cooling trend with periods of decadal to centennial climate variability. At the centennial and multi-decadal scale major climate variations that have been identified in the Northern Hemisphere include the Roman Warm Period (RWP; ~1-300 CE; Ljungqvist, 2010), Dark Ages Cold Period (DACP; ~300-800 CE; Ljungqvist, 2010), Medieval Climate Anomaly (MCA; ~950-1250 CE; Goosse et al., 2012; Mann et al., 2009) and Little Ice Age (LIA; ~1300-1900 CE; Ljungqvist, 2010). There is no widely agreed upon start and end dates for these periods, which is likely because they were not spatially nor temporally homogenous across the Northern Hemisphere. Although few studies have focussed on climate variability in the first millennium of the Common Era (Ljungqvist, 2010), the temporal and spatial extents of the MCA and LIA in the Northern Hemisphere have been extensively studied (Graham et al., 2011; Ljungqvist, 2010; Mann et al., 2009; PAGES2k, 2013; Wanner et al., 2008; Xing et al., 2016) and regional differences in the timing of these periods have been identified (PAGES2k, 2013). For example, global reconstructions identified the MCA as starting anywhere between 890 and 1100 CE, and ending between 1170 and 1300 CE (Bradley et al., 2003; Crowley & Lowery, 2000; Diaz et al., 2011; Jungclaus et al., 2014; Mann et al., 2009; Osborn & Briffa, 2006). The onset of colder conditions during the LIA also varied regionally, occurring earlier in the Arctic, Europe, and Asia than the rest of the globe (PAGES2k, 2013). Moreover, many records indicate climatic shifts during these periods, but they likely manifested as different regional expressions of temperature and hydroclimatic changes rather than uniform warming or cooling (Graham et al., 2011; Hunt, 2006).

Regional heterogeneity of multi-decadal and centennial climate variability in the Common Era is evident throughout the Arctic (Nicolle et al., 2018; Overpeck et al., 1997). Most temperature

reconstructions for the Arctic show a well-documented Neoglacial cooling (Hanhijärvi et al., 2013; Kaufman et al., 2009; McKay & Kaufman, 2014; Nicolle et al., 2018; PAGES2k, 2013; Shi et al., 2012; Tingley & Huybers, 2013; Werner et al., 2018), but as with hemispherical reconstructions, there is less evidence for a coherent MCA and LIA both spatially and temporally. Previous work has been based almost entirely on ice core, tree ring, and varve records, which may lose low-frequency variations and underestimate the amplitude of temperature changes over the last 2000 years (Christiansen & Ljungqvist, 2017; E. R. Cook et al., 1995; Xing et al., 2016). In addition, the geographical distribution of the proxy records is sparse, particularly in Siberia and the central and western Canadian Arctic, so reconstructions are biased towards the North Atlantic region.

There have been several paleoclimate reconstructions covering the past 2000 years for the Arctic region (Hanhijärvi et al., 2013; Kaufman et al., 2009; McKay & Kaufman, 2014; Nicolle et al., 2018; Overpeck et al., 1997; Shi et al., 2012; Werner et al., 2018). Although most show similar trends, there are differences in the amplitude and timing of periods of major variability. Kaufman et al. (2009) published a circum-Arctic, decadally-resolved summer temperature reconstruction that showed minimal climate variability before a 20th century warming. Shi et al. (2012) published an annually-resolved summer temperature reconstruction and found a strong signal of the MCA from 900-1100 CE and relative cooling from 1200-1900 CE with some warm periods from 1470-1510 CE, 1550-1570 CE and 1750-1770 CE. Hänhijarvi et al. (2013) reconstructed annual temperatures for the North Atlantic region, which has the most consistent record of the MCA and LIA (Hanhijärvi et al., 2013; Miller et al., 2010). The study showed more low-frequency variability as well as a greater amplitude of warming during the RWP and the MCA. Hänhijarvi et al. (2013) found the MCA occurred from 800-1200 CE and the LIA lasted from 1250-1900 CE. McKay and Kaufman (2014) reconstructed annual temperatures in the Arctic and obtained results similar to

other reconstructions for the area. Their reconstruction showed MCA warming beginning ~930 CE, followed by a gradual cooling to ~1800 CE. The amplitude of the LIA cooling trend was greater, which is likely because it is a reconstruction of annual temperature rather than summer temperature. Nicolle et al. (2018) adopted a regional approach to study climate variability in the Arctic and subarctic and found regional differences in the timing and length of the MCA and LIA. The authors found that MCA warming was ~200-250 years long and began between 900 and 950 CE in Siberia, 900 and 1000 CE in Alaska, 800 and 1050 CE in the North Atlantic and ended between 1100 and 1550 CE. Contrary to other studies, they found the LIA was more spatially and temporally variable than the MCA, with the length ranging from 100 to 700 years, start dates ranging between 1200 and 1770 CE, and end dates ranging between 1530 and 1930 CE. However, the regional curve for Siberia was based on five records, Alaska on 11, and the North Atlantic on 41, so it is not surprising that the range of start dates is greater in the North Atlantic. Finally, Werner et al. (2018) found a pronounced MCA from 920-1060 CE and two periods of centennial-scale cooling from 1100-1450 CE and 1600-1900 CE that they identified as the LIA.

Although the Neoglacial cooling is thought to be been driven by a reduction in solar insolation in northern latitudes (Kaufman et al., 2009; Miller et al., 2012), the causes of centennial climate variability in the Canadian Arctic are still under discussion. During the MCA, reconstructions show minimal volcanism and that solar insolation was relatively stable near the long-term mean (Bradley et al., 2016; Sigl et al., 2015; Vieira et al., 2011). Explosive volcanism increased around 1250 CE (Sigl et al., 2015) and, along with associated changes in sea ice and snow cover, may have been a significant factor in the onset and peak of the LIA (Miller et al., 2012).

1.4 Vegetation History of the Canadian Arctic

Presently, the Arctic can be divided broadly into three bioclimate zones – Low, Middle, and High Arctic – based on diversity and ground cover, or into more detailed classifications as seen in the Circumpolar Arctic Vegetation Map (CAVM; Walker et al., 2002; also see Figure 2.1, panel A). The distribution of the major vegetation zones in the Arctic is generally controlled by July temperature, soil moisture, and surficial materials. Plant diversity and ground-cover tend to follow a regional pattern correlated to mean July isotherms, whereas differences within the regions are greatly controlled by the available moisture and soil composition. For example, highly acidic or alkaline soils tend to lack necessary plant nutrients and remain mostly unvegetated. Where soil conditions provide sufficient nutrients for plant growth, the summer moisture regime can alter plant communities. On weakly alkaline soils, for example, plant communities may be dominated by sedge meadows in poorly-drained soils and prostrate shrubs in well-drained soils (Edlund & Alt, 1989; Gould et al., 2003b, 2003a; Walker et al., 2002).

Pollen records are used in paleoclimate reconstructions and also provide evidence of past vegetation history. Although there have been several vegetation reconstructions for North America (Ritchie, 1987; Viau et al., 2012; Viau & Gajewski, 2009; Williams & Shuman, 2008), data from the Arctic have only recently become available (Gajewski, 2015a) to enable conclusions about the vegetation history to be made. Following deglaciation, plants arrived almost immediately in the CAA. Pollen records generally show the same taxa present throughout the entire record, indicating that changes are typically seen in vegetation abundance and density rather than dominant plant species. The early Holocene generally had high plant production, indicated by higher pollen influx values, which decreased throughout the late Holocene.

CHAPTER TWO

Detailed Methodology

This thesis analyzed sediment cores from four lakes spread across the CAA: from Banks Island (B503), Prince of Wales Island (SW08), Bathurst Island (PR01), and Ellesmere Island (CV03; Figure 2.1). Since paleoenvironmental studies based on lake sediment cores in the Arctic present more challenges than comparable work in temperate regions, standard methods for analyzing physical and biotic proxies and developing age-depth models are often not applicable or do not yield useful results. The cores analyzed in this thesis were no exception. Sections 2.1 and 2.2 describe the general methodology applied to each core. Details regarding which analyses were successful can be found in Sections 2.3 and 2.4. Section 2.5 describes the development of new biogenic silica calibration samples, a task necessary for the analyses described below. These new standards can be widely used so a detailed description is provided here.

2.1 Field Methods

The fieldwork for this study was conducted over the course of four seasons. The cores were extracted using a plastic tube fitted with a piston ensuring the water-sediment interface was obtained. Deeper cores were extracted using a Livingstone corer. The samples from the uppermost, unconsolidated sediment were extruded in the field into plastic bags or centrifuge tubes at 0.5 cm intervals. The rest of the core sections were extruded and wrapped in plastic wrap and aluminum foil to retain moisture then shipped back to the University of Ottawa in plastic tubes and refrigerated at 4°C.

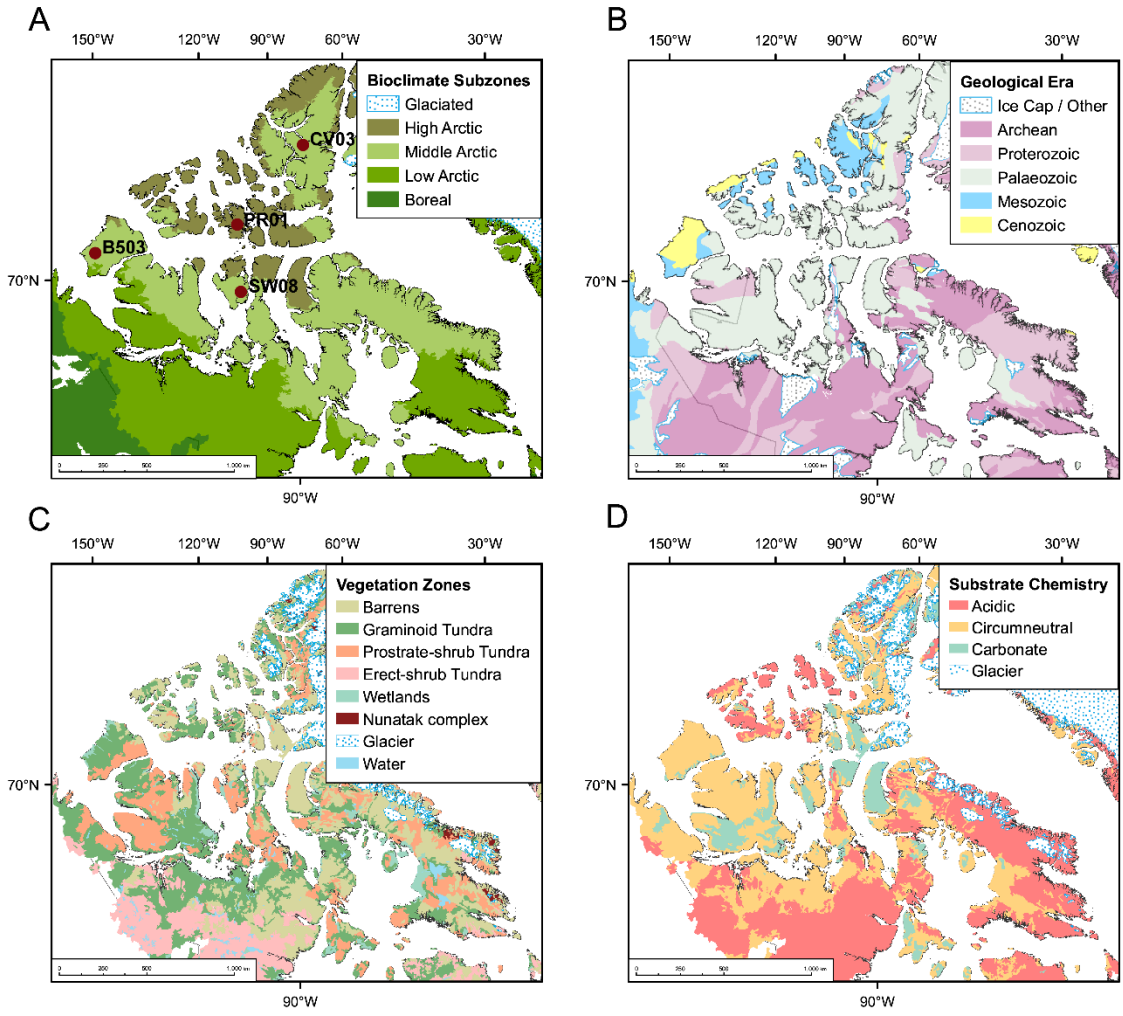

Figure 2.1: Maps of the Canadian Arctic Archipelago: (A) Bioclimate (CAVM et al., 2003), (B) Geological Era (Wheeler et al., 1997), (C) Vegetation Zone (CAVM et al., 2003), and (D) Substrate Chemistry (CAVM et al., 2003). Study sites for Chapters 3 and 4 are shown in panel A.

2.2 Laboratory Methods

In order for the data to be comparable between studies, standard laboratory methods were used as outlined on the Laboratory for Paleoclimatology and Climatology's website (LPC; www.lpc.uottawa.ca). The sediment cores were first split and all changes in stratigraphy, texture, and colour, along with any distinctive features were noted. Colour was described using a Munsell chart. Changes in mineral content were then estimated using a Bartington MS2C Magnetic Susceptibility Meter. Loss-on-ignition was performed to estimate the weight percent organic and carbonate contents of the sediment. Radiocarbon (^{14}C) and Lead-210 (^{210}Pb) dating techniques were used to date the core, and pollen and biogenic silica were then analyzed as described below.

2.2.1 Magnetic Susceptibility

Before opening each core, magnetic susceptibility was analyzed at 1 cm intervals. The analysis provided information regarding the magnetic mineral concentrations of the sediment throughout the core. In cores with relatively high organic matter or carbonates the values are too low and cannot be estimated using the instrument.

2.2.2 Loss-On-Ignition (LOI)

The approximate organic and carbonate content was determined by measuring the loss-on-ignition using a LECO Thermogravimetric oven. A sample of calcium oxalate was run with each batch to ensure an analytical uncertainty no greater than 0.1%. The following formulas were applied to determine the weight percent organic matter and carbonate:

$$weight\ \%\ organic\ matter = \frac{100(dry\ weight_{105} - ignited\ weight_{550})}{dry\ weight_{105}}$$

$$weight\ \%\ carbonate = \frac{100(ignited\ weight_{550} - carbonate\ weight_{950})}{dry\ weight_{105}}$$

2.2.3 Pollen

Since the samples in this study are from the High Arctic and are relatively inorganic, the standard method for processing sediment to extract the pollen was not sufficient. Instead, a method based on heavy-liquid separation was used (Zabenskie et al., 2006). Two cubic centimeters were subsampled at 0.5 cm intervals throughout the core. The samples were then "spiked" with two *Lycopodium* tablets (batch #938934; 53,394±953/5 tablets) to enable the estimation of the absolute concentration of pollen and spores. The samples were then washed with 10% hydrochloric acid (HCl) to remove carbonates and spun in a centrifuge at 4000 rpm for 5 minutes. After the supernatant liquid was decanted the samples were washed with deionized water and topped off with a squirt of ethanol, stirred, centrifuged and decanted. A deionized water wash occurred between every step with the exception of acetolysis and the final ethanol and tertiary butyl alcohol ($(CH_3)_3COH$) rinses. Ten percent potassium hydroxide (KOH) was then added to remove humic acids. The samples were placed into a hot water bath for 6-8 minutes, centrifuged and decanted. At this point, 5 mL of Sodium Polytungstate (SPT; density: 1.9 g/cm^3) was added to each sample and they were shaken using a vortex mixer for at least 5 minutes and centrifuged at 1800 rpm for 10 minutes. The lower speed was to ensure the pollen would not be spun down to the bottom of the centrifuge tube. The material that floated was decanted into a second centrifuge tube and any remaining sediment from the bottom of the tube was discarded. Each sample was then split between two tubes to which deionized water was added to lower the density of the liquid, then centrifuged and decanted. The two tubes that contained the same sample were combined using deionized water, then centrifuged and decanted. At this point, if the samples still contained significant quantities of silt, hydrofluoric acid (HF) was added to bring silica and many silicates into solution (Bennett & Willis, 2001). Next, glacial acetic acid was added to remove any water in

preparation for acetolysis. The acetolysis solution consisted of acetic anhydride ($C_4H_6O_3$) and sulphuric acid (H_2SO_4), which removed any polysaccharides in the sediment and the pollen grains (Bennett & Willis, 2001). This step concentrated the pollen and facilitated easier identification of pollen grains. The samples in the acetolysis solution were placed in a water bath for 3 minutes, centrifuged and decanted. Next, another wash in glacial acetic acid was performed to remove the remaining acetolysis solution. The samples were then rinsed in 95% ethanol with a drop of safranin stain to enhance the visibility of the sculpturing on the pollen grains (Bennett & Willis, 2001). Finally, the samples were rinsed in tertiary butyl alcohol and transferred into vials with a drop of silicone oil for permanent storage. Slides were prepared as needed using silicone oil.

A minimum of 300 fossil pollen grains was counted and identified per level using a light microscope at 400X magnification. More grains per sample would be preferable, however concentrations were too low in these sediments to permit higher pollen sums. Pollen concentration was determined using the following formula from Bennett and Willis (2001, p.19):

$$fossil\ pollen\ concentration = \frac{exotic\ pollen\ added * fossil\ pollen\ counted}{exotic\ pollen\ counted}$$

2.2.4 Biogenic Silica

Biogenic Silica (BSi) measures the opal silica content in sediments and has been used as a proxy for diatom abundance and productivity (Conley & Schelske, 2001). These factors should be associated with climate variability although dissolution is an issue in Arctic diatom analyses (Paull et al., 2017; Ryves et al., 2006). To measure the biogenic silica content in sediments a wet chemical digestion technique was employed.

The chemical digestion technique consists of adding a weak base solution to the sample to dissolve all of the amorphous silica in the sediment, but only a small amount of the mineral silicates (Conley

& Schelske, 2001). The assumption is that diatoms will be dissolved in the first two hours of digestion, and anything dissolved thereafter is due to digestion of mineral silicates.

The sediment cores were subsampled at 0.5 cm intervals and dried for 24 hours at 105°C. After being ground up using a mortar and pestle, subsamples were weighed out (0.02 g ± 0.002 g) and placed in polypropylene bottles to which 40 mL of 1% sodium carbonate (Na_2CO_3) was added. The samples were placed in an 85°C shaking water bath at 70 rpm. After 2, 3, 4, and 5 hours, the samples were removed, cooled, and 1 mL subsamples were placed into centrifuge tubes with 3.2 mL of 0.06 N HCl in order to neutralize the digestion solution. Each new sample was diluted with 10 mL deionized water. A micropipette was used to transfer 0.64 mL of the sample, 0.84 mL ammonium molybdate, 0.64 mL oxalic acid, and 0.84 mL ascorbic acid to a cuvette, which was placed in a spectrophotometer to measure the absorbance at 660 nm of each sample. A duplicate and two reference samples were processed alongside each batch to assess the error and ensure processing was successful.

2.2.5 Chronology

The cores were dated using Lead-210 (^{210}Pb) for the upper sediments and Radiocarbon (^{14}C) for the remainder of the core. Subsamples of the uppermost sediments were dried at 75°C for 24 hours then ground using a mortar and pestle. Samples weighing a minimum of 0.1 g dry weight were sent to MyCore Scientific Inc. (Ottawa, ON) where they were processed using alpha spectroscopy and the age-depth curve was generated based on a constant-rate-of-supply model (CRS; Appleby & Oldfield, 1978).

Radiocarbon dates were obtained for all four cores. After sieving 1 cm thick samples through a 90 µm mesh, organic matter was manually picked using forceps at a dissection microscope. The samples were then processed and analyzed by personnel at the André E. Lalonde Accelerator Mass

Spectrometry Laboratory at the University of Ottawa. The radiocarbon carbon results are expressed as the fraction modern carbon, $F^{14}C$, and the age is calculated as $-8033\ln(F^{14}C)$. Samples were calibrated using OxCal v4.2.4 (Bronk Ramsey, 2009) and the IntCal13 calibration curve (Reimer et al., 2013).

2.3 Age-Depth Modelling

Developing a reliable chronology is a pervasive issue in paleolimnology due to uncertainties resulting from ^{14}C-deficient carbon that cause a local reservoir effect. In the Arctic these factors can produce ^{14}C results up to 2000 years too old (MacDonald et al., 1991), although in some extreme cases age offsets of up to 10 000 years have been found (Ascough et al., 2011). Aquatic plants are not ideal for radiocarbon dating since they absorb carbon from ^{14}C-deficient water. Unfortunately, they are often the only available material in sediment cores from Arctic lakes since most lakes contain low allochtonous organic matter input due to sparse vegetation in the catchment area. Additionally, recently deglaciated regions are more likely to be contaminated due to large areas of exposed bedrock (MacDonald et al., 1991).

Presently, there is no accepted method for dealing with a reservoir effect in freshwater lakes. Several studies have indicated a significant difference in radiocarbon ages obtained from terrestrial and aquatic macrofossils at the same level (MacDonald et al., 1991; Peros & Gajewski, 2009; Philippsen, 2013; Snyder et al., 1994; Zhou et al., 2015). In an ideal situation, terrestrial macrofossils would be dated throughout the core, but this is not possible in most Arctic lakes. Different approaches have been used to estimate the reservoir effect in individual lakes. If present, a single terrestrial macrofossil dated alongside an aquatic macrofossil or bulk sediment sample may provide evidence of a reservoir effect. Similarly, the modern reservoir age can be measured;

however, it is unlikely that the reservoir age remained constant over time (Grimm et al., 2009; Zhou et al., 2015) so neither of these methods provides results that can be applied to the entire record. In fact, a recent study has qualitatively linked changes in reservoir age to regional climate variability (Zhou et al., 2015). There is also evidence that suggests a freshwater reservoir effect can vary spatially throughout a lacustrine system (Ascough et al., 2011). Based on the knowledge that the water-sediment interface represents the present, Peros and Gajewski (2009) estimated the reservoir effect in an individual lake on Victoria Island, Nunavut, Canada using the intercept of a linear regression of radiocarbon results. This method is further tested in this thesis (discussed below and in Chapters 3 and 4).

Chronologies were established for each core using both ^{14}C and ^{210}Pb results. Although several modelling techniques were tested, developing chronologies proved difficult. Dissolution of calcareous bedrock or surficial deposits likely contributed to the dating errors associated with lakes SW08 and PR01. In B503 and CV03, the presence of Tertiary coal in the region likely contaminated some of the samples, resulting in age reversals and anomalously old dates throughout the cores. Age-depth models showed that the radiocarbon dates, if accepted, led to extremely low sedimentation rates (0.01-0.02 cm/yr) for a period of 900-1200 years. Although we could not prove the reason for this, a local reservoir effect due to hard water or old carbon could explain this issue.

Following Peros and Gajewski (2009), a reservoir correction was estimated for each core, except for site B503 from Banks Island, where a correction was not needed, by calculating the intercept of a linear regression of the accepted radiocarbon dates, which was then subtracted from all ^{14}C dates and a new age-depth model was fit to the corrected data (Figure 2.2). This method assumes a linear relationship between depth and age throughout the sediment core and that the surface sample is modern. Although this method does not take into account temporal changes in reservoir

age, it is our best estimate based on the information available. Cores SW08, PR01, and CV03 each had an estimated reservoir effect of between 800 and 1000 years.

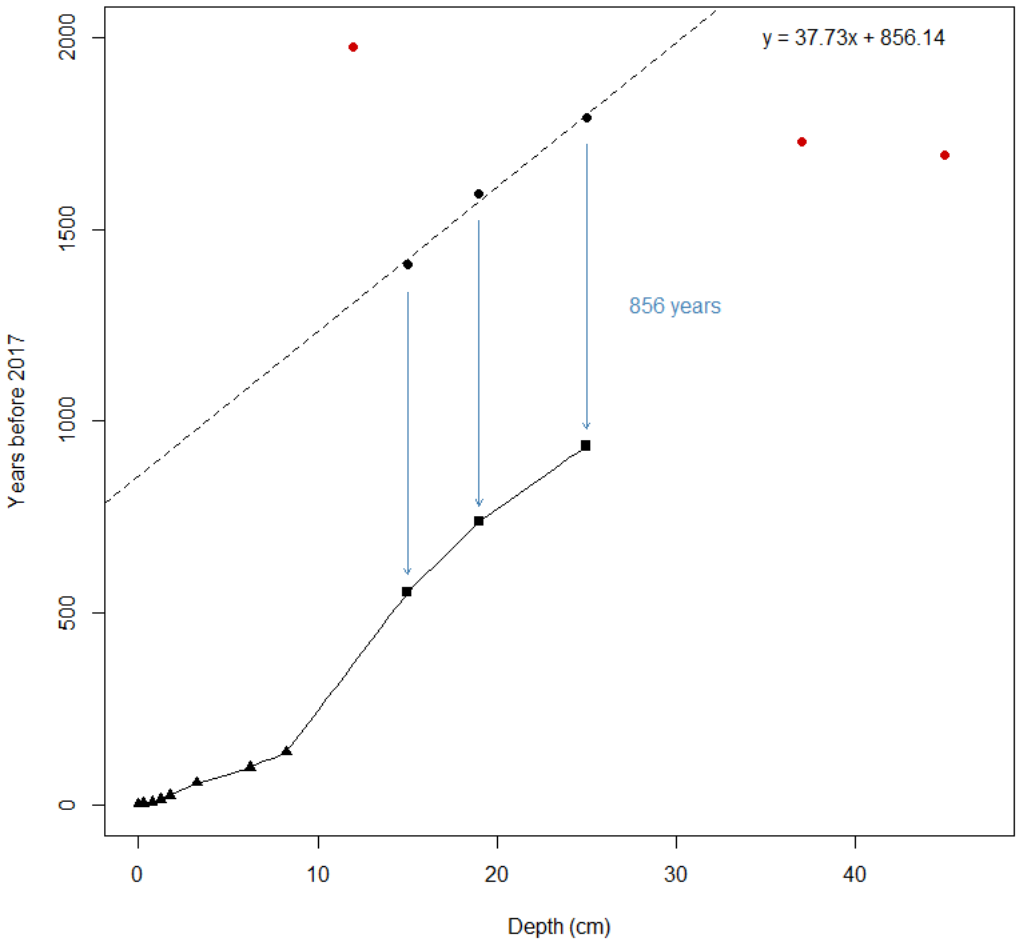

Figure 2.2: Example of the method used to calculate the reservoir effect in Lake SW08. *Triangles* are ^{210}Pb ages; *Circles* are the ^{14}C median calibrated dates; *black circles* are ^{14}C dates retained for the age-depth curve; *red circles* are ^{14}C dates rejected from age-depth model; *Squares* are hardwater-corrected ^{14}C dates (see text for details). *Solid line* represents the corrected age-depth model; *dashed line* is the linear model produced by regressing the age and depth of the accepted radiocarbon dates showing a y-intercept of 856; this is the value subtracted from the radiocarbon ages to correct the dates.

Choosing a model

Developing accurate age-depth models is important for the interpretation and comparison of proxy records. In this study, the ^{210}Pb and uncorrected ^{14}C results were first modelled using the R software package BACON (Blaauw & Christen, 2011), linear regression, and linear interpolation and the resulting age-depth curves were assessed (Figure 2.3). Including all of the dates resulted in several age reversals throughout the models; therefore, decisions regarding which dates to retain and exclude had to be made. The R software package BACON (Blaauw & Christen, 2011) provides a more objective method to exclude dates because it is robust against outlying dates (Christen & Perez, 2009) and includes prior information about sediment accumulation rates. Therefore, dates flagged as outliers by the BACON model were also ignored in the final age-depth models used in this thesis. In cases where the BACON model produced unlikely results from an ecological perspective, the model with a linear accumulation was selected.

The regression-based method did not produce strong models; the analysis of the residuals showed that the models violated the assumptions of the linear regression. The mean of the residuals were greater or less than 0 and all models contained points with a Cook's distance greater than 1. Additionally, the resulting interpolated points deviated significantly from ^{210}Pb and ^{14}C results. BACON and linear interpolation-based models produced similar results, although the BACON models tended to result in more abrupt changes in sedimentation rate. The modelling techniques produced results with an unusually low sedimentation rate between the last ^{210}Pb and the first ^{14}C date using the uncorrected ^{14}C dates, which prompted us to apply a reservoir correction. Since the BACON models did not offer any new information and the abrupt changes in sedimentation rate are unlikely, linear interpolation was deemed most appropriate for the data and the reservoir correction previously discussed was applied where necessary.

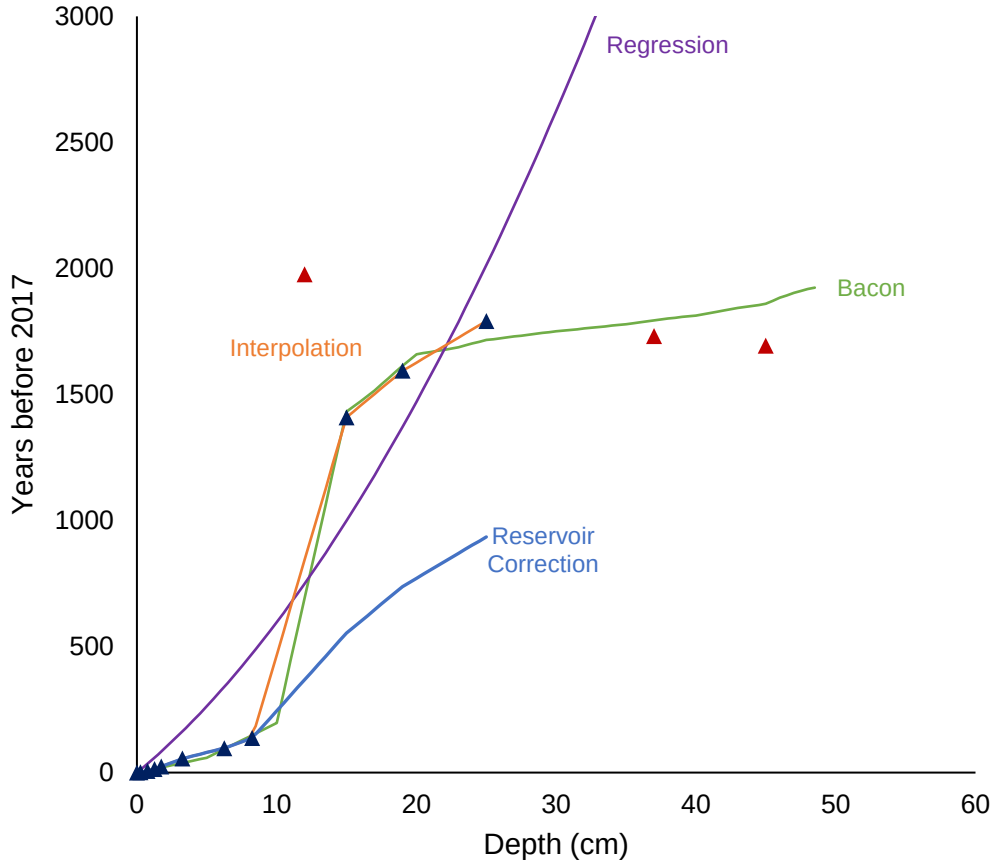

Figure 2.3: Comparison of different age-depth modelling techniques for Lake SW08. Red triangles are ^{14}C results that were omitted from all models except BACON. Models based on linear interpolation (orange), regression (purple), and BACON (green) were performed using the uncorrected ^{14}C dates and all showed a poor fit. The reservoir correction is the age-depth model derived from subtracting the y-intercept (856 years) of a linear regression of the accepted radiocarbon dates (Figure 2.2).

2.4 Cores Analyzed

There are several challenges when conducting paleoecological and paleolimnological studies in the Arctic. Pollen analysis is frequently not possible from many lake sediment cores due to low pollen concentrations or contamination by Tertiary deposits or non-pollen palynomorphs (Gajewski et al., 1995). Biogenic silica is often absent in sediments, which may be due to dissolution in carbonate-rich sediment or alkaline lake water (Fortin & Gajewski, 2009; Paull et al., 2017; Ryves et al., 2006). Where proxies are present, interpretation of records is complicated by difficulties dating lacustrine sediments (Section 2.3). Eight cores were analyzed but as a result of these problems, only four yielded interpretable results.

Table 2.1: List of cores tested to determine suitable cores for analysis. Cores analyzed in this thesis are denoted by an asterisk (*). BSi = biogenic silica, LOI = loss-on-ignition, MS = magnetic susceptibility.

Core ID	Latitude	Longitude	Successful Analyses
Banks Island			
B503*	72.32	-123.40	BSi, LOI
B504	71.89	-123.63	N/A
B505	71.99	-125.02	N/A
Bathurst Island			
PR01*	75.66	-99.11	BSi, LOI
Prince of Wales Island			
SW08*	72.32	-97.27	Pollen, LOI
Ellesmere Island			
CV01-D	79.93	-82.95	N/A
CV02-B	79.92	-82.93	N/A
CV03*	79.92	-82.94	BSi, LOI, MS

2.4.1 Magnetic Susceptibility

Magnetic susceptibility was only successful on core CV03 from Ellesmere Island. Measurements from Lake PR01 showed large inconsistencies between multiple measurements of the same core and measured values for Lake B503 were below detection throughout the entire core. Low susceptibility values likely indicate the proportion of minerogenic material is low and organic matter or carbonate content are high (Thompson et al., 1975), which is the case in B503 and PR01, respectively.

2.4.2 Pollen

Preliminary analyses of several cores from Banks, Bathurst and Ellesmere Island showed very low (<10 grains) to low (< 100 grains) pollen counts per slide. Initial results from processing brought forth concerns with the heavy-liquid processing technique. Both the pollen and exotic pollen counts seemed to be too low, possibly indicating the pollen and spores were not being suspended in the heavy-liquid and were instead being discarded with the sediment. Additionally, some samples had visible floating material during the second glacial acetic acid rinse after acetolysis that would not settle regardless of how many times the sample was centrifuged. To test the heavy-liquid technique, a batch from PR01 and B503 was processed with half the samples being processed using the heavy-liquid technique and half using the sieving technique. Pollen counts were still low and the sieving technique proved to be less effective since it reduced the concentration of the pollen grains because it did not remove as much non-pollen material as the heavy-liquid technique.

Pollen counts on Banks Island varied depending on lake. Cores were available from 3 lakes – B503, B504, and B505 – and point samples were processed from each core to check for pollen. Pollen counts were too low in all three lakes to enable a pollen analysis, which was surprising

since the vegetation is relatively dense for the Arctic islands. Lake B504 had the most pollen of all the lakes examined (54 grains), which is to be expected since it is in a Low Arctic region. Analysis of Lake B504 might have been possible, but the presence of abundant *Pediastrum* (a type of algae) in the samples obscured the pollen grains making counting impossible. Surface samples for Lake B505 were analyzed and also had low pollen concentrations (37 grains). Lake B503 contained among the lowest counts of the lakes tested (8 – 32 grains).

One core (PR01) was available from a lake south of Polar Bear Pass on Bathurst Island. Pollen counts were very low (6 – 26 grains), which is unsurprising given the sparse vegetation. Large areas of Bathurst Island are covered by weathered carbonate-based silt and rocks, which lack necessary plant nutrients and remain unvegetated (Edlund & Alt, 1989).

Samples were obtained from a small valley just to the east of the Hot Weather Creek region of Ellesmere Island, Nunavut where the land starts to rise above the plain. The samples from Ellesmere Island were difficult to analyze, mainly due to non-pollen palynomorphs and other material that made counting difficult. Lake CV01-D contained mostly coal, which indicates contamination by Tertiary deposits. The coal inhibits counting because it obscures the pollen and reduces the concentration per slide. Additionally, large trilete spores and other Tertiary pollen grains were identified, further indicating contamination. Lake CV02-B had low pollen counts (~40 grains per slide). The lake is located upstream from CV01-D and did not contain the same contamination by Tertiary palynomorphs.

Finally, a lake from Prince of Wales Island (SW08) was processed and pollen counts were high enough to enable analysis. With the exception of a few levels, at least 300 grains were counted at 0.5 cm intervals throughout the core (results discussed in Chapter 4).

Table 2.2: Results from preliminary pollen analysis in several cores across the Canadian Arctic.

Island	Lake	Depth (cm)	Pollen	Exotic
Banks	B503	13.5-14	8	83
Banks	B503	10.5-11.0	11	117
Banks	B503	13-13.15	11	180
Banks	B503	17.5-18	32	302
Banks	B504	6.5-7.0	54	133
Banks	B505	0-0.5	37	103
Bathurst	PR01	19-19.5	9	327
Bathurst	PR01	15-15.5	6	211
Bathurst	PR01	28-28.5	26	-----
Ellesmere	CV02-B	9.0-9.5	38	470
Ellesmere	CV02-B	9.0-9.5 (2)	37	251

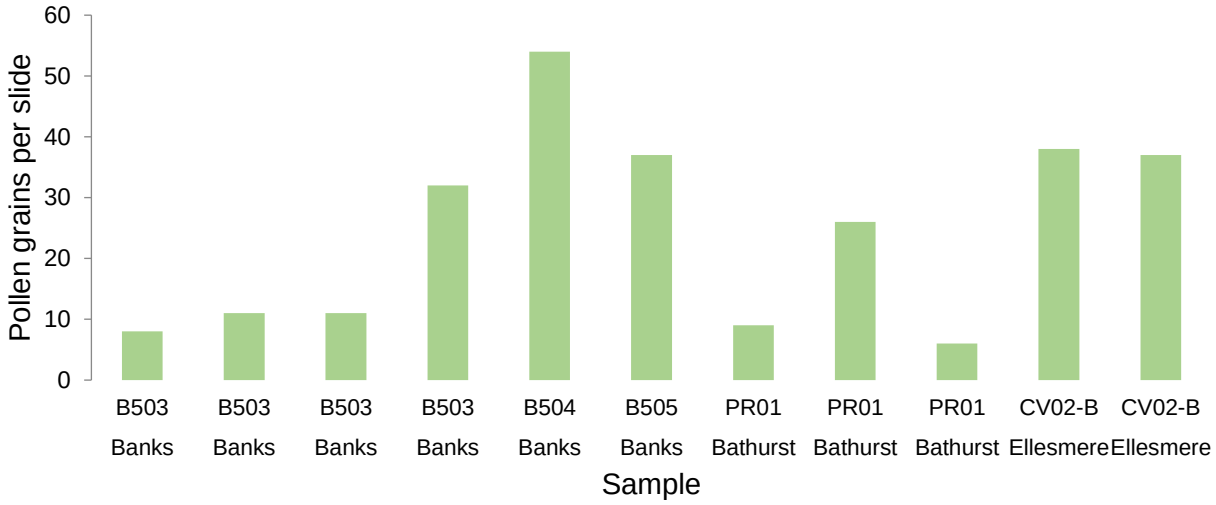

Figure 2.4: Comparison of the number of pollen grains per slide in several lakes across the Canadian Arctic Archipelago.

2.4.3 Biogenic Silica

Biogenic silica is typically low in Arctic sediments (Fortin & Gajewski, 2009) and is often absent in sections of, or entire, sediment cores. The reason for dissolution is poorly understood, but may be a result of alkaline lake water pH due to carbonate bedrock or surficial deposits (Flower, 1993; Fortin & Gajewski, 2009; Paull et al., 2017; Ryves et al., 2006). Four cores were analyzed for biogenic silica – B503, PR01, SW08, and CV03 – but only B503, PR01, and CV03 contained values above detection. The core from Banks Island (B503) contained values above detection for the entire sequence, whereas results were obtained from PR01 and CV03 for only the top 20 cm before they fell below detection. Lake water pH was reconstructed using the following calibration equation developed by Fortin and Gajewski (2009):

$$pH = 7.26 + 0.16 * \sqrt{\%\ carbonate} - 0.18 * \log(\%BSi)$$

2.5 Biogenic Silica Calibration Samples

The measurement of biogenic silica is a sensitive process and small experimental errors can lead to large inaccuracies in results. In order to verify that the processing of any particular batch of samples was successful, reference samples of known biogenic silica content are processed alongside the unknown samples. We had obtained a set of the original reference samples that were developed by Conley (1998). To create the original references, sediment samples were sent as unknowns to 31 separate laboratories for BSi determination and the results were analyzed to determine an acceptable range of BSi concentration (wt. % SiO_2) for each sample. Only a small amount of the original reference samples remained, so to facilitate future analysis of biogenic silica new reference samples were created for this study. Four samples were selected based on estimations of biogenic silica concentration and were processed using a wet chemical digestion technique (see Section 2.2.4 for details). In each batch, two reference samples developed by Conley (1998) were processed for experimental control.

Table 2.3: Original biogenic silica reference samples created by Conley (1998).

Sample	**BSi (wt. %)**	**1σ SD**	**Coefficient of variation**
1	2.82	± 1.17	± 41.6%
2	44.3	± 9.38	± 21.25%
3	6.49	± 2.09	± 32.1%
4	38.2	± 9.48	± 24.8%
5	7.37	± 2.56	± 34.8%
6	1.31	± 0.88	± 67.5%

2.5.1 Sample collection

Samples were obtained from freshwater lakes in Nova Scotia, Yukon, Northern Quebec and Northwest Territories using a Livingstone corer or Ekman dredge. In the laboratory, bulk samples were dried in an oven at 105°C for 24 hours then crushed with a mortar and pestle and homogenized. Each bulk sample was then subsampled into polypropylene vials.

2.5.2 Results and Discussion

The new reference samples ranged from 7-34 weight percent of BSi, thereby providing standards for a range of samples. The coefficients of variation ranged between 8-14%. Variations in BSi concentration for each sample were low compared to those created by Conley (1998), which were between 21-68%. When the original reference samples were created, the samples were sent out to 31 laboratories for processing, which likely introduced more error into their results due to methodological differences between laboratories. Unlike the previous reference samples, those with higher BSi concentrations had a higher coefficient of variation. As expected, BSi concentrations were lower in samples from more northern latitudes. There were seemingly large within- and between-batch variations (Figure 2.5). For example, the range of measured values for TR07 was large in batch 7 (22-38%) and small in batch 3 (30-32%). However, the coefficient of variation is small for all samples (less than 15%) and the range is more constrained than the old references so these ranges were deemed acceptable. Since the new references are more constrained than those by Conley (1998), we determined measured values within 2 standard deviations are acceptable when using as control samples.

Table 2.4: New reference samples for biogenic silica analysis, including the mean, 1-sigma standard deviation and coefficient of variation (standard deviation/mean). Since the coefficient of variation is relatively low, accepted values when using the new references must measure within 2 standard deviations.

Sample	Location	BSi (wgt %)	1σ SD	Coefficient of variation
TR07	Robertsons Lake, Nova Scotia	30.70	± 4.36	± 14.2%
BC01	Melville Island, NWT	7.21	± 0.65	± 9.0%
KP1	Northern Quebec	34.22	± 3.48	± 10.2%
K819	Yukon	17.36	± 1.41	± 8.15%

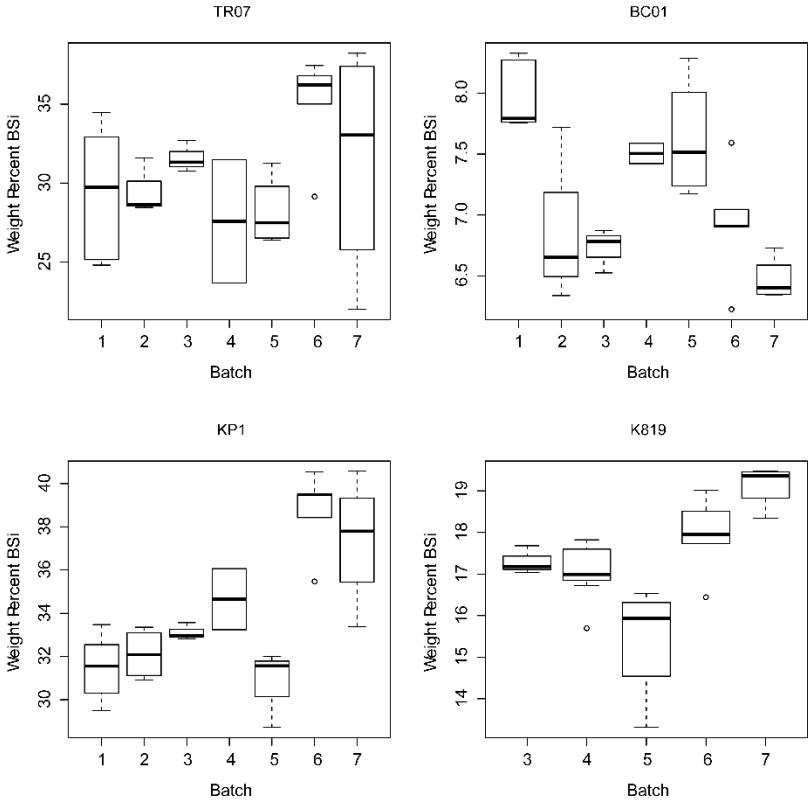

Figure 2.5: Boxplots showing the distribution of measured values for each sample by batch. *Note:* The y-axis scale is different on each graph and sample K819 was only processed in batches 3-7.

CHAPTER THREE

Lacustrine aquatic production and pH over the past 3000 years in four lakes from the Canadian Arctic Archipelago

3.1 Introduction

In the Canadian High Arctic, climate is generally considered to be the dominant control on lake ecology (Michelutti et al., 2007; Smol et al., 2005; Wolfe, 2002). Climate may directly affect organisms by controlling the duration of ice cover and water temperature, which can affect thermal stratification. Changes in precipitation can affect lake levels, which influences shallow-deep water ratios and the concentration of ions in the lake (Fritz et al., 2010). Climate can also indirectly affect lake ecology when climatic change modifies vegetation and weathering activity (Fritz & Anderson, 2013).

The long-term ecological development of Arctic lakes since deglaciation is characterized by high production and alkaline waters in the first few thousand years followed by gradual acidification and oligotrophication (Fritz & Anderson, 2013). The cause of this ecological trajectory may differ regionally throughout the Arctic. For example, in southwest Greenland, lake ontogeny processes are hypothesized to control ecological development (Fritz & Anderson, 2013; Law et al., 2015), whereas in the Canadian Arctic, climate is thought to be the dominant control due to reduced edaphic processes in the catchment area (Fritz & Anderson, 2013; Michelutti et al., 2007; Wolfe, 2002).

Changes in lake-water pH have been suggested as an indicator of past climate change, particularly in poorly-buffered Arctic lakes (Michelutti et al., 2007; Rouillard et al., 2012; Wolfe, 2002). Diatoms have frequently been used to reconstruct changes in lake pH (Lim et al., 2001; Michelutti

et al., 2007; Rouillard et al., 2012; Wolfe, 2002), either by weighted-average inference models based on fossil-diatom assemblages (Finkelstein et al., 2014; Joynt III & Wolfe, 2001) or by a transfer function based on changes in sediment carbonate and biogenic silica content (Fortin & Gajewski, 2009). In poorly-buffered Arctic lakes, diatom-inferred pH has declined over the Holocene consistent with the Neoglacial cooling (Michelutti et al., 2007; Wolfe, 2002).

In this study, we present limnological characteristics from four lakes across the Canadian Arctic Archipelago to examine late Holocene changes in aquatic production and pH. Due to the presence of dissolution in most records biogenic silica cannot be associated with climate; in such cases, additional proxies should be assessed alongside BSi for a robust analysis.

3.2 Site Description

Lake sediment cores were analyzed from four sites across the Canadian Arctic Archipelago. The cores selected from storage were estimated to span at least 1000 years. The sites are from different vegetation zones, are in areas of differing bedrock and surficial geology, and are located roughly along a southeast-northwest transect of the Canadian Arctic Archipelago (Figure 3.1).

3.2.1 Core B503; southern Banks Island

Banks Island is located in the western Arctic, Northwest Territories. Cores were extracted from a lake on the southern portion of the island. Lake B503 (unofficial name; 72.3245, -123.4036, 94 masl) is located approximately 70 km inland from the western coastline in an area underlain by continuous permafrost. The area of the lake is approximately 535,579 m^2 and the land surrounding the lake consists of poorly lithified sand, silt, and clay (Vincent, 1989). The bioclimate zones on Banks Island range from Low Arctic in the south, to High Arctic in the north (Gajewski et al., 2000); the study lake falls near the Low to Middle Arctic transition zone in a graminoid tundra.

The soil surrounding the lake is circumneutral (pH 5.5-7.2) and likely provides the essential plant nutrients to allow a higher density and diversity of plant growth (CAVM et al., 2003). The closest weather station is located ~75 km west of Lake B503 at Sachs Harbour, NWT where the mean July temperature (1956-1980) is 5.9 ± 1.8°C (Environment and Climate Change Canada, 2018c).

3.2.2 Core PR01; Bathurst Island

Bathurst Island is located in the central High Arctic, Nunavut, Canada. Two cores were taken from a lake (unofficially designated PR01; 75.6497, -99.1144, 60 masl) just to the south of Polar Bear Pass National Wildlife Area. The lake has an area of ~74,080 m^2, is 3.46 m deep at the coring site, and is approximately 20 km inland from the west coast of Bathurst Island. The geology is characterized by lower and middle Devonian limestone of the Blue Fiord Formation (Kerr, 1974). The vegetation surrounding the lake is High Arctic and characterized as an herb-shrub transition zone; herbaceous species dominate but there are some shrubs present (CAVM et al., 2003). There are also barrens to the east of the lake where the land is characterized by exposed bedrock with limited vegetation (CAVM et al., 2003). The closest weather station is located 160 km to the southeast at Resolute Bay, Cornwallis Island, Nunavut where the mean July temperature (1948-1980) is 4.2 ± 1.2°C (Environment and Climate Change Canada, 2018b).

3.2.3 Core SW08; Prince of Wales Island

Prince of Wales Island is located in the central High Arctic, Nunavut, Canada. Lake SW08 (unofficial name; 72.3177, -97.2678, 104 masl; Figure 4.1) is located in a drumlin field ~20 km inland from the eastern coast of Prince of Wales Island. The lake has an area of ~128,850 m^2. Although the site is located primarily on sandstone bedrock, glacial activity likely deposited carbonate-rich till throughout the area (Dyke & Morris, 1988). The vegetation is defined as a dry prostrate-shrub tundra (Walker et al., 2002). The nearest weather station is 275 km to the northeast

in Resolute Bay, Nunavut where the mean July temperature (1948-1980) 4.2 ± 1.2°C (Environment and Climate Change Canada, 2018b).

3.2.4 Core CV03; Ellesmere Island

Ellesmere Island is located in the northeastern Canadian Arctic, Nunavut. The lake (unofficially named CV03; 79.9211, -82.9348, 363 masl) is small with an area of 4,460 m^2 and is over 2.5 m deep. It is located in an area characterized by late Triassic/early Jurassic sandstone and quartz (Harrison et al., 2015). The site is located near the Hot Weather Creek Area, which is sheltered from cold air masses by the surrounding mountains making it an 'Arctic Oasis' (Garneau & Alt, 2000). Therefore, despite the high latitude, the regional vegetation is characterized as Middle Arctic with a high density and diversity of vascular plant species. However, the higher altitude of the site limits the vegetation, which is characterized as a graminoid tundra. The lake is north of a small glacier and is in a valley surrounded by steep slopes. The closest weather station is 56 km to the west at Eureka, Ellesmere Island where the mean July temperature (1950-1980) is approximately 5.5 ± 0.96°C (Environment and Climate Change Canada, 2018a), although it can often be upwards of 10°C (Edlund & Alt, 1989).

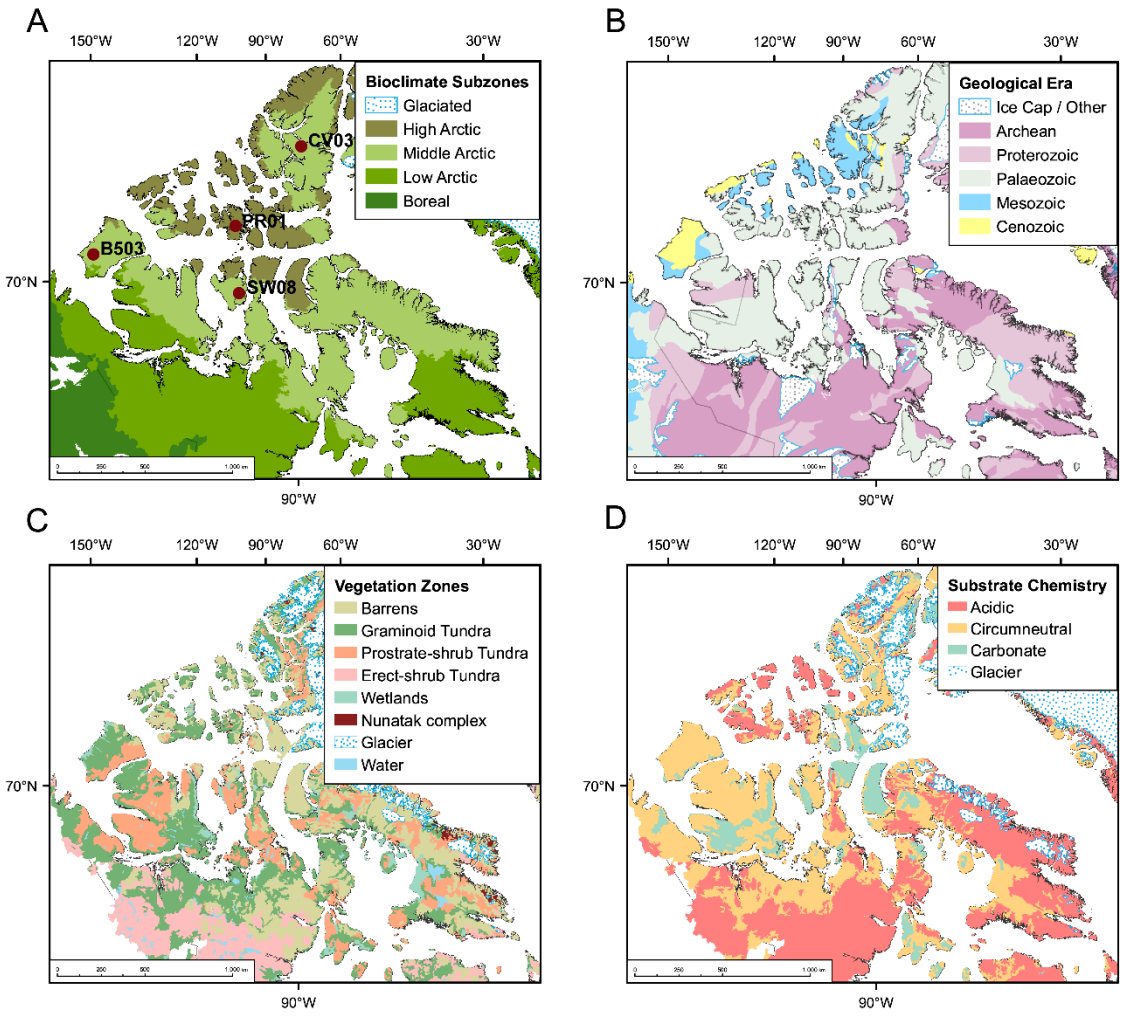

Figure 3.1: Maps of the Canadian Arctic Archipelago: (A) Bioclimate (CAVM et al., 2003), (B) Geological Era (Wheeler et al., 1997), (C) Vegetation Zone (CAVM et al., 2003), and (D) Substrate Chemistry (CAVM et al., 2003). Study sites are shown in panel A.

3.4 Methods

Sediment cores were extracted over four field seasons – 2007, 2015, 2016, and 2017 – using a plastic tube fitted with a piston. The samples from the uppermost, unconsolidated sediments were extruded in the field into plastic bags or centrifuge tubes at 0.5 cm intervals. The rest of the core sections were extruded and wrapped in plastic wrap and aluminum foil to retain moisture then shipped back to the University of Ottawa in plastic tubes and refrigerated at 4°C.

Before opening each core, magnetic susceptibility was analyzed at 1 cm intervals using a Bartington MS2C Magnetic Susceptibility Meter. This provided information regarding the magnetic mineral concentrations of the sediment throughout the core; however, it was only successful on the core from Lake CV03.

Organic matter and carbonate content were determined by measuring loss-on-ignition using a LECO Thermogravimetric Analyzer. The mass at each temperature step was recorded by the analyzer once its variation reached less than 0.1%. Standards of known organic and carbonate content were run alongside each batch to ensure experimental control (Section 2.5). Using a wet chemical digestion technique (Conley & Schelske, 2001; DeMaster, 1981; Parsons, 1984), biogenic silica was analyzed at 0.5 cm intervals for the entire sequence in core B503. In cores CV03 and PR01 biogenic silica was analyzed continuously for the top 20 cm; point samples were analyzed in the deeper sediments but no values above detection were found. In core SW08, point samples were analyzed throughout the core. Samples were weighed (0.02g ± 0.002) and placed in polypropylene bottles with 40mL of 1% sodium carbonate (Na_2CO_3). Each sample was placed in an 85°C water bath and subsamples were taken after 2, 3, 4, and 5 hours for analysis using a spectrophotometer.

Cores were dated using both ^{210}Pb and ^{14}C techniques. Lead-210 samples were processed by MyCore Scientific Inc (Ottawa, Ontario) and ages were determined using a constant rate of supply model (Table 3.1). Samples of aquatic macrophytes were sent to the André E. Lalonde Accelerator Mass Spectrometry Laboratory at the University of Ottawa for ^{14}C analysis (Table 3.2), and the results were calibrated using OxCal v4.2.4 (Bronk Ramsey, 2009) and the IntCal13 calibration curve (Reimer et al., 2013).

3.5 Results

3.5.1 Core B503; southern Banks Island

Chronology

The age-depth model for core B503 was established using nine ^{210}Pb and four ^{14}C dates. The unsupported ^{210}Pb activity in the surface sample was 447.25 Bq/kg (Table 3.1). After a slight reversal at 0.25 cm, the unsupported activity decreased below the supported amount of 84 Bq/kg by 7.25 cm corresponding to an age of 1896 CE. Five ^{14}C results (Table 3.2) were obtained but contained several age reversals that may be a result of contamination of old carbon from Tertiary organic matter in the area (Gajewski et al., 2000). The intercept for the regression of the ^{14}C results was negative, which did not allow a reasonable model to be produced to estimate a reservoir effect. Without other information to assist in dating the core the most suitable approach was to exclude any age reversals. Consequently, the resulting age-depth model (Figure 3.2) excludes three ^{14}C results and is truncated at 50 cm (900 BCE; ~2850 BP).

Sediment stratigraphy and characteristics

The sediment of core B503 (Figure 3.3) was uniformly grayish olive (5Y 4/2) with a band of olive black (5Y 3/1) sediment between 48 and 52 cm (800-900 BCE). Percent organic matter, carbonate,

and biogenic silica were measured continuously at 0.5 cm intervals for the entire 56.5 cm of core B503. Organic matter varied between 14% and 48% and was relatively constant except in the top 5 cm (1920-2015 CE) where it increased from 25% to 48%. Percent carbonate was low, between 1% and 3% and there were no significant changes in the core. Biogenic silica was present throughout the entire core with values up to 12%. Between 40 and 50 cm (900 BCE - 0 CE) BSi percentages were low, never exceeding 2%. BSi increased to ~4% between 28 and 35 cm (85 BCE - 435 CE) and again to ~6% between 12 and 18 cm (1150 – 1650 CE). Percentages were highest in the uppermost 5 cm (1900-2015 CE), reaching 12% in the surface samples. Lake water pH was reconstructed using a transfer function developed by Fortin and Gajewski (2009). There was a long-term decrease in pH from ~7.5 to 7.3 towards present day. Magnetic susceptibility was measured but values were below detection level.

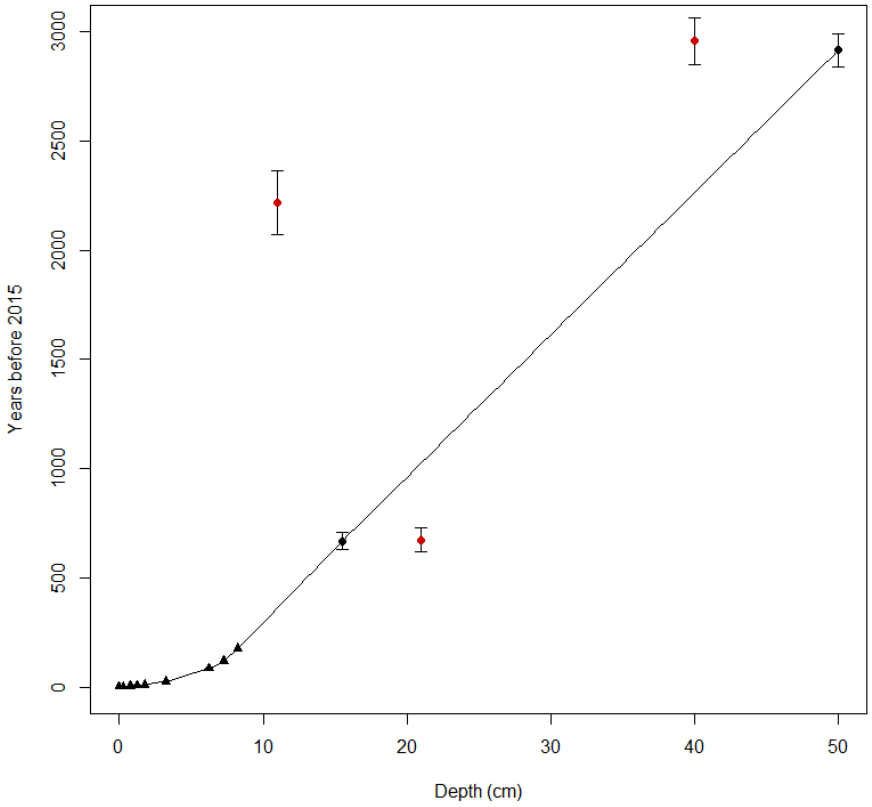

Figure 3.2: Age-depth curve for core B503. *Triangles* are ^{210}Pb results; *circles* are the ^{14}C median calibrated dates with 2σ age range; *red circles* are ^{14}C results omitted from age-depth model.

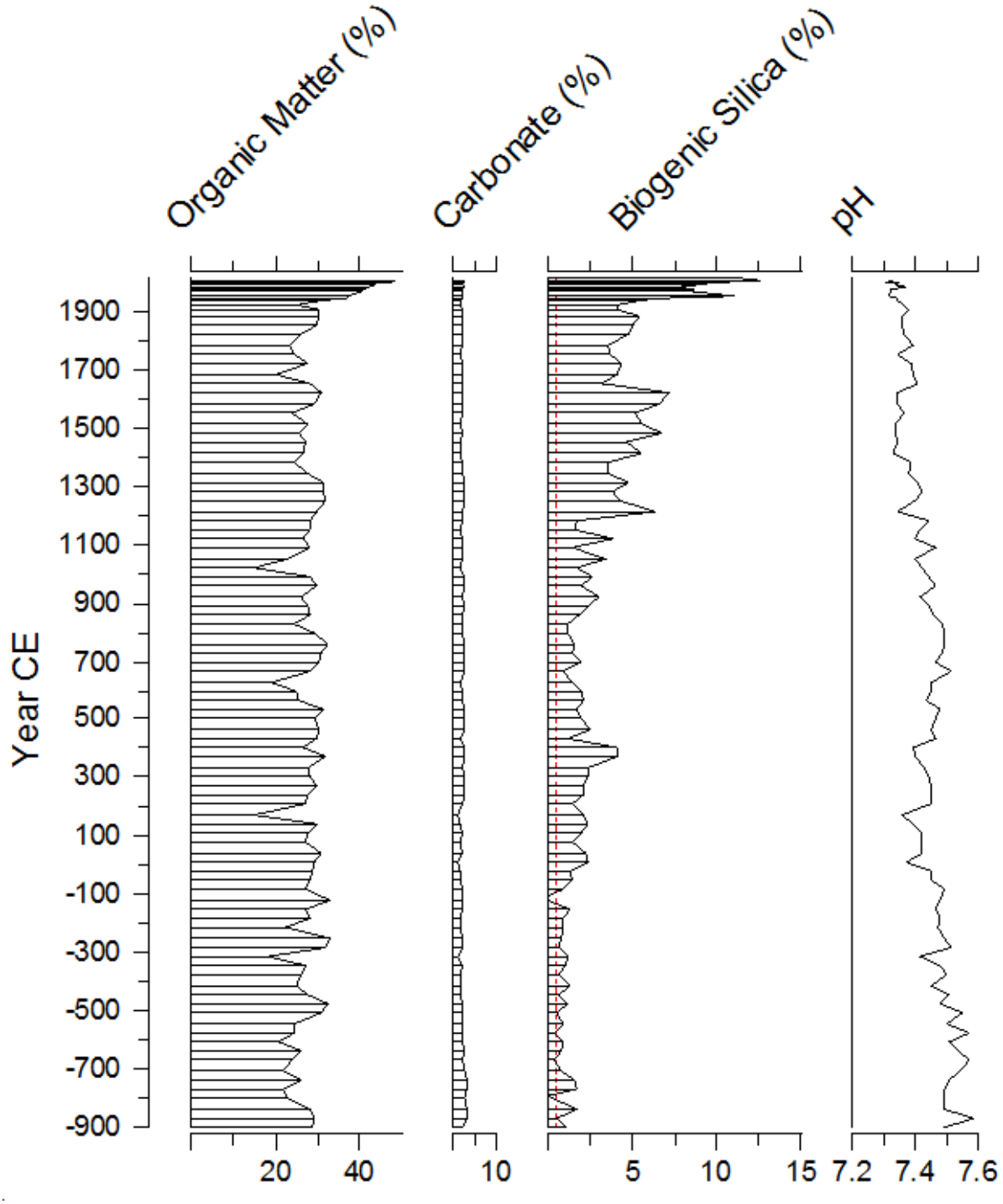

Figure 3.3: Sediment characteristics and pH reconstruction for core B503. *Dashed red line* on biogenic silica curve represents detection level (0.5).

3.5.2 Core PR01; Bathurst Island

Chronology

Nine samples were analyzed for ^{210}Pb from core PR01. In the uppermost sediments the unsupported activity was 263 Bq/kg and decreased below the supported activity of 84 Bq/kg by 6.25 cm at 1912 CE. Some age reversals were present in the top 1 cm, which may be a result of mixing of the sediment. Six ^{14}C dates were obtained which included three anomalously old dates at 12, 15, and 67 cm. The resulting age-depth model was generated using the nine ^{210}Pb and remaining three ^{14}C dates. Given the calcareous bedrock, a hardwater correction of 842 years was applied to core PR01 based on the intercept from linear regression of the three accepted ^{14}C dates. The corrected dates were used to generate an age-depth model truncated at 41 cm (853 CE; Figure 3.4).

Sediment stratigraphy and characteristics

Core PR01 (Figure 3.5) was 71 cm long and relatively uniformly dark greyish brown (2.5Y 4/2) with some irregular banding of olive brown (2.5Y 4/3) sediment between 30 and 41 cm. Organic matter percentages ranged between 9 and 22% with a mean of 14%. There were four periods of increased organic matter between 58 and 65 cm, 47 and 55 cm, 31 and 40 cm, and in the uppermost 7 cm of the core. Carbonate content was low, never exceeding 5%. Biogenic silica percentages for the top 20 cm of the core were low, never exceeding 2% except in the uppermost 3 cm where percentages increased to 12%. Below 20 cm, point samples were measured but no biogenic silica was detected. Lake pH was reconstructed for the top 20 cm of the core where BSi was available and shows a general tendency to decrease over time from 7.6 to 7.4.

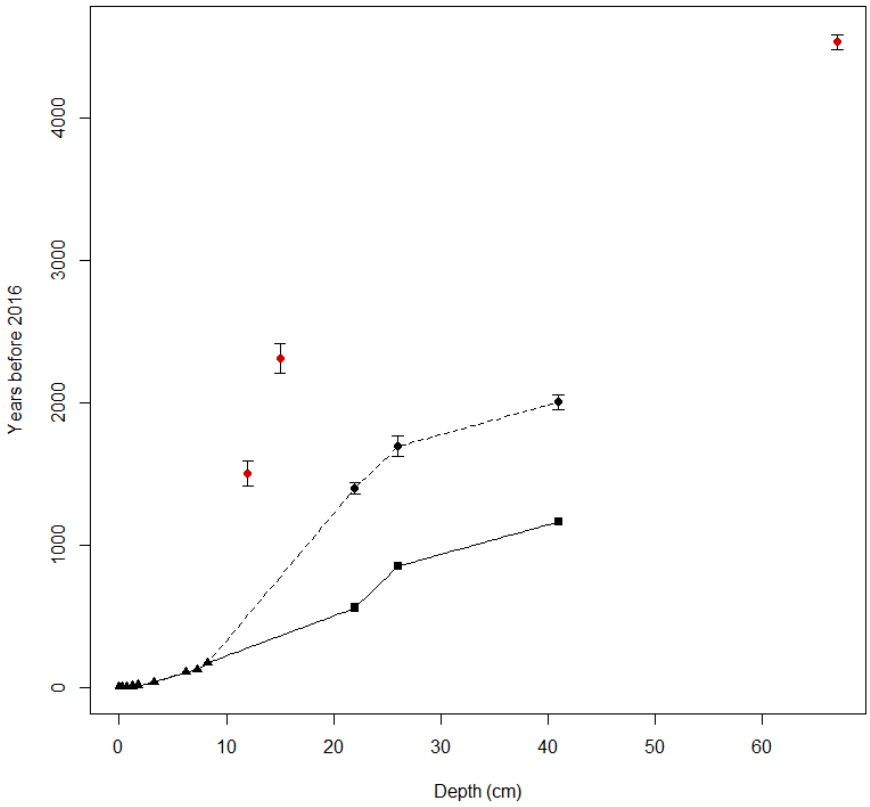

Figure 3.4: Age-depth curve for core PR01. *Triangles* are ^{210}Pb results; *circles* are the ^{14}C median calibrated dates with 2σ age range; *red circles* are ^{14}C results omitted from age-depth model; *squares* are hardwater-corrected ^{14}C dates. *Solid line* represents the corrected age-depth model; *dashed line* is the age-depth model without the hardwater correction.

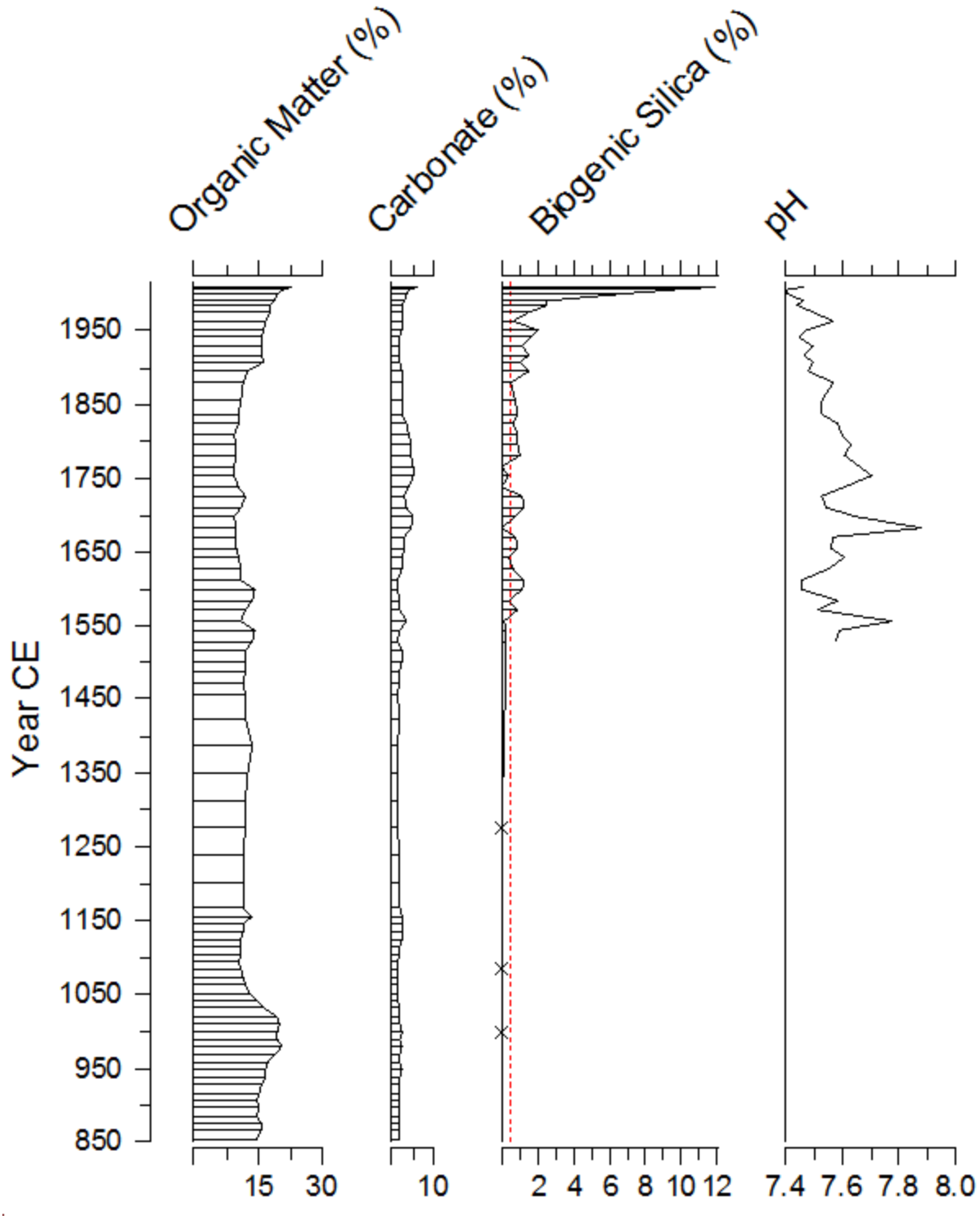

Figure 3.5: Sedimentary characteristics and reconstructed pH for core PR01. *Dashed red line* is biogenic silica detection level (0.5).

3.5.3 Core SW08; Prince of Wales Island

Chronology

The unsupported ^{210}Pb activity in the uppermost sediment was 134 Bq/kg and reached the supported level of 64 Bq/kg by 3.25 cm at 1962 CE (Table 3.1). The six ^{14}C dates included one anomalously old age and two age reversals at 12, 37 and 45 cm, respectively, which were excluded from age-depth modelling (Table 3.2). The resulting age-depth model was created by linear interpolation of eight ^{210}Pb and three ^{14}C dates, however, this only established a reliable chronology for the top 25 cm of the core (1082 CE). The age-depth curve (Figure 3.6) shows an unusually large sedimentation rate between 10 and 15 cm. Results such as this are frequently seen in Arctic sediments (Gajewski et al., 2000; MacDonald et al., 1991; Peros & Gajewski, 2009) and suggest a reservoir effect due to hardwater. Following Peros and Gajewski (2009), a hardwater correction was estimated by calculating the intercept of a linear regression of the accepted radiocarbon dates. The estimated hardwater correction for core SW08 is 856 years, which was subtracted from the remaining radiocarbon dates to generate an age-depth model whose oldest date at 25 cm is 1082 CE (Figure 3.6).

Sediment stratigraphy and characteristics

The sediment in core SW08 (Figure 3.7) was very dark grey (10YR 3/1) in the top 7 cm (1900-2017 CE) then became mottled with dark yellowish brown (10YR 3/4) sediment until 12 cm (1650-1900 CE). From 12 to 32 cm the sediment was uniformly dark yellowish brown (10YR 3/4). Below 32 cm, the sediment was dark greyish brown (10YR 4/2). Organic matter was low throughout the core, never exceeding 6%, and carbonate percentages were high, ranging between 22% and 27%. Nineteen samples were analyzed for biogenic silica along the core, but no values above detection were measured.

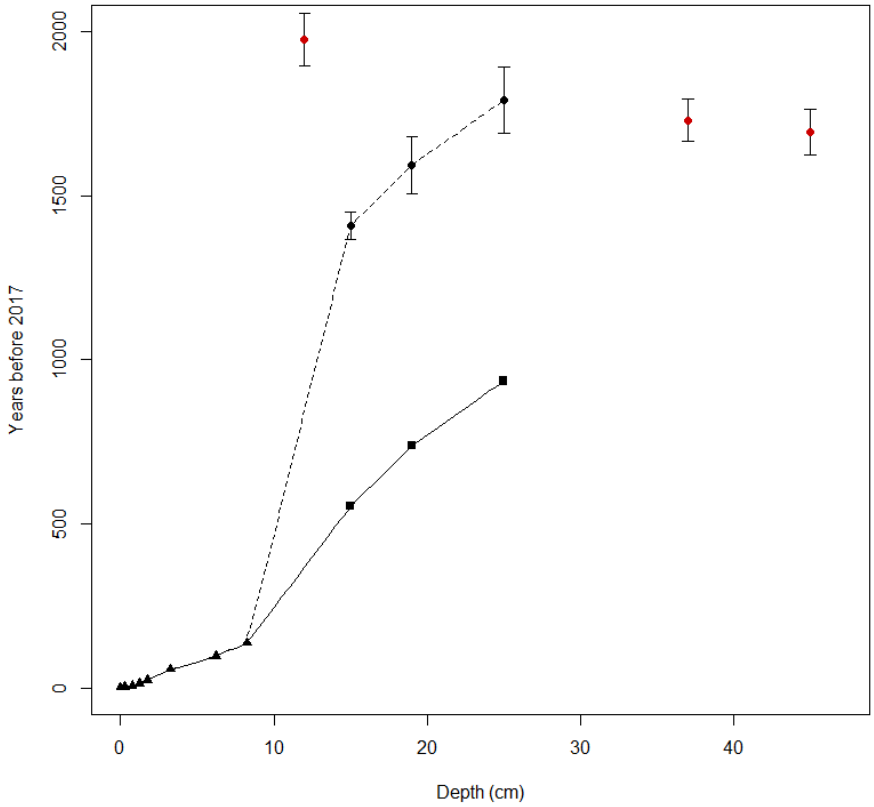

Figure 3.6: Age-depth curve for core SW08. *Triangle*s are ^{210}Pb ages; *Circles* are the ^{14}C median calibrated dates with 2σ age range; *red circles* are ^{14}C dates rejected from age-depth model; *Squares* are hardwater-corrected ^{14}C dates (see text for details). *Solid line* represents the corrected age-depth model; *dashed line* is the age-depth model without hardwater correction.

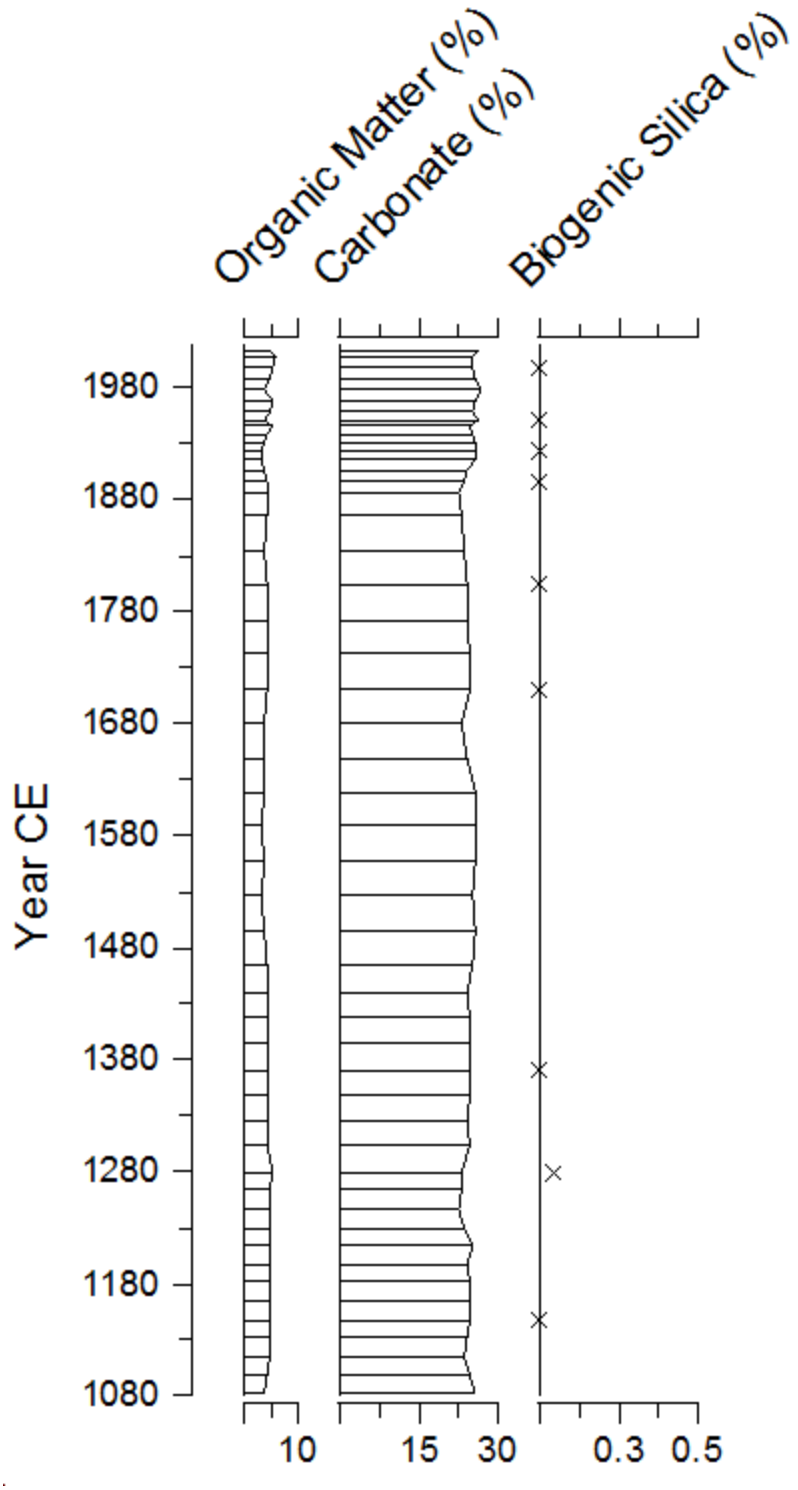

Figure 3.7: Sedimentary characteristics of core SW08.

3.5.4 Core CV03; Ellesmere Island

Chronology

In core CV03, the unsupported ^{210}Pb activity was 202 Bq/kg in the uppermost sediments and decreased below the supported level of 31.50 Bq/kg by 6.25 cm, corresponding to an age of 1872 CE. Five ^{14}C determinations were obtained that included one anomalously old and one age reversal at 15 and 40 cm, respectively. Tertiary coal was identified in a neighbouring lake and could explain the anomalously old dates. The resulting age-depth model (Figure 3.8) was based on seven ^{210}Pb and three ^{14}C dates and was truncated at 30 cm since no reliable dates were obtained in the lowermost sediments. As above, a rapid increase in age between the oldest ^{210}Pb and the youngest ^{14}C date indicates there is likely a reservoir effect, either from hardwater or Tertiary coal. A reservoir correction of 929 years was applied to each accepted date.

Sediment stratigraphy and characteristics

Core CV03 (Figure 3.9) had several distinct changes in sediment characteristics. Between 6 and 12 cm (1860-1880 CE) there were several visible white fragments, potentially of mineral origin, in the sediments. There was a large band of dense, grey clay (5Y 4/1) between 15 and 20 cm (1645-1772 CE), followed by brown sandy (10YR 4/4) sediment that had been oxidized (red) between 20 and 21 cm (1637-1645 CE). Below 30 cm, the sediment was characterized by grey clay (5Y 4/1) typical of Arctic lacustrine sediments.

Percentages of organic matter and carbonate were measured at 0.5 cm intervals for the length of core CV03 (47 cm). Organic matter remained between 5 and 10% in most of the core except between 18 and 28 cm (1588-1682 CE) where it increased to ~14% and in the uppermost 4 cm (1923-2007 CE) where it increased to 32%. Carbonate content ranged between 1 and 16%, with three distinct periods of increased carbonate between 25 and 30 cm (1574-1610 CE), 19 and 22

cm (1630-1650 CE), and 6 and 13 cm (1830-1880 CE). Biogenic silica percentages in the top 20 cm were mostly near or below detection, except in the top 3 cm (1960-2007 CE) where they reached 6%. Lake water pH was reconstructed for the top 30 cm of the core; however, the results should be interpreted with caution since BSi values were very low. Magnetic susceptibility measured some distinct increases in magnetic mineral concentrations between 13 and 20 cm (1645-1830 CE), and below 30 cm, which corresponded to the sections of clay-rich sediments.

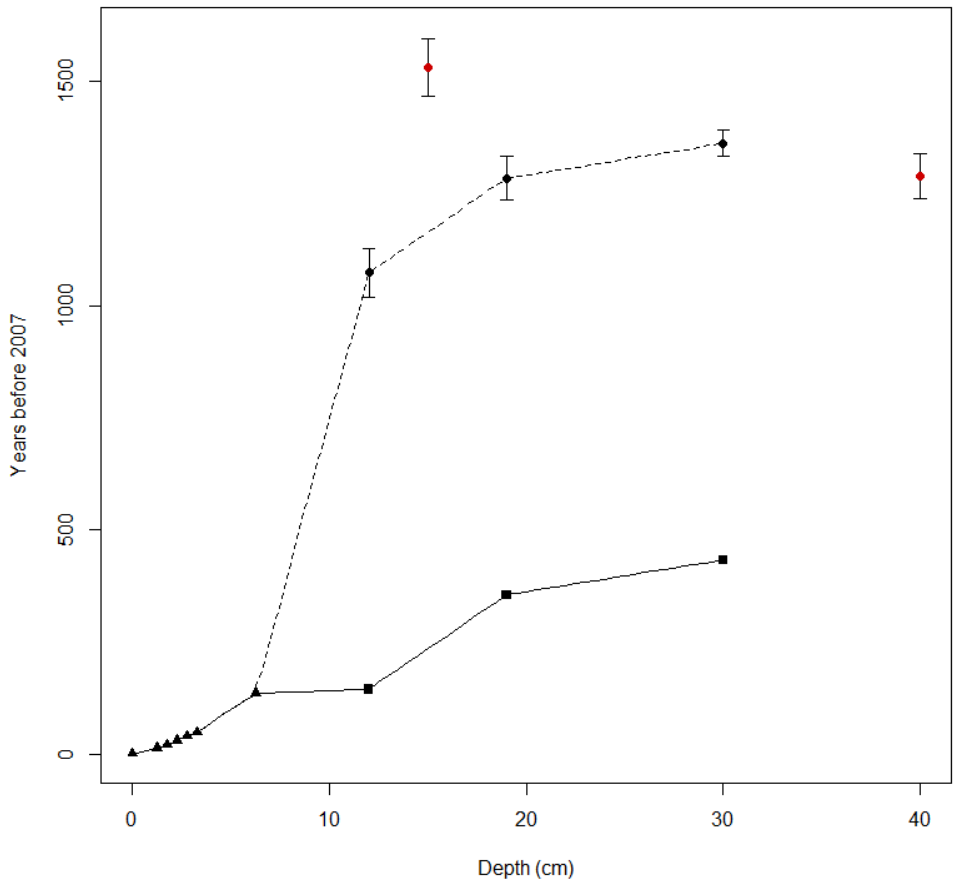

Figure 3.8: Age-depth curve for core CV03. *Triangles* are ^{210}Pb results; *circles* are the ^{14}C median calibrated dates with 2σ age range; *red circles* are ^{14}C results omitted from age-depth model; s*quares* are hardwater-corrected ^{14}C dates. Solid line represents the corrected age-depth model to be interpreted; dashed line is the age-depth model without hardwater correction.

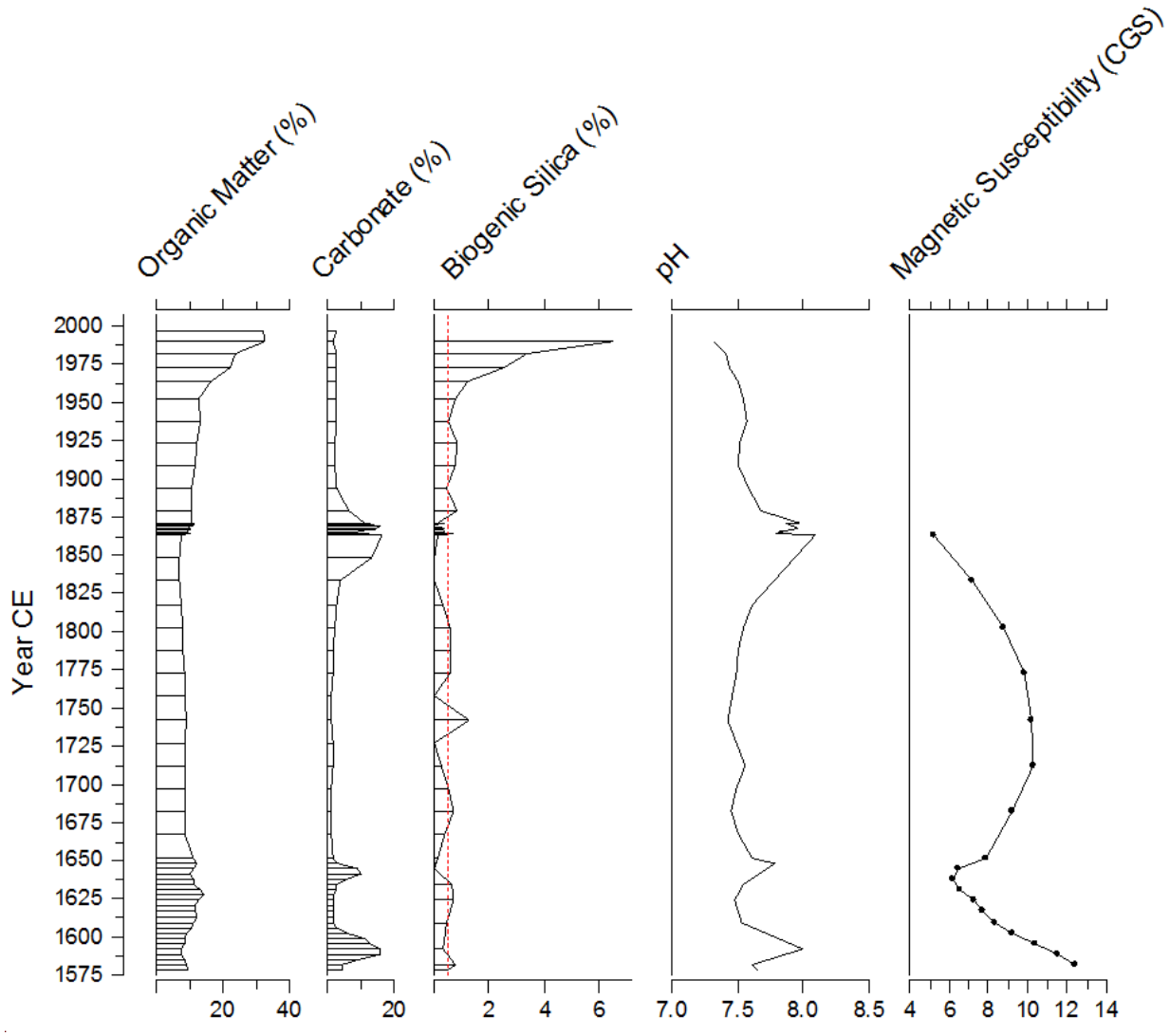

Figure 3.9: Sedimentary characteristics for core CV03. *Dashed red line* is biogenic silica detection level (0.5).

Table 3.1 ^{210}Pb results and ages based on constant-rate-of-supply (CRS; Appleby & Oldfield, 1978) model.

B503				**CV03**			
Midpoint Depth (cm)	Unsupported Activity (Bq/kg)	Year CE	CRS Error (years)	Midpoint Depth (cm)	Unsupported Activity (Bq/kg)	Year CE	CRS Error (years)
0.00	447.27	2015.58	0	0.00	202.54	2007.46	0.29
0.25	369.72	2014.84	0.11	1.25	202.54	1994.28	1.46
0.75	443.11	2012.94	0.24	1.75	185.9	1987.47	1.72
1.25	431.93	2009.88	0.42	2.25	179.6	1977.83	2.20
1.75	424.25	2005.97	0.59	2.75	76.58	1967.91	2.93
3.25	312.82	2989.99	1.31	3.25	49.43	1960.32	3.69
6.25	116.98	1931.14	4.04	6.25	8.04	1872.10	20.72
7.25	34.25	1896.79	10.22	7.25	4.21		
8.25	23.85	1838.67	16.29	8.25	0.39		
8.75	0.10			8.75	3.40		
PR01				**SW08**			
Midpoint Depth (cm)	Unsupported Activity (Bq/kg)	Year CE	CRS Error (years)	Midpoint Depth (cm)	Unsupported Activity (Bq/kg)	Year CE	CRS Error (years)
0.00	263.49	2016.39	0	0.0	134.78	2017	0
0.25	292.34	2014.87	0.17	0.25	78.22	2015	0.23
0.75	98.10	2012.47	0.29	0.75	132.24	2011	0.72
1.25	284.16	2009.59	0.53	1.25	137.3	2004	1.25
1.75	269.24	2003.95	0.92	1.75	152.96	1993	2.12
3.25	134.76	1981.10	2.42	3.25	18.89	1962	7.23
6.25	20.07	1912.87	10.56	6.25	12.73	1920	17.90
7.25	8.77	1892.26	17.87	8.25	0.00	1880	19.11
8.25	10.20	1845.21	43.34	8.75	22.39	N/A	
8.75	0.00						

Table 3.2: Radiocarbon dates for cores B503, PR01, SW08, and CV03. Asterisk (*) indicates dates rejected and not used in developing the chronology. All samples were mixed terrestrial and aquatic matter. Samples were calibrated using OxCal v4.2.4 (Bronk Ramsey, 2009) and the IntCal13 calibration curve (Reimer et al., 2013).

	Lab ID	Depth (cm)	^{14}C yr BP	Error (+/-)	2σ cal BP range	Median cal BP	Hardwater-corrected median cal BP
B503							
	UOC-5315	11-13	2136	25	2007-2255	2153	N/A
	*UOC-5316	15.5-16	685	24	564-642	603	N/A
	UOC-5317	21-22	634	24	555-663	609	N/A
	UOC-5318	40-43	2798	41	2787-3000	2893	N/A
	*UOC-5319	50-51	2752	30	2775-2925	2850	N/A
PR01							
	UOC-5306	12-13	1523	24	1348-1521	1424	N/A
	UOC-5307	15-16	2243	52	2141-2350	2245	N/A
	*UOC-5308	22-23	1433	24	1296-1370	1333	491
	*UOC-2638	26-27	1709	27	1553-1698	1625	783
	*UOC-2637	41-42	1986	24	1886-1991	1938	1096
	UOC-2636	67-68	3996	27	4418-4522	4470	N/A
SW08							
	*UOC-5309	12-13	1961	29	1830-1989	1909.5	N/A
	UOC-5310	15-16	1449	26	1300-1385	1342.5	486.5
	UOC-5311	19-20	1647	24	1441-1613	1527	671
	UOC-5312	25-26	1812	34	1623-1825	1724	868
	*UOC-5313	37-38	1756	24	1600-1727	1663.5	N/A
	*UOC-5314	45-46	1710	24	1556-1696	1626	N/A
CV03							
	*UOC-5320	12-13	1120	24	961-1071	1016	87
	UOC-5321	15-16	1588	24	1411-1537	1474	N/A
	*UOC-5322	19-20	1270	24	1178-1276	1227	298
	*UOC-5323	30-31	1377	24	1275-1334	1304	375
	UOC-5324	40-41	1286	24	1180-1283	1232	N/A

3.6 Discussion

The biogenic silica records in the sediment were affected by the sedimentary carbonate at each lake, resulting in likely diatom dissolution in both PR01 and CV03. Consequently, Lake B503 was the only site with a reliable biogenic silica sequence. Biogenic silica concentrations may be related to climate or other environmental variables, but these relationships could not be quantitatively assessed due to the absence of other climate proxies.

Clear stratigraphic changes occurred in Lake CV03 and, although the causes can not be quantitatively assessed here, they roughly relate to climatic events observed in the instrumental record (Jones et al., 2016) and published reconstructions (Shindell et al., 2001; Vieira et al., 2011). The first stratigraphic change was a carbonate spike between 1865 and 1870 CE. An increase in carbonate precipitation could occur either from increased productivity in the lake or increased erosion in the catchment area, both of which would occur during warmer conditions. This recent carbonate spike in the sedimentary record occurred when the instrumental records showed warm season temperatures were warmer than average (Jones et al., 2016). Another abrupt stratigraphic change was a thick clay band that was deposited between 1645 and 1772 CE corresponding to the Maunder Minimum, which was a period of reduced total solar irradiance. If temperatures were colder during this period, prolonged ice cover at the lake would reduce the influx of allochthonous material from the catchment area and lead to the deposition of finer clay particles (Håkanson & Jansson, 1983). The link between the earlier two carbonate peaks and climate is less clear since the instrumental record does not extend that far back and the decadal climate variability in the Arctic not well-resolved.

Stratigraphic changes in percent organic matter, carbonate and BSi were subtle at Lake PR01, which was expected due to the unproductive landscape and harsher climate characteristic of High

Arctic locations. Apart from the last 150 years, peak organic matter content occurred between 950 and 1050 CE, corresponding with the MCA, whereas carbonate and biogenic silica did not show any relationship with climate.

The results from Lake SW08 showed consistently high carbonate values (> 20%) and no biogenic silica above detection. Although it is possible that there were no diatoms present in the lake, it is also likely that the diatoms were dissolved by the carbonates in the sediment similar to what occurred in Lake CV03.

The changes in biogenic silica content at B503 roughly corresponded to periods of climate variability, mainly the Roman Warm Period (RWP; 1 – 300 CE), Dark Ages Cold Period (DACP; 300 CE – 800 CE), Medieval Climate Anomaly (MCA; 800-1300 CE) and the Little Ice Age (LIA; 1300-1900 CE; Ljungqvist, 2010). As seen in other pH reconstructions from the Arctic (Fortin & Gajewski, 2010a, 2010b; Michelutti et al., 2007; Wolfe, 2002), the long-term trend indicates decreasing pH, which is consistent with the Neoglacial cooling. The results from the pH reconstruction also produced contradictory results. In warmer conditions, increases in algal productivity are expected, which would remove CO_2 from the water and increase the pH. However, the record from B503 shows an inverse relationship between productivity (inferred from BSi) and pH. Fortin and Gajewski (2009) suggested this negative relationship may to due to increased CO_2 from respiration from higher-order consumers which would decrease lake water pH. Alternatively, they suggested that pH may control the sediment BSi content and preservation (discussed below).

The rapid increase in biogenic silica concentration in the uppermost samples of cores B503, PR01, and CV03 may be a result of either diatom dissolution in the deeper sediments (Paull et al., 2017) or recent climate change (Douglas et al., 1994). Several studies have linked diatom dissolution with increased lake-water alkalinity (Flower, 1993; Fortin & Gajewski, 2009; Paull et al., 2017;

Ryves et al., 2006); however, no threshold for dissolution has been identified. Dissolution has been identified at a pH as low as 7 (Flower, 1993), but diatoms have also been found in lakes with a pH as high as 9.9 (Ryves et al., 2006). Bedrock composition is thought to be a major control on lake water pH, particularly influencing the buffering ability of the lake (Dranga et al., 2017; Fortin & Gajewski, 2009; Michelutti et al., 2007; Ryves et al., 2006; Wolfe, 2002). In areas of carbonate bedrock, dissolution of carbonate minerals maintains a neutral to slightly alkaline lake water, whereas areas with low carbonate content are more susceptible to acidification from changing environmental conditions such as increased precipitation or decreased air temperatures (Fortin & Gajewski, 2009; Michelutti et al., 2007; Wolfe, 2002). Diatom dissolution is suspected in cores PR01, SW08, and CV03 due the presence of carbonates in the surrounding bedrock and lake sediments. In Lake CV03, biogenic silica falls below detection at each period of increased carbonate, which supports post-depositional dissolution as the cause. Increased carbonate precipitation in lakes has been attributed to increased productivity since it occurs via the removal of CO_2 by algae during photosynthesis (Dean, 1981; Håkanson & Jansson, 1983; Kelts & Hsü, 1978). As such, the increased carbonates in the sediment should correspond with increased BSi; however, post-depositional dissolution prevents this from being recorded in the sedimentary record (Figure 3.10).

Although the records obtained in this study may not be directly associated with climate, the results provided insight into the issue of diatom dissolution. The transfer function developed by Fortin and Gajewski (2009) from surface samples across the Canadian Arctic was likely significantly influenced by dissolution since many of the lakes were located on or near carbonate bedrock or surficial materials. Complete or partial post-depositional dissolution of diatoms indicates that the concentrations present in the sediment do not accurately reflect what was living in the lake at the

time of deposition. In addition to post-depositional dissolution, Paull et al. (2017) suggested that diatom-free zones may occur during warmer conditions as a result of increased productivity where silica would be recycled and fewer remains would be buried in the sediment. In some cases, increased temperatures may also increase carbonate precipitation into the sediment, further reducing the sediment BSi. Given the complex relationships between biogenic silica, climate, hydrochemistry, and sedimentary characteristics, biogenic silica records should be supplemented with independent temperature reconstructions (i.e. pollen- or chironomid-based). Furthermore, analyzing only the uppermost sediments in a core is insufficient, even if the target study period is in the last 200 years, because abrupt changes may simply be a result of post-depositional dissolution.

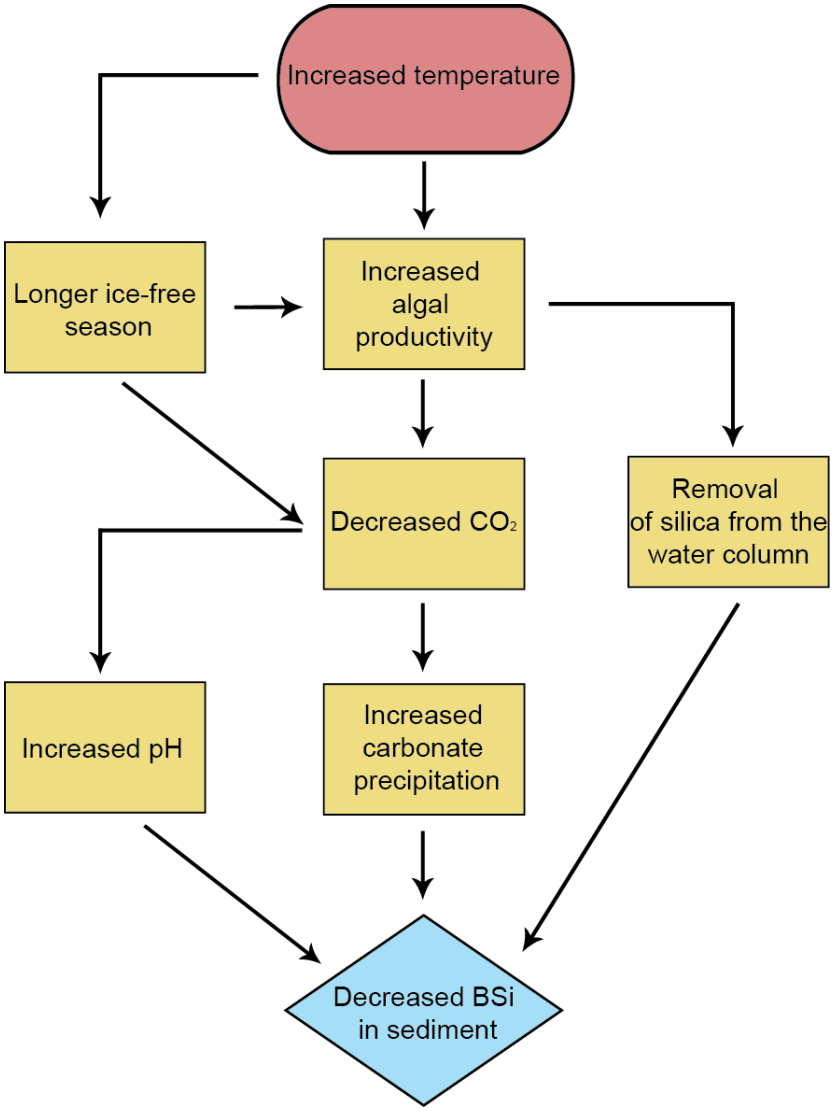

Figure 3.10: Model of proposed interactions between climate, lake ecology and sediment BSi,

3.7 Conclusion

Biogenic silica records can be directly associated with climate (McKay et al., 2008), but the reliability of the record is strongly controlled by the sedimentary characteristics of the lake. The results from Lake CV03 show evidence of post-depositional dissolution linked to changes in carbonate content. Lake PR01 also shows evidence of post-depositional dissolution since it is only present in the uppermost sediments. In Lake SW08, percent carbonate was consistently measured above 20% and no biogenic silica was detected in the sediments. The observed relationship between carbonate and biogenic silica cautions the use of the transfer function based on sedimentary characteristics since the carbonate influences the amount of biogenic silica preserved in the sediment and the transfer function was developed using several hardwater lakes (Fortin & Gajewski, 2009). Results from Lake B503 may be more closely associated with climate; however, the proxies analyzed are crude and a climate signal would need to be verified using a multi-proxy study. As is typical in the Arctic, no other proxies existed in sufficient quantities to allow for a quantitative study.

CHAPTER FOUR

Environmental changes of the last 1000 years on Prince of Wales Island, Nunavut, Canada

4.1 Introduction

High-resolution paleoclimate studies are key to understanding the scales of climate variability and provide insight into how ecosystems responded to previous periods of decadal-, centennial-, and millennial-scale climate variability. Robust large-scale reconstructions for the last 2000 years have been hindered by poor spatial coverage, dating uncertainties, and low resolution data (Christiansen & Ljungqvist, 2017). These problems are exacerbated in the Arctic because annually-resolved records (ice cores, tree rings and varves) are spatially limited and non-annually resolved records often lack the temporal resolution to address decadal- or centennial-scale climate variability. Consequently, there are currently large gaps in our understanding of regional climate variability across the Arctic, particularly in the Canadian Arctic Archipelago and Siberia. Previous studies have demonstrated the value of pollen-based temperature reconstructions to understand climate variability in the Canadian Arctic (Gajewski, 2015b; Peros & Gajewski, 2009), but none have produced high-resolution reconstructions (<50 years between samples) for the last 2000 years. In this study, we demonstrate that pollen-based reconstructions can capture low and high frequency variability as long as the sampling resolution is fine enough. Since lake sediments are the only archives available in certain regions of the Arctic, such as the central CAA, using pollen-based reconstructions can provide important information about these data-poor regions.

The climate of the Common Era has been extensively studied, but spatio-temporal differences and forcing mechanisms contributing to the MCA, LIA, and the transition between them, remain under discussion. External forcing mechanisms that have been used to explain the transition from the

MCA to the LIA include changes in orbital position and total solar irradiance (TSI; Bond et al., 2001; Goosse et al., 2012; Kaufman et al., 2009), sustained explosive volcanism and associated feedbacks (i.e. sea ice and ocean circulation shifts; Andres & Peltier, 2016; Miller et al., 2012; Schleussner & Feulner, 2013; Schurer et al., 2014; Zhong et al., 2011), and variations in greenhouse gases (GHGs; Schurer et al., 2014; Servonnat et al., 2010). The relative contributions of each forcing factor over time is still under study. For example, Andres and Peltier (2016) suggested TSI and volcanism were the most important factors to explain the MCA and LIA, whereas Schurer et al. (2014) argued TSI had only a weak influence on the climate of the last 1000 years and variability was instead driven by volcanism and GHGs. The issue is further complicated by associated feedbacks and the response of internal climate dynamics to changes in external forcing. Centennial and decadal climate variability has been commonly linked to ocean-atmosphere interactions, particularly in the North Atlantic (Goosse et al., 2012; Goosse & Renssen, 2006; Mignot et al., 2011; Trouet et al., 2009). Volcanism has been associated with changes in the Atlantic Meridional Overturning Circulation (AMOC; Church et al., 2005; Iwi et al., 2012; Stenchikov et al., 2009; Zhong et al., 2011) and may affect the phases of the North Atlantic Oscillation (NAO; Ortega et al., 2015; Trouet et al., 2009). Attribution studies have suggested internal variability may be more important in explaining the MCA, whereas the LIA and modern warming may be largely explained by external forcing (Goosse et al., 2012; Schurer et al., 2013). In order to understand the impacts of internal and external forcing on the climate, robust reconstructions and maps of the timing, amplitude, and spatial characteristics of climate variability are needed.

Current large-scale reconstructions characterize the climate of the last 2000 years by a long-term cooling trend with periods of centennial and decadal climate variability, including the Medieval

Climate Anomaly (MCA; 950-1250CE) and the Little Ice Age (LIA; 1500-1800CE) and the Early Twentieth Century Warming (ETCW; 1920-1940). Although the long-term cooling is documented throughout the Northern Hemisphere, there are regional differences in intensity as well as spatio-temporal heterogeneity in the manifestation of the MCA and LIA (Graham et al., 2011; Mann et al., 2009; PAGES2k, 2013).

There have been several paleoclimate reconstructions of the Common Era for the Arctic region (Hanhijärvi et al., 2013; Kaufman et al., 2009; McKay & Kaufman, 2014; Nicolle et al., 2018; Overpeck et al., 1997; Shi et al., 2012; Tingley & Huybers, 2013; Werner et al., 2018), but these have been primarily based on ice core, tree ring, and varve records since these can be annually-resolved. Although most of the reconstructions show similar trends, there are differences in amplitude and timing of major variability. Kaufman et al. (2009) published a circum-Arctic, decadally-resolved summer temperature reconstruction that showed minimal climate variability before 20th century warming. Shi et al. (2012) found a strong signal of the MCA in a reconstruction of summer temperature from 900-1100 CE and relative cooling from 1200-1900 CE punctuated by warm periods from 1470-1510 CE, 1550-1570 CE and 1750-1770 CE. Hänhijarvi et al. (2013) reconstructed annual temperatures for the North Atlantic region, which tends to have the most consistent record of the MCA and LIA (Hanhijärvi et al., 2013; Miller et al., 2010). The study showed a greater amplitude of warming during the Roman Warm Period (~250 BCE-400 CE) and the MCA. Hänhijarvi et al. (2013) found the MCA occurred from 800-1200 CE and the LIA lasted from 1250-1900 CE. McKay and Kaufman (2014) reconstructed annual temperatures in the Arctic and obtained results similar to other reconstructions for the area. Their reconstruction showed MCA warming beginning ~930 CE, followed by a gradual cooling to ~1800 CE. The amplitude of the LIA cooling trend is greater than in other reconstructions, which is likely because it is a

reconstruction of annual temperature rather than summer temperature. Nicolle et al. (2018) adopted a regional approach to study climate variability in the Arctic and subarctic and found regional differences with the timing and length of the MCA and LIA. The authors found that MCA warming was ~200-250 years long and began between 900 and 950 CE in Siberia, between 900 and 1000 CE in Alaska, and between 800 and 1050 CE in the North Atlantic and ended between 1100 and 1550 CE. Contrary to other studies, they found the LIA was more spatially and temporally variable than the MCA, with its length ranging from 100 to 700 years, start dates ranging between 1200 and 1770 CE and end dates ranging between 1530 and 1930 CE. Werner et al. (2018) found a pronounced MCA from 920-1060 CE and two periods of centennial-scale cooling from 1100-1450 CE and 1600-1900 CE that they identified as the LIA.

Although there are broad-scale similarities between these reconstructions, there are important differences in the timing and magnitude of the reconstructed conditions. This is probably due to the kinds of records used (whether they preserve all frequencies accurately), the reconstruction method applied, and the still sparse distribution of sites. Reconstructions based solely on annually-resolved records may lose low frequency variations (Christiansen & Ljungqvist, 2017; E. R. Cook et al., 1995; Xing et al., 2016), and are limited to specific regions of the Arctic. Pollen and chironomid records from lake sediments are frequently used to reconstruct past climates of the Holocene (Clegg et al., 2011, 2010; Gajewski, 2015b; Luoto & Helama, 2010; Peros & Gajewski, 2009; Rolland et al., 2009); however, dating uncertainties are greater resulting in less precise chronologies. The geographical distribution of the proxy records is sparse, particularly in Siberia and the Canadian Arctic, which can lead to spatial underrepresentation and regional biases when attempting large-scale temperature reconstructions (Christiansen & Ljungqvist, 2017).

This study presents a new quantitative temperature reconstruction for the last 1000 years from Prince of Wales Island, Nunavut, based on fossil pollen assemblages. Pollen records preserve low frequency variability, and the high frequencies available from these records are determined by the temporal resolution of the sampling along the core. There are no quantitative records from this region, so these new data provide information about this understudied region. We also combine these data with others from the literature and analyze long-term and centennial climate variability based on existing proxy records across the Arctic.

4.2 Site Description

Prince of Wales Island is located in the central High Arctic, Nunavut, Canada. Lake SW08 (unofficial name; 72.3177, -97.2678, 104 masl; Figure 4.1) is located in a drumlin field ~20 km inland from the eastern coast of Prince of Wales Island. The lake has an area of ~128 850 m^2. Although the site is located primarily on sandstone bedrock, glacial activity likely deposited carbonate-rich till throughout the area (Dyke & Morris, 1988). The vegetation is defined as a dry prostrate-shrub tundra (Walker et al., 2002). The nearest weather station is 275 km to the northeast in Resolute Bay, Nunavut where the mean July temperature (1948-1980) 4.2 ± 1.2°C (Environment and Climate Change Canada, 2018b).

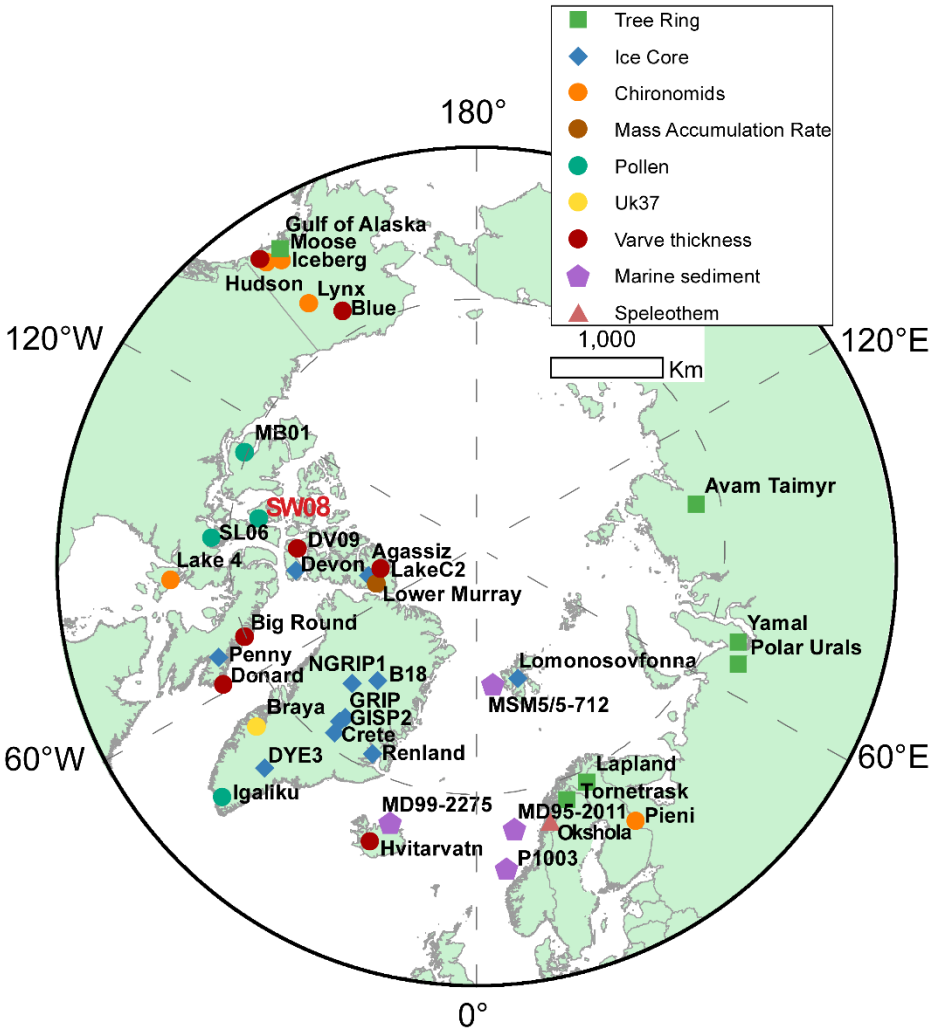

Figure 4.1: Map of sites with paleoclimate reconstructions of the past 1000-2000 years used in this study. Lake sediment records are denoted by a *circle* and colour-coded by proxy type. Records were obtained from the literature (Table 4.A1), except for site SW08 (red text), which is described here.

4.3 Methods

A sediment core was extracted from Lake SW08 in July 2017 using a plastic tube fitted with a piston. The sediment-water interface was preserved in the tube by adding sodium polyacrylate, and the core was shipped back to the University of Ottawa and refrigerated at 4°C.

In the laboratory, the core was extruded and changes in stratigraphy, texture, and colour were noted. Loss-on-ignition was measured at 0.5 cm intervals using a LECO Thermogravimetric Analyser to estimate weight percent organic and carbonate contents. Samples throughout the core were analyzed for biogenic silica using a wet chemical digestion technique (Conley & Schelske, 2001; DeMaster, 1981; Parsons, 1984). Sediment samples were digested in 1% sodium carbonate (Na_2CO_3) for 5 hours in an 85°C water bath. Subsamples were taken at 2, 3, 4, and 5 hours and analyzed using spectrophotometry. Reference samples of known BSi content were processed alongside each batch to ensure experimental control.

Fossil pollen was analyzed at 0.5 cm resolution, where possible, from the top 25 cm of the core. Pollen was extracted using a heavy-liquid separation technique (Zabenskie et al., 2006). Two cubic centimeters of sediment were subsampled and two *Lycopodium* tablets (batch #938934; 53,394±953/5 tablets) were added to enable the estimation of the absolute concentration of pollen and spores. Samples were washed in 10% HCl and 10% KOH prior to heavy-liquid separation using sodium polytungstate (SPT; density: 1.9 g/cm^3). The samples were then treated with HF and acetolysis before being transferred to vials with silicone oil (2000 cs) for permanent storage. At least 300 grains were counted for each level, except at 0.5, 1.5, 6, 8, and 12.5 cm where pollen concentrations were too low to reach 300 grains. In two cases, at 10 and 16.5 cm, there was no material left to count after processing.

4.3.1 Chronology

The core was dated using ^{210}Pb for the uppermost sediments and ^{14}C for the remainder of the core. Eight bulk sediment samples were processed by MyCore Scientific Inc. (Ottawa, Ontario) to analyze the ^{210}Pb activity and ages were determined using a constant rate of supply model (CRS). There was no terrestrial material present in the cores, so six 0.5 cm samples of aquatic moss fragments were sent to Andre E. Lalonde Accelerator Mass Spectrometry Laboratory at the University of Ottawa for ^{14}C analysis. The results were calibrated using OxCal v4.2.4 (Bronk Ramsey, 2009) and the IntCal13 calibration curve (Reimer et al., 2013).

4.3.2 Numerical analyses and Climate Reconstruction

Arctic samples often contain several pollen types that have been transported from the boreal or other forest regions. These long-distance taxa were removed from the pollen sums prior to calculating percentages to ensure the reconstruction was not influenced by boreal or more southern plant communities. Three sums were calculated for the pollen stratigraphic diagrams: (1) pollen sums based on only local and regional pollen, (2) based on the entire assemblage (excluding *Pediastrum* and aquatics), and (3) based on the entire assemblage including aquatics and *Pediastrum*. The third sum was only used to compare *Pediastrum* to the pollen assemblages in Figure 4.4. The pollen assemblages were analyzed using Principal Components Analysis and the scores were grouped based on major periods of climate variability in the Arctic (i.e. MCA, LIA; Ljungqvist, 2010) to examine the how the vegetation was altered during each period.

Mean July temperatures were reconstructed from the pollen data using the modern analogue technique (MAT; Sawada, 2006). The training set used for calibration included Arctic samples from Gajewski (2015b), which were obtained from the North American Modern Pollen Database (Whitmore 2005). The calibration set contained local and regional taxa but excluded pollen

transported from south of the Arctic (Table 4.1). The average of the closest three analogs was used to estimate past July temperatures and the squared chord distance between the fossil and all modern samples was analyzed to determine if the fossil level had a good analog.

The reconstruction for Lake SW08 was compared to existing records from the Arctic 2k Database (version 1.1.1; McKay & Kaufman, 2014) and from primary sources (Courtney Mustaphi & Gajewski, 2013; Lecavalier et al., 2017; Peros & Gajewski, 2009). For this analysis, only records that contained data between 1000 and 1960 CE were retained. The new dataset prepared for this study contains 11 ice core, 18 lake sediment (eight varve, five chironomid, four pollen, and one U^{k}_{37} alkenone), four marine sediment, one speleothem, and six tree ring records (Appendix Table 4.A1). To enable comparison between records, those with non-annual resolution were interpolated to 10-year intervals and 10-year block means were calculated for records with annual resolution. Although interpolation will inflate the explained variance of statistical analyses, the dominant trends and relationships should be unaffected. Each record was truncated to the common time period for which all records contained data (1090-1960 CE) then standardized by subtracting the mean and dividing by the standard deviation. Principal Components Analysis (PCA) was then used to summarize these data and groups were established using cluster analysis with a Euclidean distance measure and Ward's method of clustering. A second PCA was performed using only records with data covering all of the last 2000 years (10-1960 CE). Each record was again standardized relative to the mean and standard deviation for the entire period and clusters were established as above.

Table 4.1: Pollen taxa used for MAT reconstructions and others identified in core SW08. The local and regional taxa were used in the MAT temperature reconstruction. Taxa denoted with an asterisk (*) were part of the training set but were not found in the core.

Local and Regional	
Betula	*Saxigfraga oppositifolia*
Alnus	Saxifragaceae undiff
Salix	Polygonaceae undiff
Ericaceae	Ranunculaceae undiff
Artemisia	*Thalictrum**
Caryophyllaceae	Rosaceae undiff
Chenopodiaceae	Potentilla*
Brassicaceae	*Rubus chamaemorus*
Asteraceae	*Lycopodium annotinum**
Cyperaceae	*L. clavatum**
Dryas	*L. selago**
Poaceae	*Lycopodium* undiff
Leguminosae*	*Selaginella*
Oxyria	Polypodiaceae*
Papaver	*Equisetum*
*Pedicularis**	*Sphagnum*
Long Distance	
Picea undiff	
Abies	
Pinus	
Populus	
Carpinus/Ostrya	
Juglans	
Acer	
Juniperus	
Fraxinus	
Morus	
Celtis	
Corylus	
Ulmus	
Urtica	

4.4 Results

4.4.1 Sedimentary stratigraphy and characteristics

The sediment in core SW08 (Figure 4.2) was very dark grey (10YR 3/1) in the top 7 cm (1900-2017 CE) then became mottled with dark yellowish brown (10YR 3/4) sediment until 12 cm (1650-1900 CE). From 12 to 32 cm the sediment was uniformly dark yellowish brown (10YR 3/4). Below 32 cm, the sediment was dark greyish brown (10YR 4/2). Organic matter was low throughout the core, never exceeding 6%, and carbonate percentages were high, ranging between 22% and 27%. Nineteen samples were analyzed for biogenic silica along the core, but no values above detection were measured.

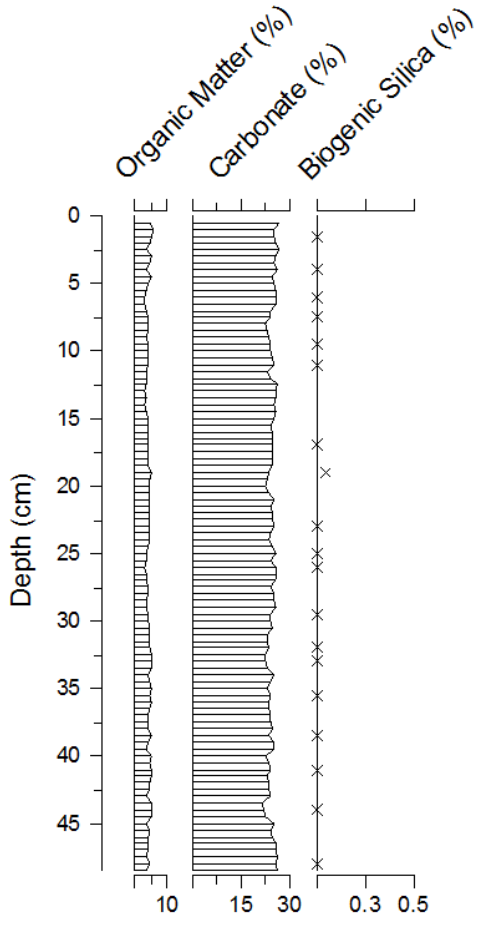

Figure 4.2: Sedimentary characteristics of core SW08 plotted against depth.

4.4.2 Chronology

The unsupported ^{210}Pb activity in the uppermost sediment was 134 Bq/kg and reached the supported level of 64 Bq/kg by 3.25 cm at 1962 CE (Table 4.2). The six ^{14}C dates included one anomalously old age and two age reversals at 12, 37 and 45 cm, respectively, which were excluded from age-depth modelling (Table 4.3). The resulting age-depth model was created by linear interpolation of eight ^{210}Pb and three ^{14}C dates; however, this only established a reliable chronology for the top 25 cm of the core (1082 CE). The age-depth curve (Figure 4.3) shows an unusually large sedimentation rate between 10 and 15 cm. Results such as this are frequently seen in Arctic sediments (Gajewski et al., 2000; MacDonald et al., 1991; Peros & Gajewski, 2009) and suggest a reservoir effect due to hardwater. Following Peros and Gajewski (2009), a hardwater correction was estimated by calculating the intercept of a linear regression of the accepted radiocarbon dates. The estimated hardwater correction for core SW08 is 856 years, which was subtracted from the remaining radiocarbon dates to generate an age-depth model whose oldest date at 25 cm is 1082 CE (Figure 4.3).

Table 4.2: ^{210}Pb results and ages based on constant-rate-of-supply (CRS) model.

Midpoint Depth (cm)	Unsupported Activity (Bq/kg)	Year CE	CRS Error (years)
0.0	134.78	2017	0
0.25	78.22	2015	0.23
0.75	132.24	2011	0.72
1.25	137.3	2004	1.25
1.75	152.96	1993	2.12
3.25	18.89	1962	7.23
6.25	12.73	1920	17.90
8.25	0.00	1880	19.11
8.75	22.39	N/A	

Table 4.3: Radiocarbon results and hardwater-corrected dates. Asterisk (*) indicates dates rejected and not used in developing the chronology. All dates were measured on aquatic mosses extracted from the sediment. Samples were calibrated using OxCal v4.2.4 (Bronk Ramsey, 2009) and the IntCal13 calibration curve (Reimer et al., 2013).

Lab ID	Depth (cm)	^{14}C yr BP	Error (+/-)	2σ cal BP range	Median cal BP	Hardwater-corrected median cal BP
*UOC-5309	12-13	1961	29	1830-1989	1909.5	N/A
UOC-5310	15-16	1449	26	1300-1385	1342.5	486.5
UOC-5311	19-20	1647	24	1441-1613	1527	671
UOC-5312	25-26	1812	34	1623-1825	1724	868
*UOC-5313	37-38	1756	24	1600-1727	1663.5	N/A
*UOC-5314	45-46	1710	24	1556-1696	1626	N/A

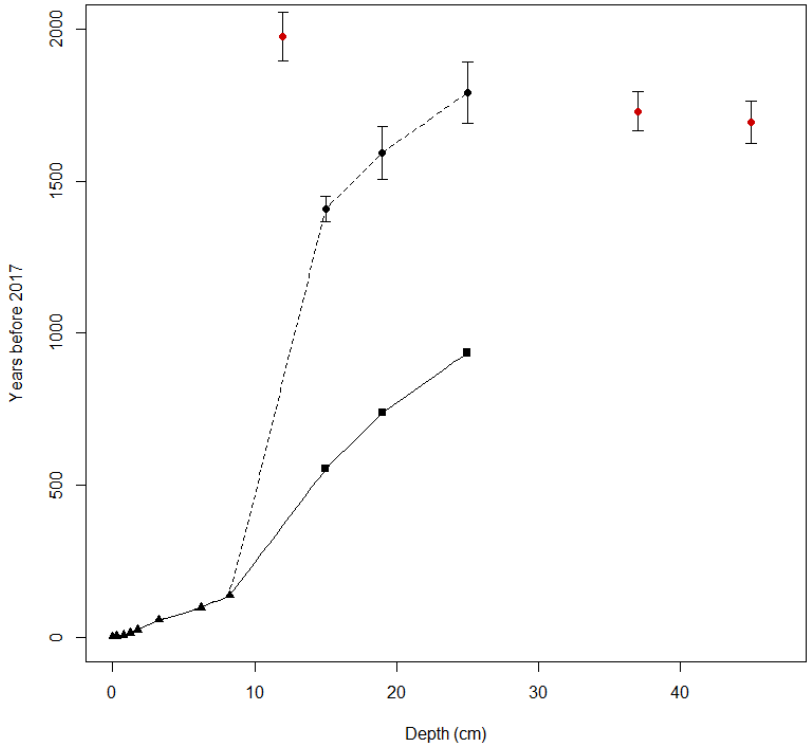

Figure 4.3: Age-depth curve for core SW08. *Triangle*s are ^{210}Pb ages; *Circles* are the ^{14}C median calibrated dates with 2σ age range; *red circles* are ^{14}C dates rejected from age-depth model; *Squares* are hardwater-corrected ^{14}C dates (see text for details). *Solid line* represents the corrected age-depth model; *dashed line* is the age-depth model without hardwater correction.

4.4.3 Pollen stratigraphy

The local and regional pollen (Figure 4.4) were dominated by Cyperaceae, Poaceae and *Salix*. At the bottom of the core Cyperaceae pollen dominated, comprising up to 80% of the assemblage. The general trend of Cyperaceae was a decrease to the present, while Poaceae percentages increased. Both Cyperaceae and Poaceae percentages decreased in the uppermost 5 cm (1930-2017 CE), concurrent with an increase in both *Betula* and *Salix*. Other local taxa, such as *Dryas*, *Oxyria*, *Papaver*, and *Saxifraga oppositofolia*, were present but the percentages were low (<5%). The *Oxyria* curve was similar to that of Poaceae, but with a lower amplitude of change.

Pollen transported from forested areas in the south (long-distance pollen), such as *Pinus* and *Picea*, remained relatively constant throughout the core (Figure 4.5). *Betula*, which probably originated from the Low Arctic tundra, showed a similar trend as *Salix*, with a rapid increase in uppermost 2 cm (1970-2017 CE).

Pollen concentration fluctuated between 2000 and 4000 grains cm^{-3} during the period between 1080-1700 CE. Concentration was highest in the 1800s CE, corresponding to an increase in Poaceae and decrease in Cyperaceae, then decreased for the last 100 years. Pollen accumulation rate (grains cm^{-2} yr^{-1}) was highest in the earliest samples (1080-1250 CE), then low until 1885 CE where it increased until the present (Figure 4.5).

The green coccal algae *Pediastrum* was present throughout the core, and comprised mainly of the species *P. boryanum var. longicorne*. Percentage (computed using a sum of all pollen, spores, and *Pediastrum*) was generally low, averaging around 8%, then increased between 6 and 12 cm (1650-1920 CE). The increase, which peaked at 30% at 8 cm (1885 CE), occurred during a decrease in Cyperaceae and increase in Poaceae. Tardigrade eggs were also present throughout the core; however, no pattern of change was observed and they were not enumerated.

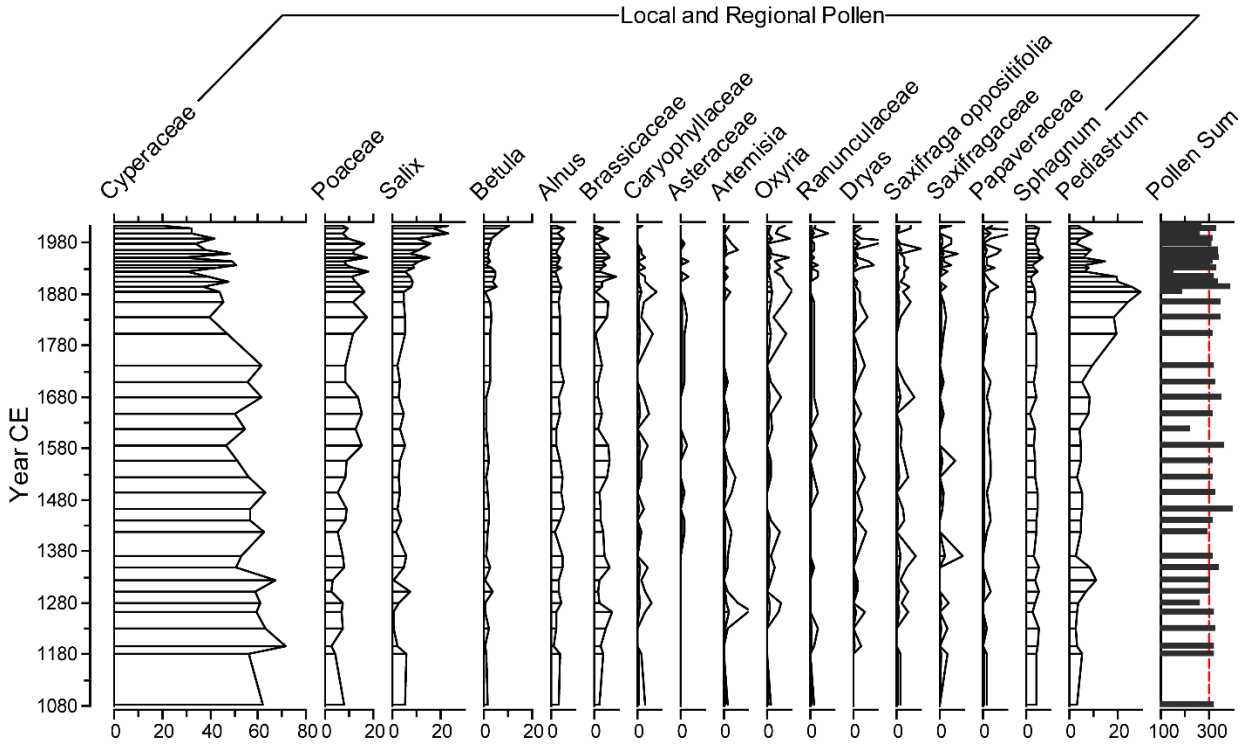

Figure 4.4: Local and regional pollen in core SW08. The second line in the curves of the rarer taxa is a 5x exaggeration. The pollen sum used for calculating percentages included only the local and regional taxa, although the numbers in the final column include all pollen and spores counted. The sum used to calculate the percentage of *Pediastrum* included all pollen, spores, and *Pediastrum*.

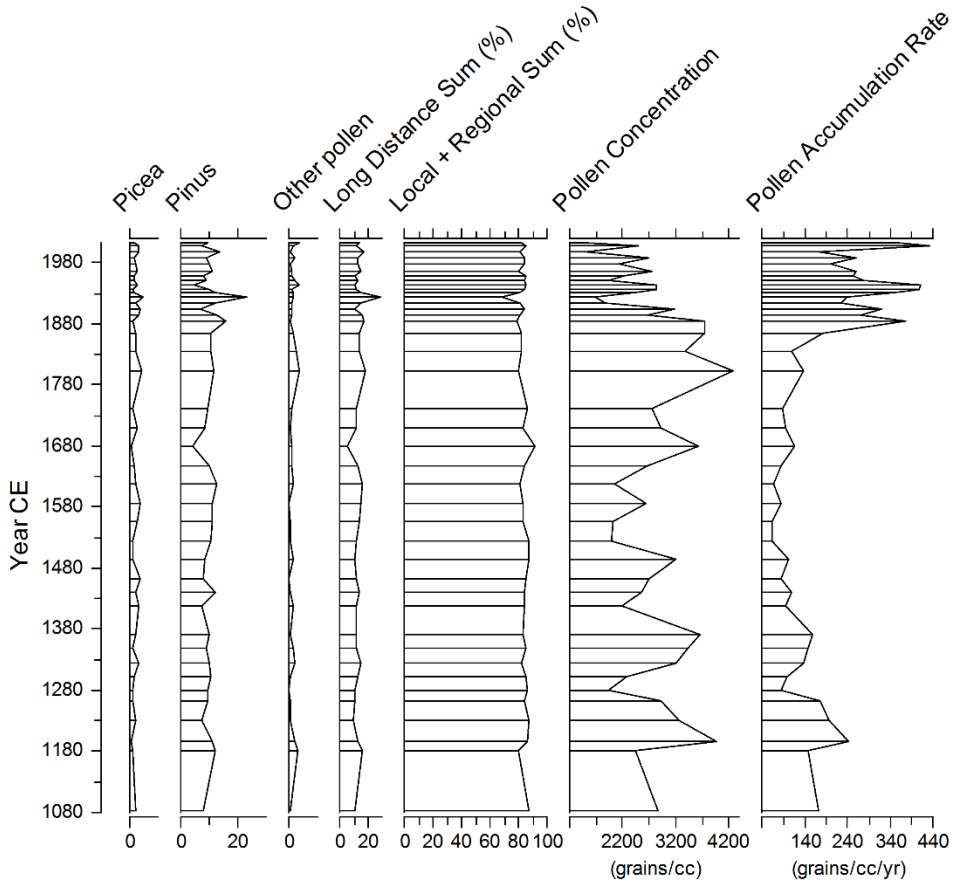

Figure 4.5: Long-distance pollen percentages, pollen concentration and accumulation rates for core SW08. Sums were calculated based on entire pollen assemblage (local, regional and long-distance).

4.4.4 Ordination of pollen assemblages from SW08

The pollen stratigraphy was analyzed with a principal components analysis of all taxa included in the July temperature reconstruction. Component 1 explains 42.5% of the variance and component 2 explains 11% (Figure 4.6). Cyperaceae is positively correlated, while *Salix* and *Betula* are both negatively correlated with the first axis. Brassicaceae and Poaceae are both positively correlated with the second axis. The scores of the first component were positive until the last 200 years and negative thereafter. The scores show a temporal separation on the biplot. Scores from the MCA and late 20th /21st century were negative on the second component and positive (MCA) or negative (20th century) on the first component. Scores from 1500 – 1980 CE tended to be positive on the second component.

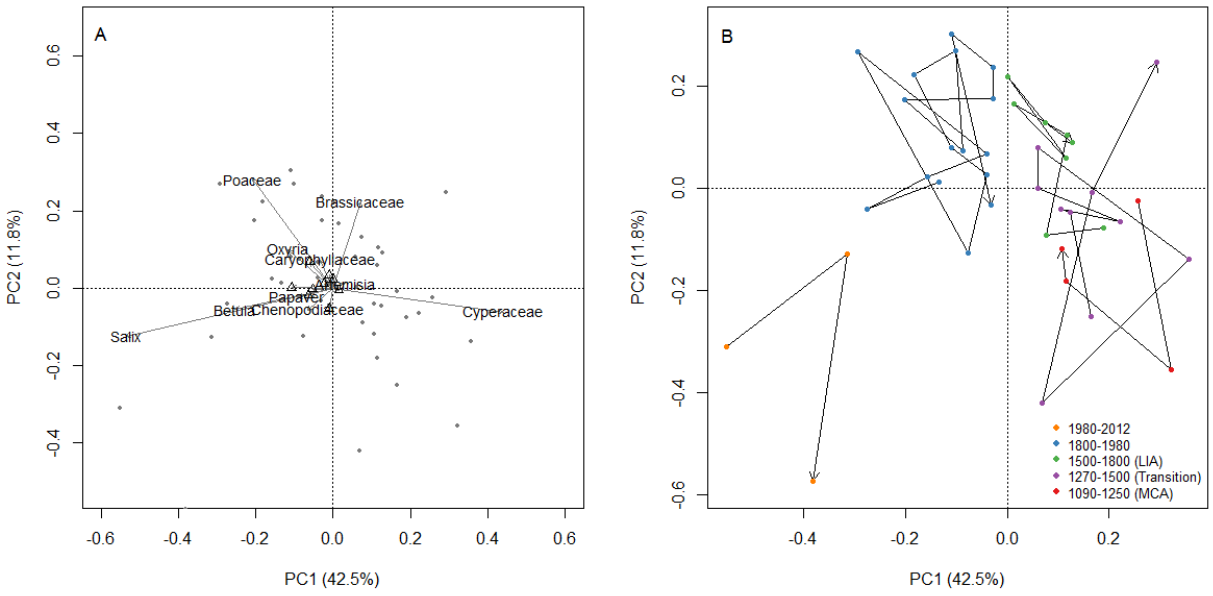

Figure 4.6: Principal components (PCA) biplots for SW08 pollen assemblages. Only taxa used in the MAT reconstruction (Table 4.1) were included in the PCA. Panel (A) shows the loadings and (B) shows the scores grouped by major periods of climate variability in the Arctic (i.e. MCA, LIA; Ljungqvist, 2010).

4.4.5 Climate Reconstruction

Reconstructed July temperatures ranged from 4.3 to 8.2°C and showed a cooling trend from 1080-1915 CE and with lowest temperatures (4.3°C) reconstructed between 1800 and 1915 CE. Temperatures rose over the last 100 years to between 5 and 6°C (Figure 4.7).

Gajewski (2015b) determined that a good analog has a dissimilarity value of less than 0.2 in the modern dataset used for these analyses; in the present study, all fossil levels were considered good analogs (Figure 4.7). The sites chosen as the best analogs were generally from Boothia Peninsula (n=24), Banks Island (n=12), and Somerset Island (n=5). One analog was found on Baffin Island and one on Cornwallis Island.

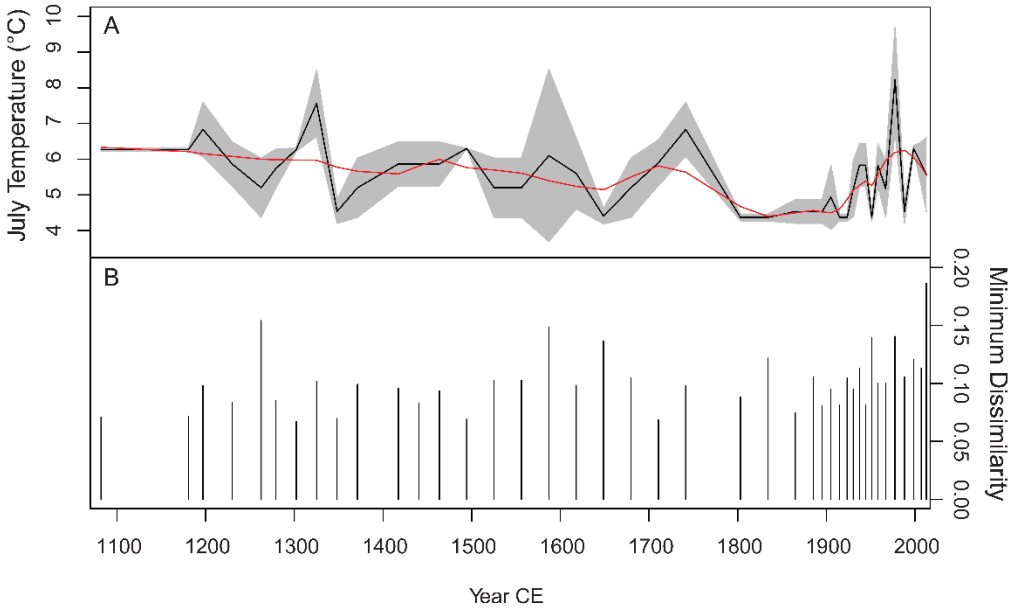

Figure 4.7*:* (A) Reconstructed July temperatures using the modern analog technique (MAT) from fossil pollen assemblages in core SW08. Solid black line is the average of the 3 best analogs. Grey shaded area is the standard deviation of the 3 analogs and the red line is a loess curve (span = 0.25) fitted to the reconstruction. (B) Minimum dissimilarity (squared-chord distance) between fossil and associated modern sample.

4.5 Discussion

4.5.1 Environmental Change on Prince of Wales Island, Nunavut

As is typical in the Arctic, the sediment core from SW08 was inorganic and sedimentation rates were low. This led to difficulties establishing a chronology, which was further complicated by the likely presence of a freshwater reservoir effect due to hardwater. Applying a reservoir correction was deemed appropriate for this site to enable the derivation of a reasonable chronology. The reservoir correction calculated here is consistent with others for Arctic (e.g. MacDonald et al., 1991; Peros & Gajewski, 2009; Snyder et al., 1994) and temperate lakes (e.g. Ascough et al., 2011; Philippsen, 2013; Zhou et al., 2015).

The pollen assemblages were dominated by herbaceous taxa Cyperaceae and Poaceae, but also contained smaller percentages of Brassicaceae, Caryophyllaceae, *Artemisia*, *Oxyria*, and *Saxifraga oppositifolia*. Gajewski (2002) described regional differences between High Arctic assemblages, which were dominated by Poaceae, Caryophyllaceae, and *Papaver*, and Middle Arctic sites dominated by Cyperaceae and *Artemisia*. The decrease in Cyperaceae and increase in Poaceae at this site therefore suggests a shift from warmer to colder conditions. This change is further supported by changes in less abundant taxa, such as the increase in Caryophyllaceae and *Oxyria* observed throughout the core.

A principal components analysis summarizing the local and regional pollen data (Figure 4.6) showed clear changes in vegetation composition over time roughly corresponding to periods of climate variability that have been reconstructed for the circum-Arctic region (Kaufman et al., 2009; McKay & Kaufman, 2014; Nicolle et al., 2018; Overpeck et al., 1997; Shi et al., 2012; Werner et al., 2018). Samples corresponding to the MCA (~1090-1250 CE) and LIA (~1500-1800 CE) formed two groups on the PCA biplot and those corresponding to the transition period (~1270-

1500 CE) overlap these zones. Samples representing the post-LIA (1800-1980 CE) are grouped together, suggesting a sustained period when the vegetation was characteristic of the High Arctic. In the samples representing 1980-2012 CE the vegetation was dominated by *Salix* and *Betula*, which is a change that is unprecedented in relation to the last 1000 years.

Reconstructed temperatures were similar (5.8-6.3°C) during the two warm periods (1090-1250 and 1980-2012 CE); however, the vegetation composition was not the same. The earliest samples, which may correspond with the end of the MCA, were dominated by Cyperaceae, while samples from the last 100 years saw an increase in *Salix* and *Betula*. It is unclear what caused the differences observed in the vegetation. Several studies have discussed the impacts of modern warming on Arctic vegetation, particularly in relation to the northward expansion of shrubs such as *Alnus*, *Betula*, and *Salix* (Myers-Smith et al., 2011; Post et al., 2009; Tape et al., 2006). *Salix* currently grows on Prince of Wales Island and has likely become more abundant with warming temperatures as documented elsewhere in the Arctic (Hill & Henry, 2010). *Alnus* and *Betula* do not presently grow on Prince of Wales Island but their increased production in the south could cause more pollen to be transported to the High Arctic. The increase in shrubs over the last 30 years may also be related to precipitation or hydrological changes. Unfortunately, precipitation reconstructions are less reliable and there are currently no comprehensive analyses of Holocene precipitation across the Arctic (Briner et al., 2016; Linderholm et al., 2018; Miller et al., 2010). Moreover, precipitation patterns are more spatially variable than temperature because they are primarily controlled by cyclonic activity, topography, and atmospheric circulation (Edlund & Alt, 1989). Most regions of the Arctic have experienced increased precipitation over the last 30 years (Hinzman et al., 2005), which may contribute to the increase in *Salix* and *Betula*. However, increased precipitation would also benefit Cyperaceae. Experimental studies have highlighted the spatio-temporal heterogeneity

of the response of tundra communities to warming (Elmendorf et al., 2012) and the complexity of controls on tundra shrub expansion (Martin et al., 2017). Consequently, without high-resolution regional climate reconstructions, it is difficult to attribute any one environmental factor to the difference observed between the vegetation in the two warmer periods.

Colder temperatures in the reconstruction were indicated by changes in both the vegetation and supported by concurrent changes in algal production. Although aquatic productivity could not be assessed using BSi, probably due to post-depositional diatom dissolution (Paull et al., 2017; Ryves et al., 2006), changes in *Pediastrum* were inversely correlated with the July temperature reconstruction. In the pollen data, colder temperatures were reconstructed when Poaceae increased, and in the lake, *Pediastrum* concentration increased when cooler temperatures were reconstructed. The dominant species, *Pediastrum boryanum var. longicorne*, is generally associated with cold, dystrophic waters (Jankovská & Komárek, 2000; Komárek & Jankovská, 2003), so its increase between 1800-1915 CE is consistent with the reconstruction of colder temperatures. Pollen concentration and influx decreased, concurrently with the peak in *Pediastrum* in the late 1800s (Figures 4.4-4.5), suggesting reduced terrestrial productivity. Although few studies have been conducted on the use of *Pediastrum* as a bioindicator, the increase in algal abundance suggests within lake processes altered at the same time as vegetation change occurred during the Little Ice Age.

4.5.2 High temporal-resolution pollen-based reconstructions from the CAA

There are several pollen-based temperature reconstructions in the Canadian Arctic spanning the entire Holocene and these have been recently quantitatively analyzed by region (Gajewski, 2015b). Although previous studies produced longer records (up to 10 000 years ago), the results from Lake SW08 are the only reconstruction with high-resolution data (<50 years between samples) for the

Common Era. Other reconstructions with a temporal resolution of less than 100 years between data points (SL06 and MB01, Peros & Gajewski, 2009; JR01, Zabenskie & Gajewski, 2007) showed some between-site congruence with SW08 (Figure 4.8). Two of the sites (SW08 and JR01) recorded warmer temperatures before 1200 CE and the longer records showed a centennial-scale cooling trend in the Common Era. All four sites reconstructed a relative cooling between 1800 and 1930 CE when temperatures decreased by 0.5-1.5°C from the mean for each record. Although each site experienced a cold period of similar amplitude, the duration varied between sites. SW08 and SL06 recorded a longer sustained cold period from 1800-1930 CE and 1775-1950 CE, respectively. At SL06, this period was an intensification of colder conditions that began at ~1100 CE, whereas at SW08 there was more variability prior to 1800 CE. MB01 is out of phase with the other sites, perhaps because it is located in the western Arctic. The timing of climatic events has been previously recorded as being out of phase in the Western Arctic during the early Holocene (Gajewski, 2015b). For example, warmer conditions in the early Holocene occurred earlier in the Western Arctic (10-8 ka) than the Eastern Arctic and Greenland (8-5 ka) and this delay may explain the earlier warmth seen in the first millennium CE at MB01.

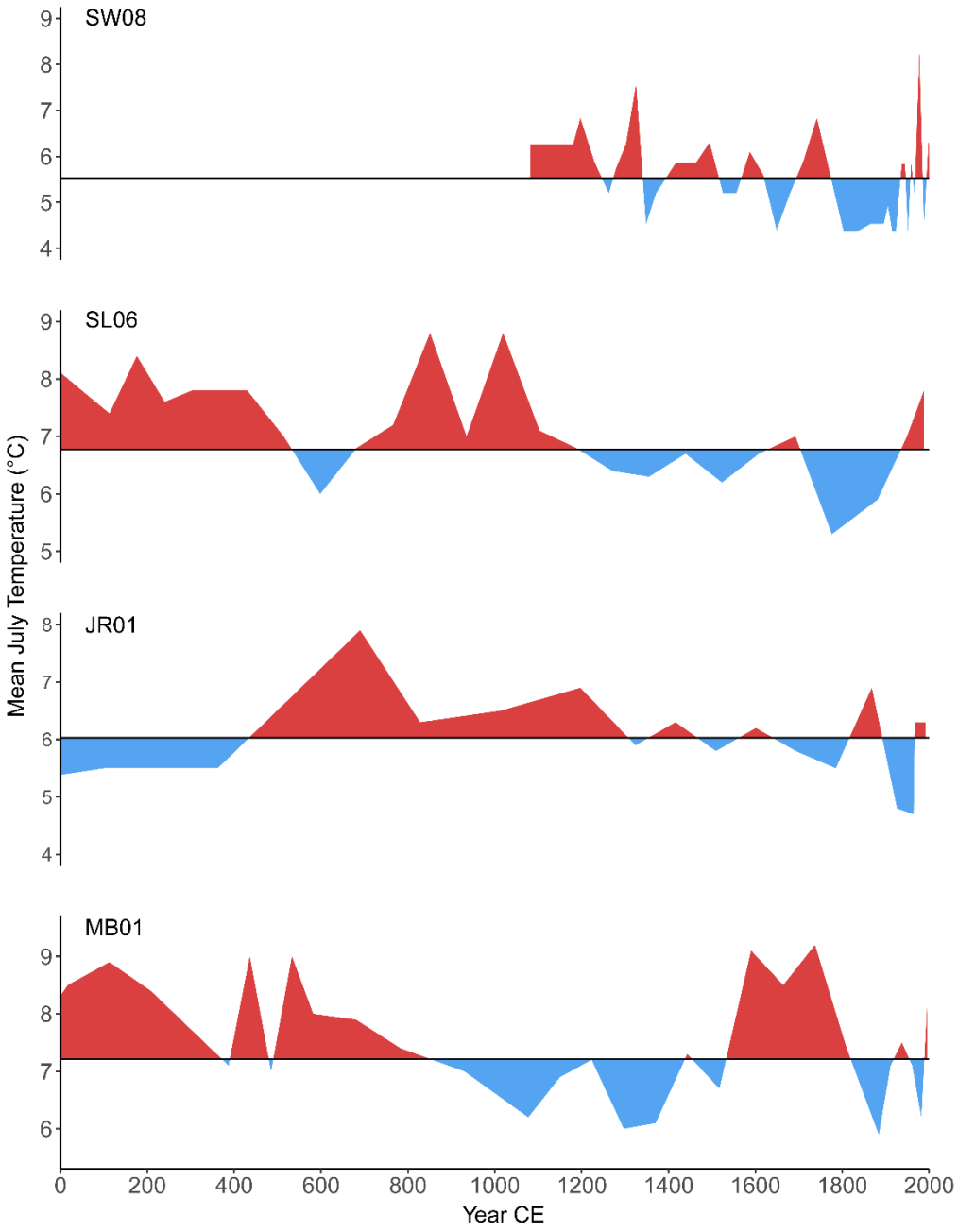

Figure 4.8: Pollen-based temperature reconstructions in the Central and Western Arctic. The horizontal line is the mean for each record based on a reference period from 1000-2000 CE.

4.5.3 Synthesis of circum-Arctic paleoclimate records of the past 2000 years

There has recently been considerable work to reconstruct the climates of the past 2000 years across the circum-Arctic region (Kaufman et al., 2009; McKay & Kaufman, 2014; Nicolle et al., 2018; Shi et al., 2012; Werner et al., 2018). However, the results from these efforts are significantly affected by data selection and availability, as well as by the methodologies applied. Using the database compiled for this study, we examined the influence of (1) increasing the spatial coverage of the proxy network, (2) including lower resolution pollen records, and (3) applying different methodologies to similar datasets. We also analyzed the spatial patterns of the dominant trends observed in the proxy records.

To study climate variability across the entire Arctic, records were compiled by the Past Global Changes (PAGES) Arctic 2k working group. The database consists of 56 proxy records (version 1.1.1; McKay and Kaufman, 2014), of which 35 are annually-resolved. There are strict conditions for records to be included in the database, which reduces potential error but also excludes useful information and results in the underrepresentation of some regions of the Arctic. Furthermore, annually-resolved records, typically tree rings, ice cores and varves, are restricted to certain regions and reconstructions based on only these proxies may introduce bias (Birks & Birks, 2006; Christiansen & Ljungqvist, 2017). Despite chronological limitations, lake sediments are the only archive with spatial representation across the entire Arctic and so should be included in a synthesis study. Notably lacking from the Arctic 2k database are quantitative pollen-based reconstructions, which is in part due to the low temporal resolution of available records. Here, we update the Arctic 2k database with the addition of three pollen-based reconstructions (SW08, this study; SL06 and MB01, Peros & Gajewski, 2009) and one varve record (DV09; Courtney Mustaphi & Gajewski, 2013) to increase the representation of the CAA in the circum-Arctic reconstruction. We also used

the updated version of the Agassiz ice core record that includes a new quantitative evaluation of the climate signal in these data (Lecavalier et al., 2017).

In this study, we used a similar methodology to Kaufman et al. (2009); the average of the records standardized relative to their common period (1090-1960 CE) was computed. These results were compared to the average for all the records (SD with respect to 980-1800 CE) from Kaufman et al. (2009) to analyze the influence of adding more proxy records to the reconstruction (Figure 4.9 A). The curves roughly paralleled each other during the last 500 years, but diverged slightly prior to 1500 CE. Although the differences are subtle, the average from this study tends to be warmer than the Kaufman (2009) average, except during the LIA.

The database assembled for this study was similar to that in the McKay and Kaufman (2014) reconstruction, but with additional records from the CAA. The averages of the records with and without those from the CAA were similar until ~650 CE, when the average containing the CAA records became slightly higher (Figure 4.9 B). These results demonstrate that the additional records modify the reconstruction but also preserve the temporal trends despite the chronological errors and lower resolution.

McKay and Kaufman (2014) applied the PaiCo method (Hanhijärvi et al., 2013) to reconstruct circum-Arctic annual temperatures. The results are similar to the average for this study, but applying the PaiCo method produced consistently colder temperatures and higher variance (Figure 4.9 C). However, the PaiCo method does not retain the magnitude of proxy values, so the variance produced may be artificial.

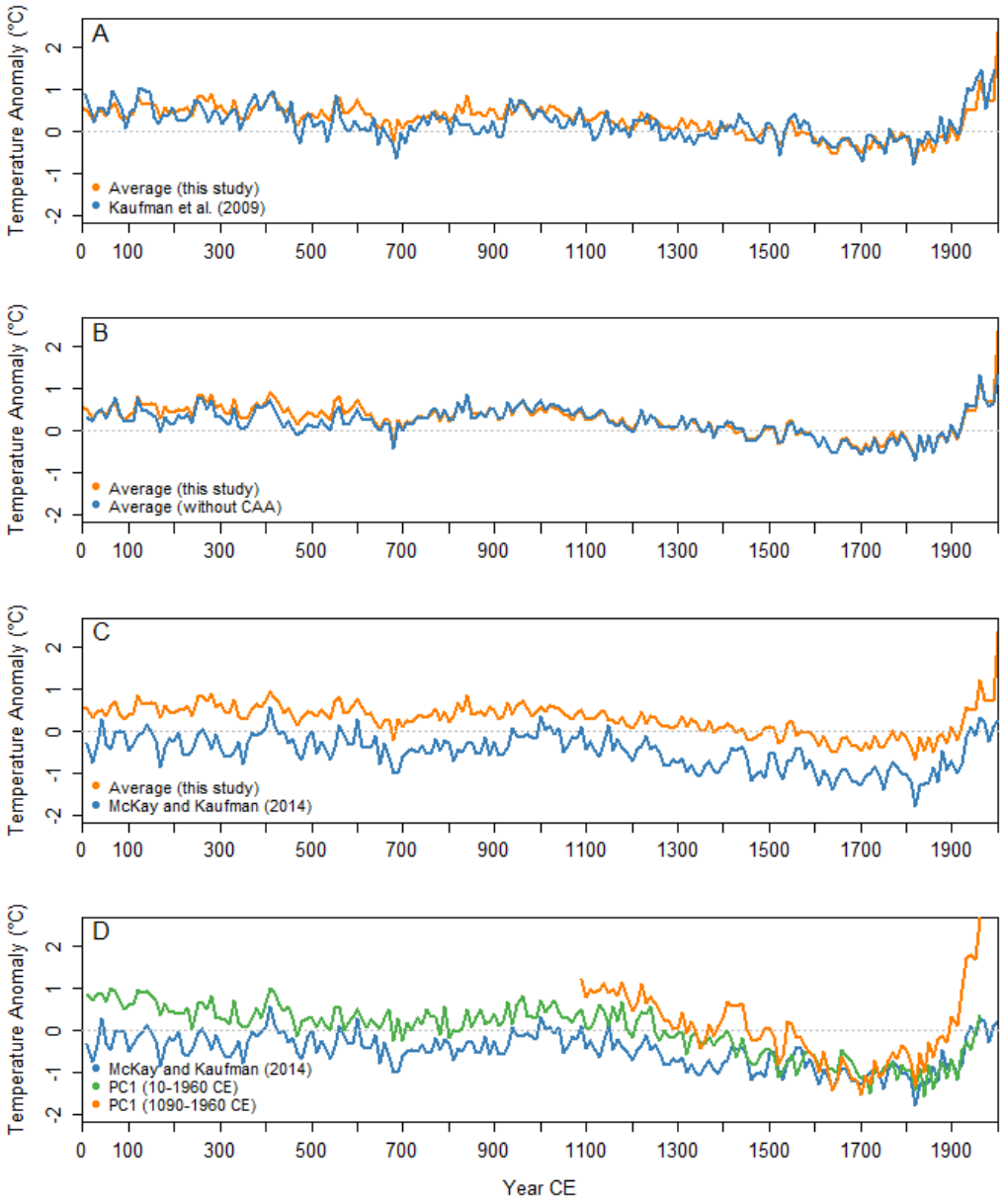

Figure 4.9: (A) Comparison of the average of all the records relative to their common period (1090-1960 CE; orange line) computed for this study and the average for all the records (SD wrt. 980-1800 CE; blue line) from Kaufman et al. (2009). (B) Average for this study with (orange line) and without (blue line) additional records from the CAA. (C) Average for this study (orange line) and the PaiCo reconstruction from McKay and Kaufman (2014). (D) McKay and Kaufman (2014) reconstruction (blue line) compared to the first principal component from both PCA_1 (1090-1960 CE; orange line) and PCA_2 (10-1960 CE; green line).

The available records (Table 4.A1; Figure 4.1) were analyzed using a principal components analysis to determine the spatial and temporal coherence of the data. A first analysis was performed on 40 records that contained data for the past 1000 years (1090-1960 CE; hereafter referred to as PCA_1). The first component of PCA_1 explains 15.5% of the variance, the second 13%, and the third explains 8% (Figure 4.10). The scores were grouped based on a cluster analysis of the matrix of reconstructions using a Euclidean distance dissimilarity measure and Ward's method, which identified four temporal groups: 1090-1260 CE, 1270-1570 CE, 1580-1910 CE, and 1920-1960 CE.

To assess whether the relationships were the same over a longer timescale, a second study (PCA_2) compared records with data for the last 2000 years (10-1960 CE). There were fewer records (n=26) spanning this longer time period: four tree ring, seven ice core, four marine sediment, one speleothem, and 10 lake sediment records (see Table 4.A1 for proxy type). The first component explains 16% of the variance, the second 9.5%, and the third 8%. Four temporal groups were identified by a cluster analysis (same method as above): 10-710 CE, 720-1400 CE, 1410-1910 CE, and 1920-1960 CE.

Despite only explaining 15-16% of the variance, the first principal component in both PCAs are markedly similar to the McKay and Kaufman (2014) reconstruction (Figure 4.9 D). These results could suggest that the dominant circum-Arctic trends are represented in the reconstruction and other variability can be attributed to regional responses. However, the dataset is biased towards the North Atlantic region, and the PCAs revealed spatial and proxy-based patterns in the dominant trends.

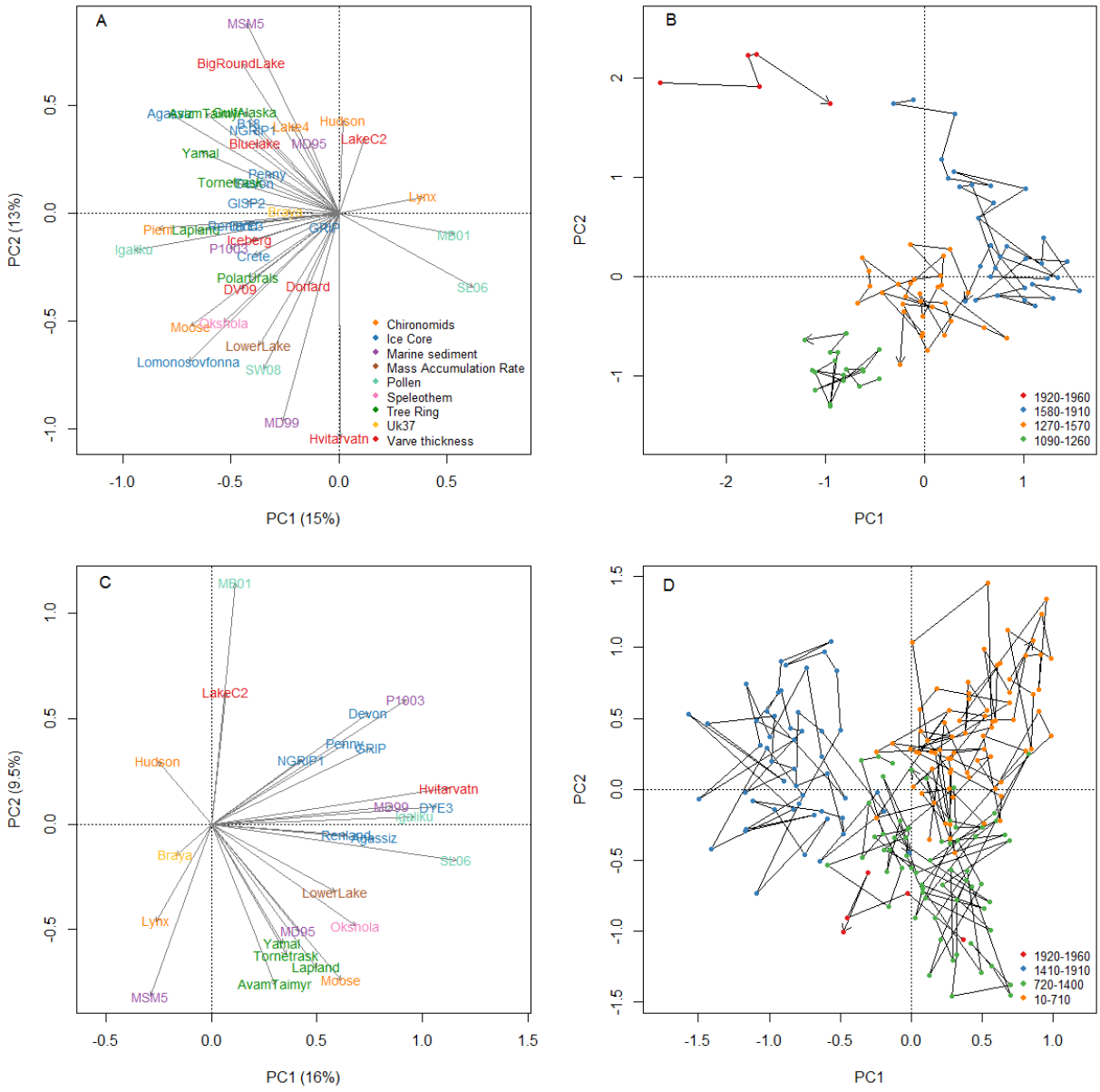

Figure 4.10: Principal components analysis of proxy climate records from the Arctic. (A) Biplot of records from 1090-1960 CE (PCA_1) showing the loadings coloured by proxy type. (B) Scores grouped by clusters established using Ward's method. (C) Biplot of records from 10-1960 CE (PCA_2) showing loadings coloured by proxy type (same legend as in panel A). (D) Scores grouped by clusters established using Ward's method. Note the different axis scales.

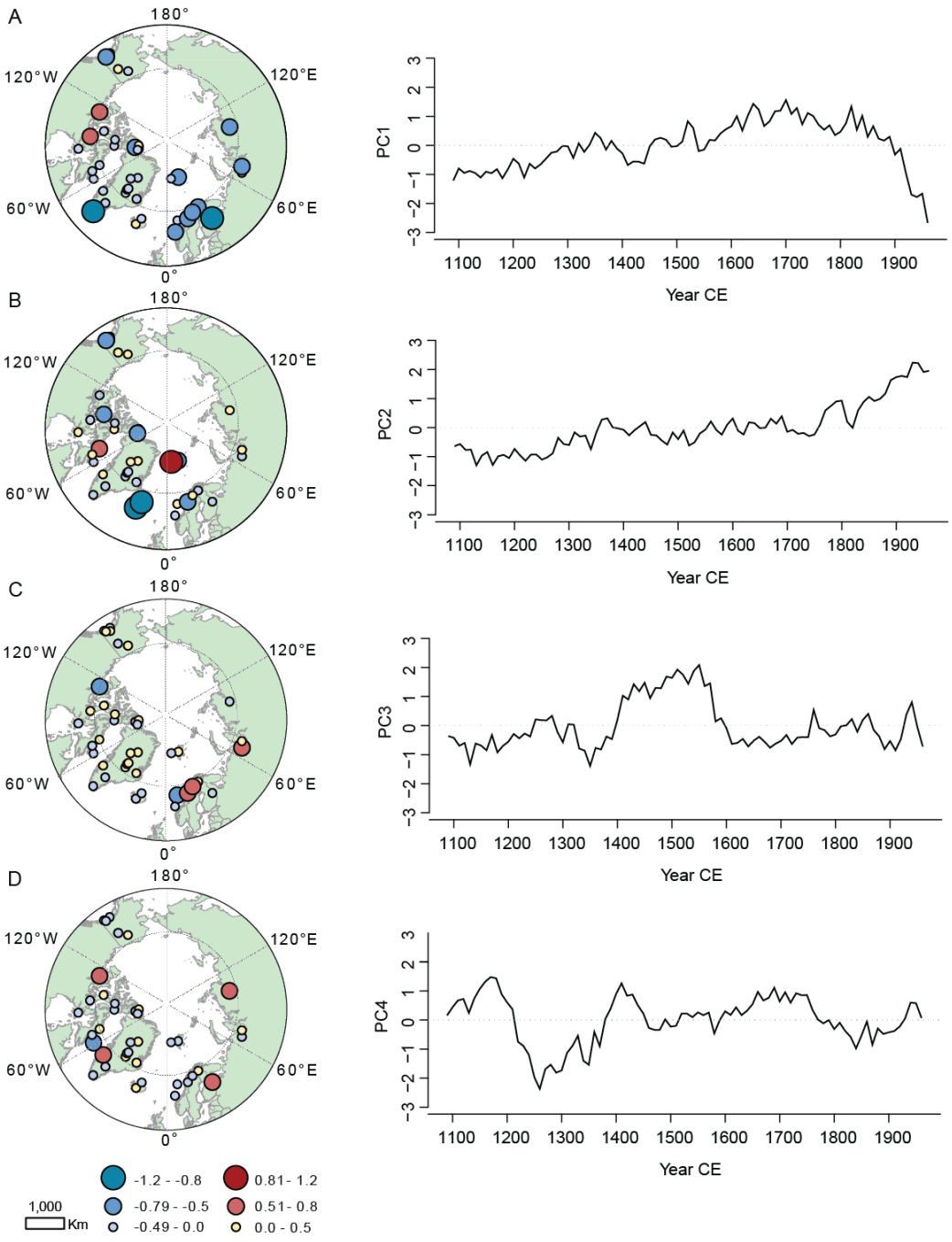

Figure 4.11: Maps of the loadings from PCA_1 and associated scores over time for (A) PC1, (B) PC2, (C) PC3, and (D) PC4. The scores over time show the dominant trend associated with each component. Blue dots on the maps are associated with the inverse of the curve.

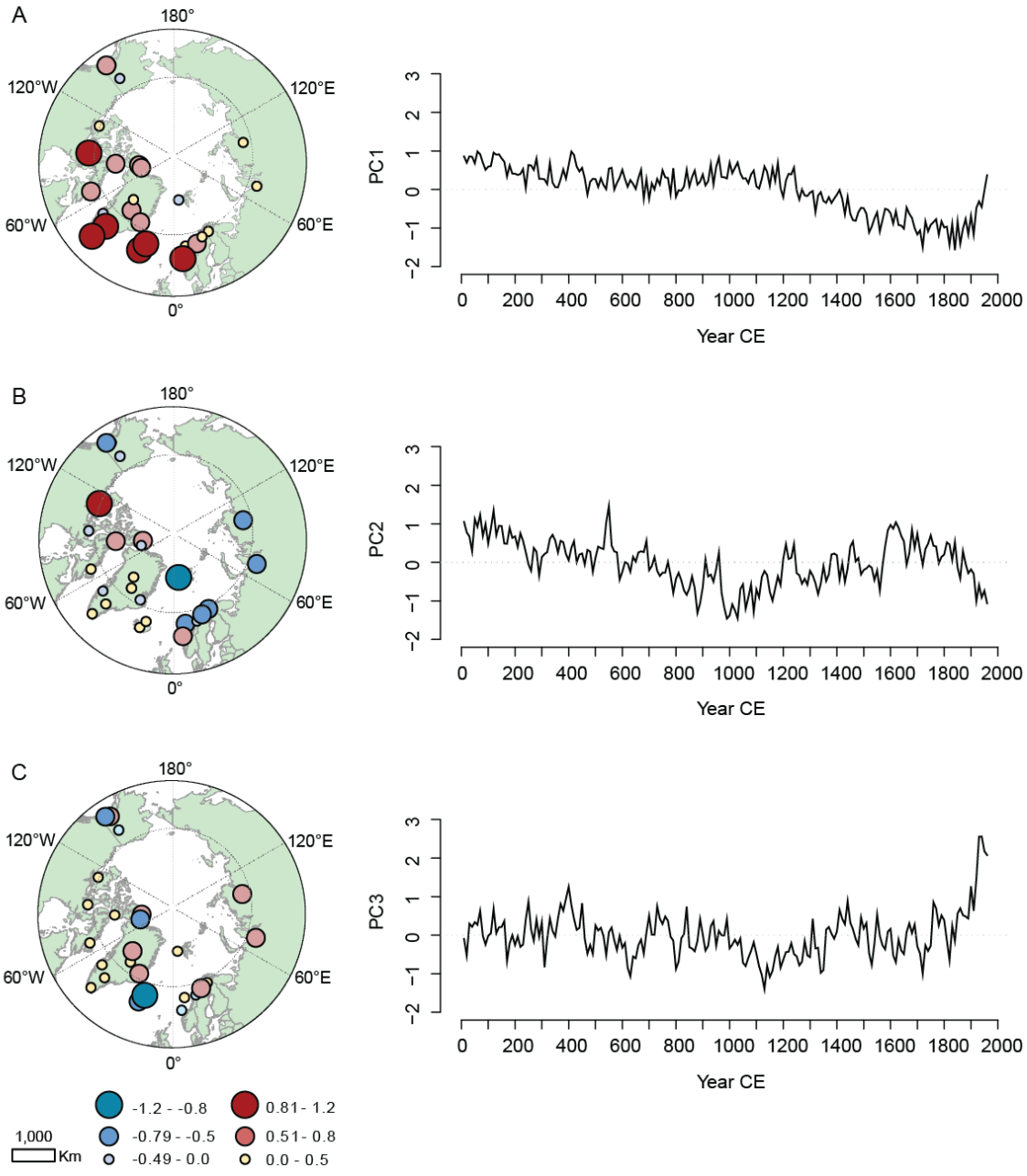

Figure 4.12: Maps of the loadings from PCA_2 and associated scores over time for (A) PC1, (B) PC2, and (C) PC3. The scores over time show the dominant trend associated with each component. Blue dots on the maps are associated with the inverse of the curve.

The first component in both PCAs shows a dominant trend that reverses at 1920 CE. In both cases, all but a few records are similarly loaded suggesting that the first component reflects variability that affected the entire Arctic at the same time. On both timescales, the records that have the highest correlation with the first component are in the North Atlantic (Figure 4.11 & 4.12); however, the spatial coherence is greater in PCA_2 and includes more ice cores and records from the CAA. Ice core records are generally weakly correlated with the first component in PCA_1 except for those that are in units of temperature (Agassiz and Lomonosovfonna). The higher correlation of uncalibrated ice core records with the first component in PCA_2 suggests the raw $\delta^{18}O$ values may have a more common signal of longer term climate variability. In addition to temperature, the isotopic signals in ice cores are influenced by the seasonality of precipitation and changes in circulation patterns and thus moisture transport (Krinner & Werner, 2003; Masson-Delmotte et al., 2005; M. Werner et al., 2001). Although there is a linear relationship between modern surface temperature and isotopic composition, changes in the hydrological regime over time could alter this relationship, thereby biasing reconstructions based on raw $\delta^{18}O$ values.

Subsequent components in both PCAs show modifications to the dominant trends that occurred in various records. Records that are highly loaded on the second component of PCA_1 have either a strong manifestation of the MCA or modern warming. For example, MD99-2275, Lower Murray Lake, SW08, and Moose Lake are all positively correlated with this component and show warming of 1-2°C between 1100 and 1300 CE. On the other hand, records from Big Round Lake and MSM5/5-712 both show a stronger signal of 20th-century warming but a relative weak medieval warming in the last 1000 years. Sites located around Iceland (Hvitarvatn and MD99-2275) show a stronger manifestation of the MCA, which may be due to the influence of an intensified AMOC due to changes in the NAO at that time (Trouet et al., 2009). The long-term temporal pattern of

the second component of PCA_2 is similar to that of the first component, but it includes several multi-decadal deviations from the long-term trend that correspond to periods of increased volcanism. These occur from 520-570 CE, 900-970 CE, 1190-1250 CE, and 1600-1680 CE. The first peak corresponds to a period of perceived global climate anomalies between 536-550 CE which has been attributed to major volcanic eruptions in both the southern and northern hemispheres (Sigl et al., 2015).

The PCA also indicates that pollen records can capture both low and high frequency variability, although they are highly dependent on the sampling resolution. For example, SW08 is in agreement with several other different proxy types (eg. Lomonosovfonna, MD99-2275, and Lower Murray Lake) over the last 1000 years, and also documents the MCA, LIA, and the 20th century warming. Although SL06 and MB01 do not show the same patterns in the last 1000 years, perhaps due to the lower sampling resolution or to regional differences in climate evolution, they do document the long-term Neoglacial cooling trend over the last 2000 years.

In recent years, several reconstructions have been attempted using different methodologies, calibration periods, and slightly different datasets (Figure 4.13). Despite these differences, they all produced relatively similar climate trends, but with different amplitudes of change. It is likely that none of the reconstructions represent the "true" amplitude of change that occurred over the last 2000 years because few of the records used in the reconstructions are calibrated into units of temperature. Obtaining quantitative, rather than index-based, reconstructions will enable the production of large-scale reconstructions without standardizing the data so that a more accurate amplitude of change can be produced.

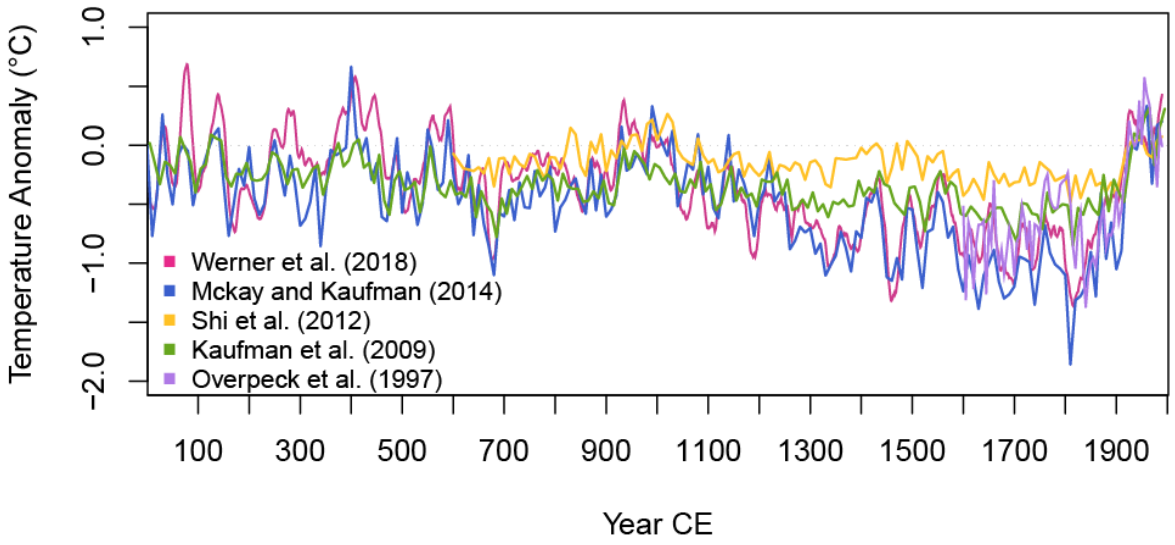

Figure 4.13: Comparison of circum-Arctic reconstructions for the past 2000 years.

4.6 Conclusion

High-resolution pollen data provide new information about climate variability in the Arctic and help put recent vegetation changes in the context of the last 1000 years. The pollen-based reconstruction from Prince of Wales Island, Nunavut, Canada shows more variability than previous Holocene-scale reconstructions (Peros & Gajewski, 2009; Zabenskie & Gajewski, 2007). Our reconstruction of temperature provides evidence for sustained colder conditions in the 1800s and unprecedented vegetation change in the last 30 years.

In order to produce more reliable circum-Arctic reconstructions, individual records from across the Arctic must be calibrated into units of temperature. Although this has recently been done for the Agassiz ice core (Lecavalier et al., 2017) and several tree ring records (Grudd, 2008; Helama et al., 2009), those proxies are regionally limited so separating proxy-based bias from regional

patterns may be difficult. Lake sediments are the only archive with spatial representation across the Arctic and changes in pollen assemblages have consistently shown direct association with climate (Gajewski, 2002, 2015b). We demonstrated that pollen provides important regional information and preserves the low and high frequency temporal trends when added to existing databases of proxy records. Despite chronological limitations, the addition of pollen and other lake sediment records into a circum-Arctic analysis of spatial and temporal climate variability is necessary to reduce spatial gaps in the proxy network to produce a robust circum-Arctic climate reconstruction.

4.7 Appendix

Table 4.A1: List of reconstructions included in the synthesis study. Sites in bold are included in both PCA_1 and PCA_2.

Site	Region	Lat	Long	Record	Proxy	Reference
Arc_1_Bluelake	Alaska	68.1	-150.5	Lake sediment	Varve thickness	Bird et al. (2009)
Arc_7_GulfAlaska	Alaska	61.0	-146.6	Tree Ring	Ring width	Wiles et al. (2014)
Arc_41_Hudson	Alaska	61.9	-145.7	Lake sediment	Chironomids	Clegg et al. (2011)
Arc_42_lynx	Alaska	66.1	-145.4	Lake sediment	Chironomids	Clegg et al. 2011
Arc_40_Moose	Alaska	61.3	-143.6	Lake sediment	Chironomids	Clegg et al. (2010)
Arc_23_Iceberg	Alaska	60.8	-143.0	Lake sediment	Varve thickness	Loso et al. (2006)
MB01	Victoria Island, NWT	69.8	-112.1	Lake sediment	Pollen	Peros and Gajewski (2009)
SW08	Prince of Wales Isl, NU	72.3	-97.27	Lake sediment	Pollen	Tamo and Gajewski, this volume
SL06	Boothia Peninsula, NU	68.6	-91.9	Lake sediment	Pollen	Peros and Gajewski (2009)
DV09	Devon Island, NU	75.6	-89.3	Lake sediment	Varve thickness	Courtney Mustaphi and Gajewski (2009)
Arc_54_Lake4	Southampton Isl, NU	65.1	-83.8	Lake sediment	Chironomids	Rolland (2009)
Arc_44_Devon	Devon Island, NU	75.3	-82.5	Ice core	$\delta^{18}O$	Fisher et al. (1983)
Arc_20_LakeC2	Ellesmere Island, NU	82.1	-77.2	Lake sediment	Varve thickness	Lamoureux and Bradley (1996)
Agassiz Ice Cap	Ellesmere Island, NU	81.0	-75	Ice core	$\delta^{18}O$	Lecavalier et al. (2017)
Arc_4_Lower Lake	Ellesmere Island, NU	81.4	-69.5	Lake sediment	Mass accumulation rate	Cook et al. (2009)
Arc_30_BigRoundLake	Baffin island, NU	69.9	-68.8	Lake sediment	Varve thickness	Thomas and Briner (2009)
Arc_53_Penny	Baffin Island, NU	67.3	-66.8	Ice core	$\delta^{18}O$	Fisher et al. (1998)
Arc_25_Donard	Baffin Island, NU	66.7	-61.4	Lake sediment	Varve thickness	Moore et al. (2001)
Arc_43_Braya	Greenland	67.0	-50.7	Lake sediment	$U^{K'}_{37}$	D'Andrea et al. (2011)
Arc_52_Igaliku	Greenland	61.0	-45.4	Lake sediment	Pollen accumulation	Massa et al. (2012)
Arc_35_DYE3	Greenland	65.2	-43.8	Ice core	$\delta^{18}O$	Vinther et al. (2010)
Arc_32_NGRIP1	Greenland	75.1	-42.3	Ice core	$\delta^{18}O$	Vinther et al. (2006)
Arc_11_GISP2	Greenland	72.1	-38.1	Ice core	$\delta^{18}O$	Grootes and Stuiver (1997)
Arc_36_GRIP	Greenland	72.6	-37.6	Ice core	$\delta^{18}O$	Vinther et al. (2010)
Arc_34_Crete	Greenland	71.1	-37.3	Ice core	$\delta^{18}O$	Vinther et al. (2010)
Arc_28_B18	Greenland	76.6	-36.4	Ice core	$\delta^{18}O$	Schwager (2000)
Arc_59_Renland	Greenland	71.3	-26.7	Ice core	$\delta^{18}O$	Vinther et al. (2008)
Arc_22_Hvitarvatn	Iceland	64.6	-19.8	Lake sediment	Varve thickness	Larsen et al. (2011)
Arc_57_MD99-2275	North Atlantic	66.6	-17.4	Marine sediment	$U^{K'}_{37}$	Sicre et al. (2011)
Arc_55_P1003	North Atlantic	63.8	5.3	Marine sediment	$\delta^{18}O$	Sejrup et al. (2011)
Arc_58_MSm5/5-712	North Atlantic	78.9	6.8	Marine sediment	Planktic forams	Spielhagen et al. (2011)
Arc_38_MD95-2011	North Atlantic	67.0	7.6	Marine sediment	Diatoms	Berner et al. (2011)
Arc_49_Okshola Cave	Scandinavia	67	15	Speleothem	$\delta^{18}O$	Linge et al. (2009)
Arc_17_Lomonosovfonna	North Atlantic	78.9	17.4	Ice core	$\delta^{18}O$	Divine et al. (2011)
Arc_12_Tornetrask	Scandinavia	68.3	19.6	Tree Ring	Ring Width	Grudd (2008)
Arc_15_Lapland	Scandinavia	69.0	25.0	Tree Ring	Ring width	Helama et al. (2009)
Arc_51_Pieni	Scandinavia	64.3	30.1	Lake sediment	Chironomids	Luoto and Helama (2010)
Arc_10_PolarUrals	Central Russia	66.8	65.8	Tree Ring	Max. density	Esper et al. (2002)
Arc_3_Yamal	Central Russia	67.5	70.0	Tree Ring	Ring width	Briffa et al. (2008)
Arc_2_AvamTaimyr	Central Russia	72.0	101.0	Tree Ring	Ring width	Briffa et al. (2008)

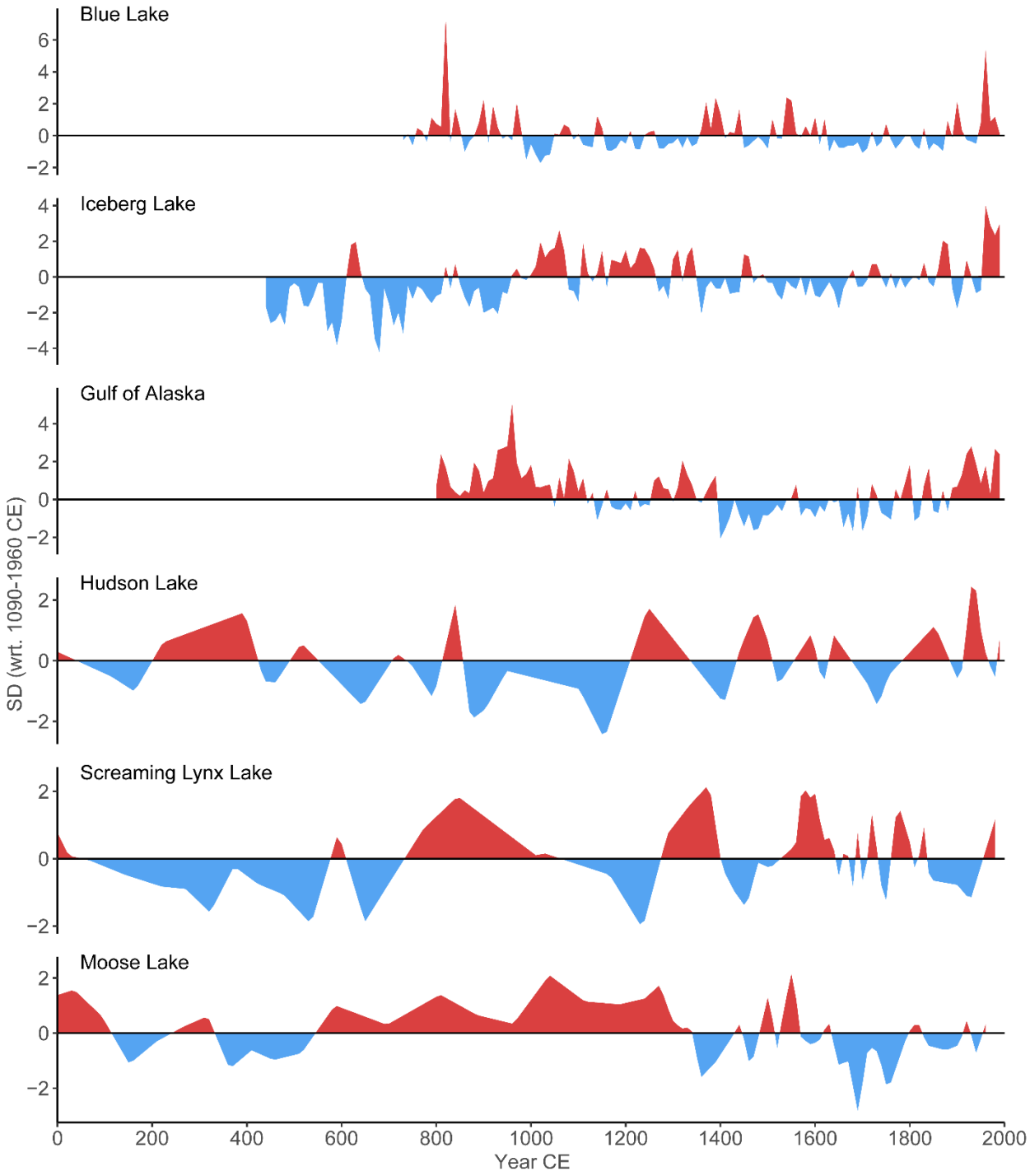

Figure 4.A1: Interpolated varve, tree ring, and chironomid records from Alaska.

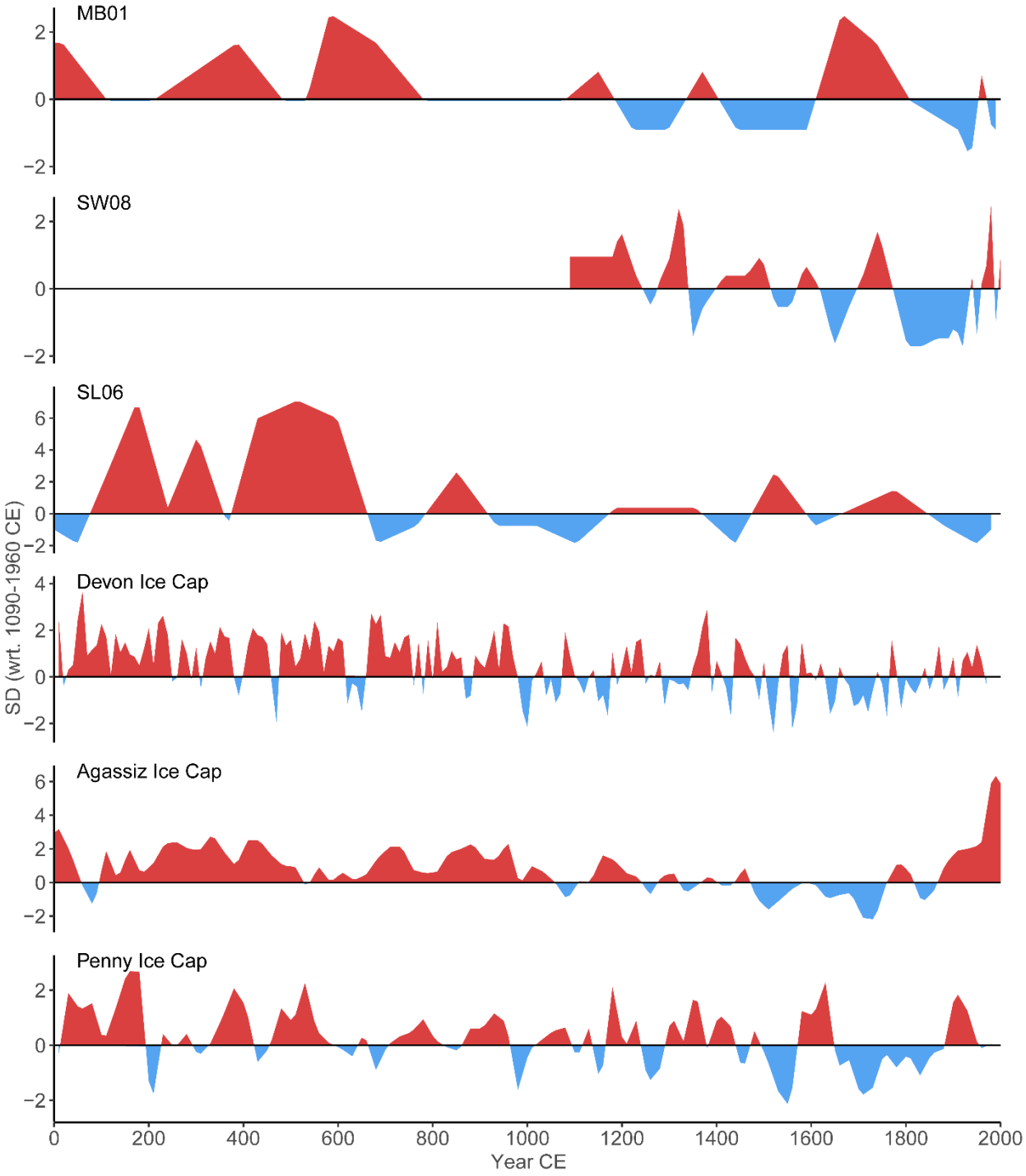

Figure 4.A2: Interpolated pollen and ice core records from the Canadian Arctic Archipelago.

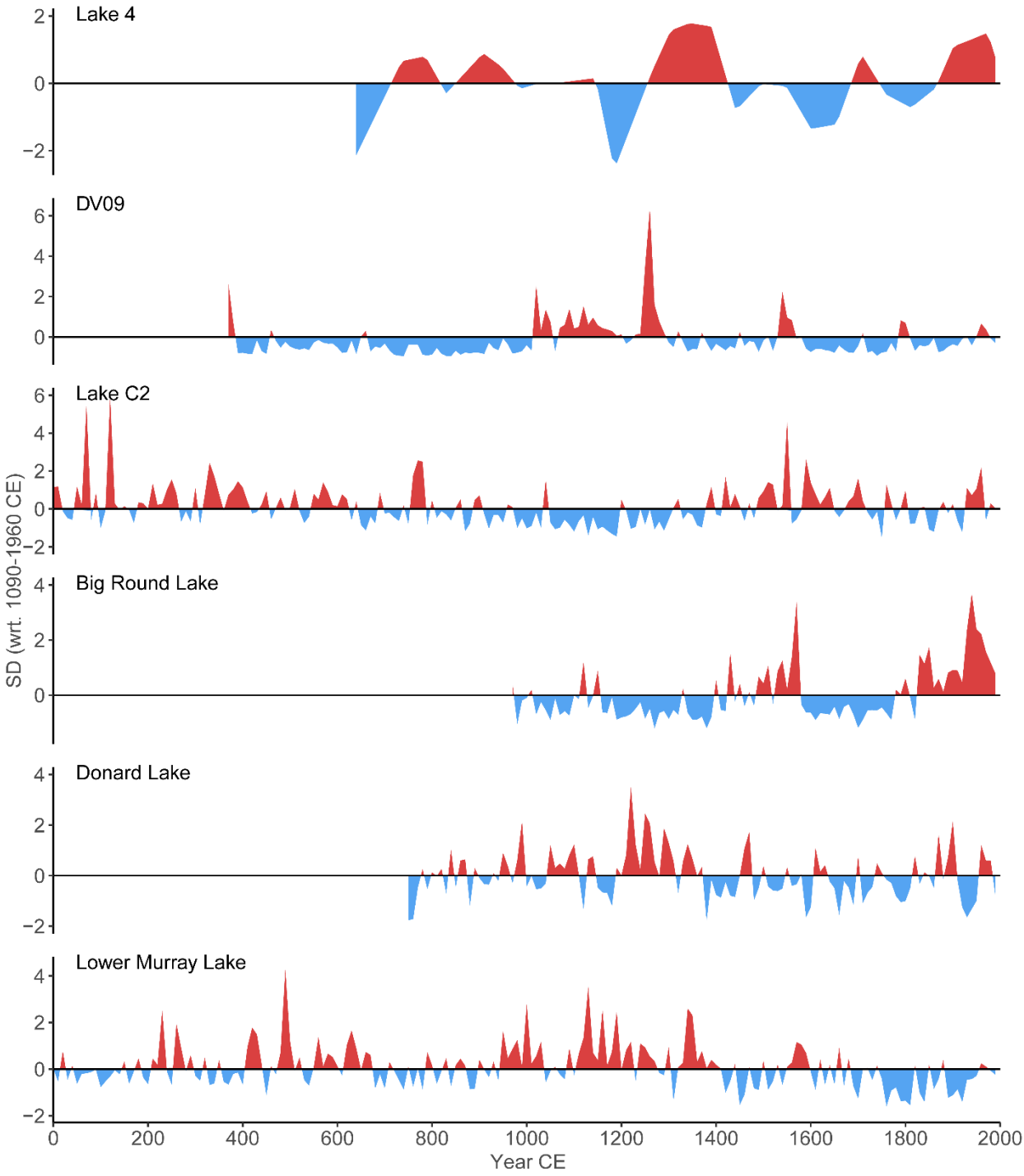

Figure 4.A3: Interpolated varve records from the Canadian Arctic Archipelago.

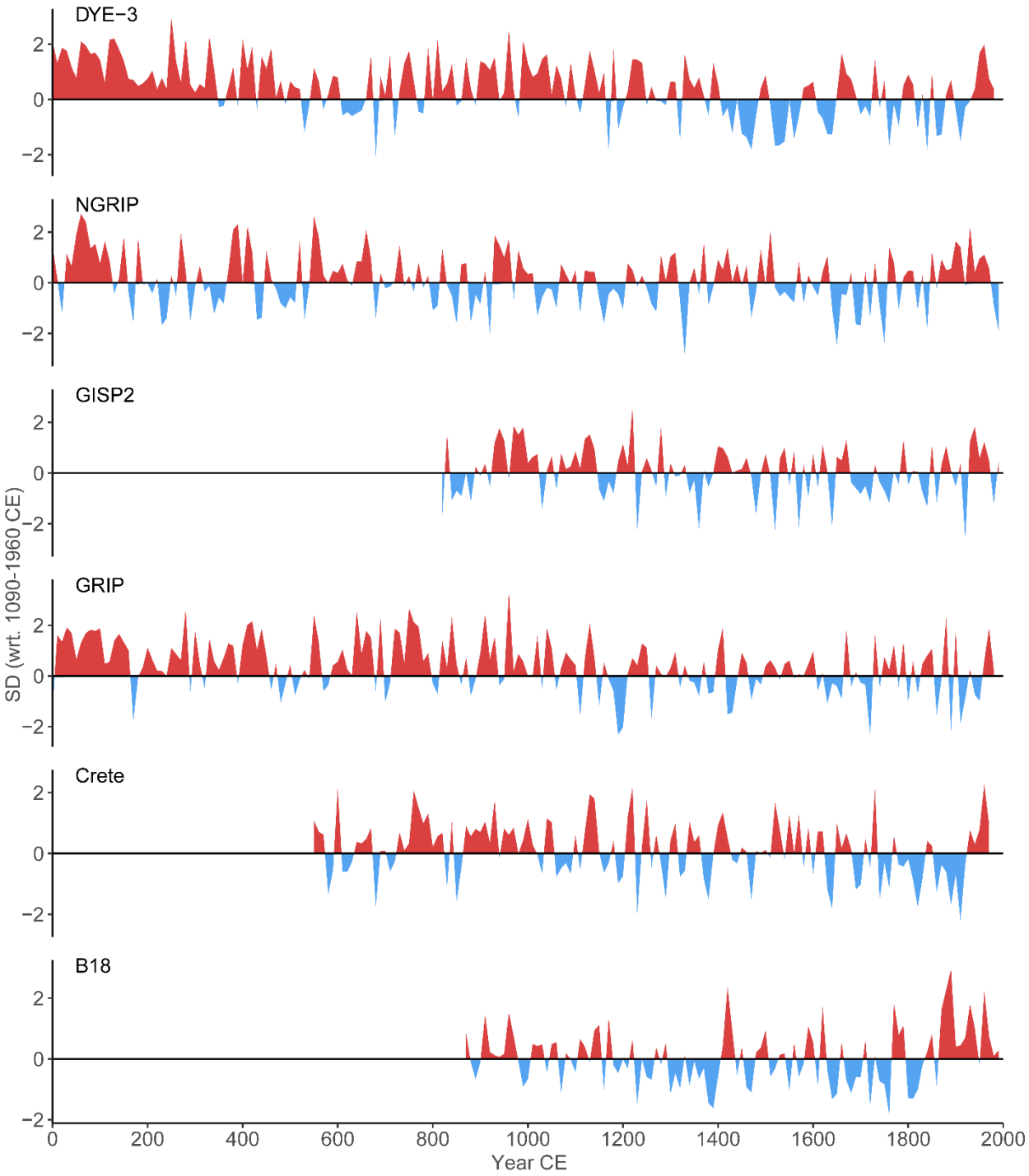

Figure 4.A4: Interpolated ice core records from Greenland.

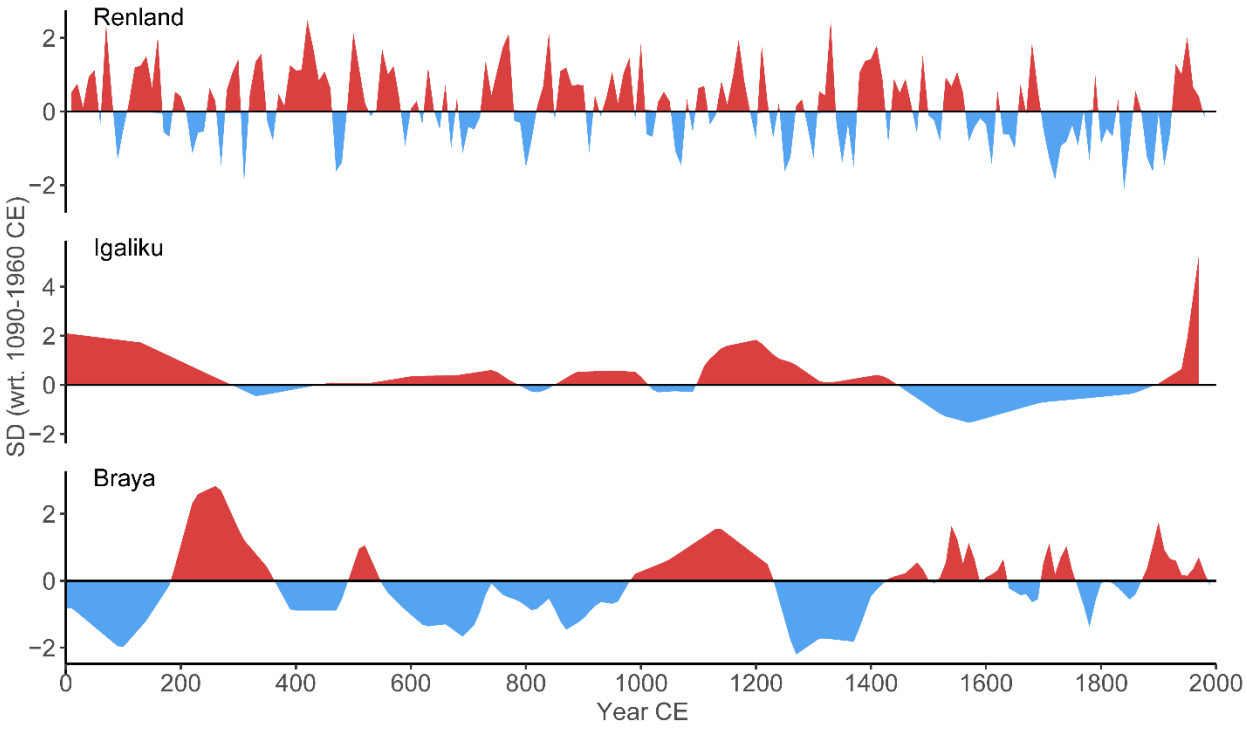

Figure 4.A5: Interpolated ice core, pollen and $U^{K'}_{37}$ records from Greenland.

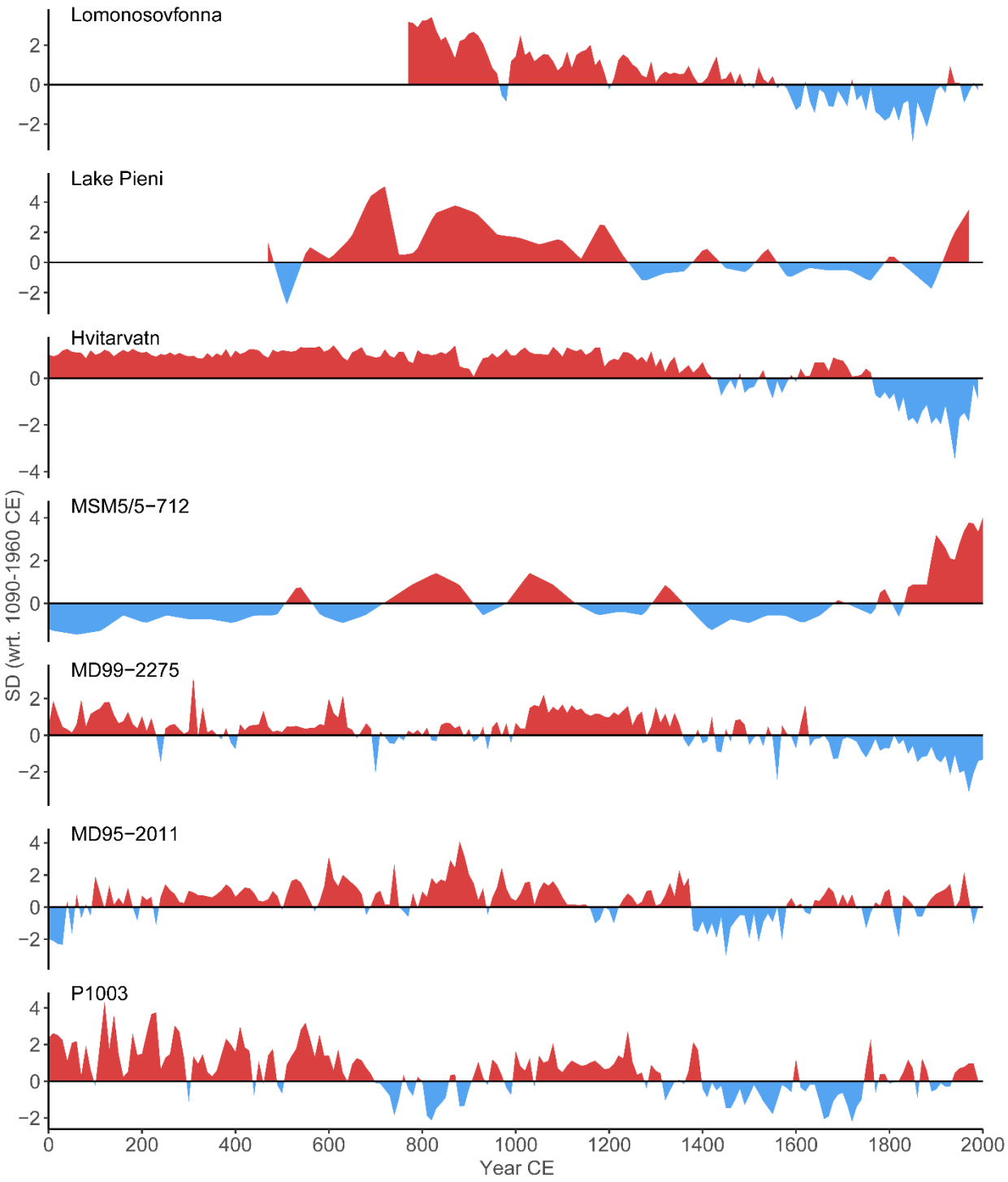

Figure 4.A6: Interpolated ice core, chironomid, varve, and marine sediment records from Scandinavia and the North Atlantic.

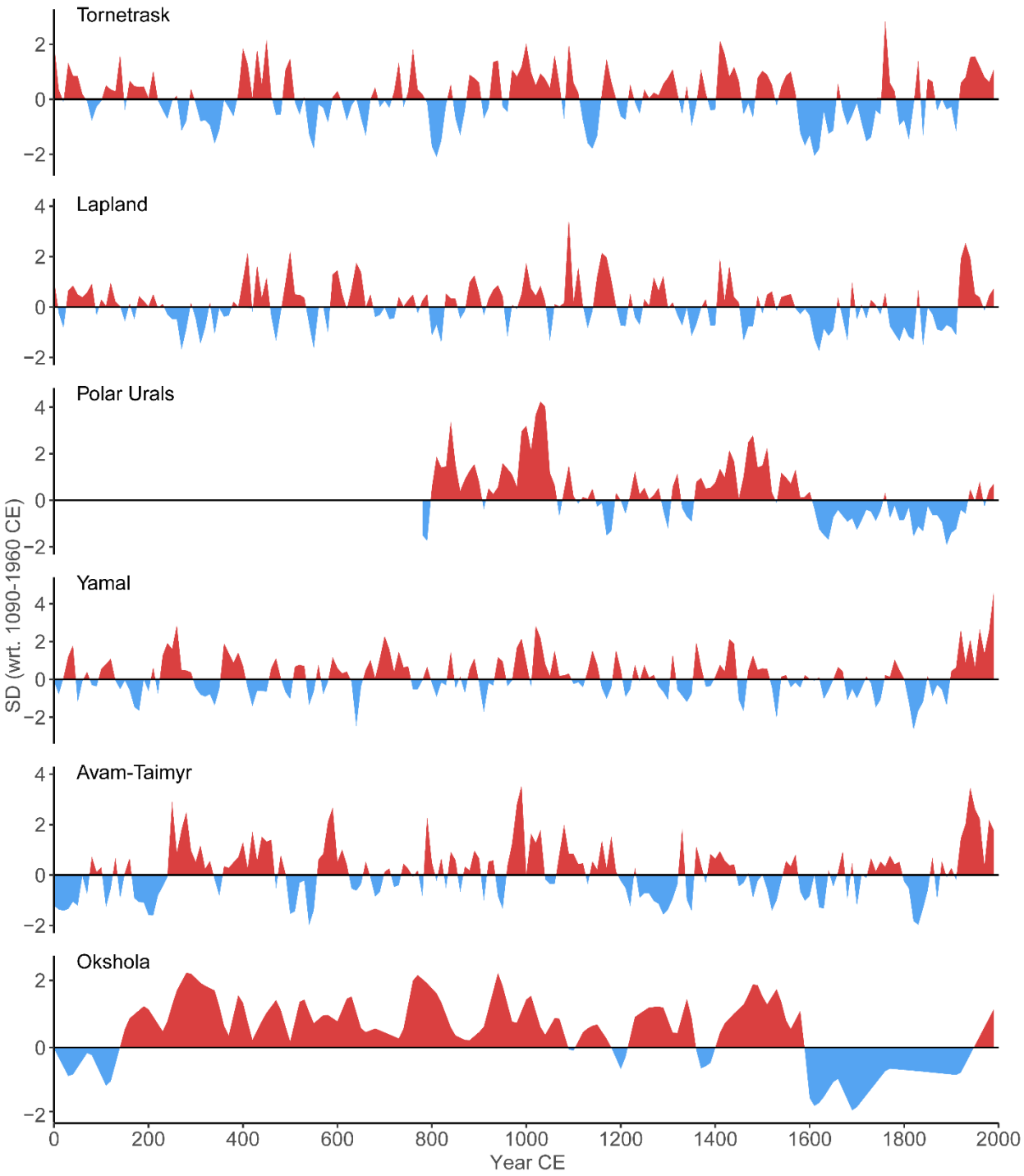

Figure 4.A7: Interpolated tree ring and speleothem records from Scandinavia and Russia.

CHAPTER FIVE

Conclusions and Future Directions

5.1 Summary

Robust circum-Arctic paleoclimate reconstructions are still hindered by the sparse geographic proxy network and lack of quantitative reconstructions. The new ~1000 year paleoclimate record from Prince of Wales Island, Nunavut presented in this thesis is the only high resolution record for the last 1000 years from the central Canadian Arctic and the four biogenic silica records and three pH reconstructions provide insight into diatom dissolution in the Arctic. Changes in the vegetation on Prince of Wales Island, Nunavut are strongly linked to climate, whereas biogenic silica records are influenced by sedimentary characteristics and probably cannot be associated to climate in hardwater lakes.

In this thesis, we encountered and addressed several methodological problems associated with working with Arctic lacustrine sediments. A pervasive issue limiting robust reconstructions from lake sediment archives is dating uncertainty. The freshwater reservoir effect is understudied and few methods have been proposed to correct for the resulting dating uncertainties (MacDonald et al., 1991). We applied a method developed by Peros and Gajewski (2009) based on linear regression with the assumption that the sediment-water interface represents the present. The resulting correction for each site was between 800 and 1000 years, which is not unusual for the Arctic (MacDonald et al., 1991; Snyder et al., 1994).

Previous studies have proposed climate as the driver of lake water pH in Arctic lakes (Michelutti et al., 2007; Rouillard et al., 2012; Wolfe, 2002). Lake water pH may be reconstructed using diatoms preserved in the sediment, either by weighted-average inference models based on fossil-

diatom assemblages (Finkelstein et al., 2014; Joynt III & Wolfe, 2001) or by a transfer function based on changes in sediment carbonate and biogenic silica content (Fortin & Gajewski, 2009). In the lakes studied here, sedimentary carbonates likely exerted a strong influence on the preservation of biogenic silica, and thus diatoms, in the sediment. Biogenic silica was measured in four lakes located along a southwest-northeast transect of the Canadian Arctic that were in differing vegetation zones with various bedrock and substrate chemistry. Dissolution was evident in three of the four lakes. In the sediment core from Prince of Wales Island, no values above detection were measured, which is likely due to consistent sedimentary carbonate values above 20%. Biogenic silica records from Banks Island, Bathurst Island, and Ellesmere Island all contained abrupt increases in biogenic silica in the last 30 years. These results could be attributed to increased productivity associated with modern warming, but the absence of biogenic silica in deeper sediments from both Bathurst and Ellesmere Island also suggests post-depositional dissolution. The record from Banks Island, NWT provided the most reliable reconstruction of pH and aquatic production since it was not influenced by sedimentary carbonates. However, the reconstructed pH values using the transfer function developed by Fortin and Gajewski (2009) produced contradictory results. Lake water pH, sedimentary carbonate, and aquatic productivity have all been independently positively associated with climate (Dean, 1981; Finkenbinder et al., 2018; Fritz & Anderson, 2013; Kelts & Hsü, 1978; Wolfe, 2002), but analyses of surface samples across the Arctic showed an inverse relationship between sediment BSi and carbonate (Fortin & Gajewski, 2009). The transfer function based on this inverse relationship thus produced a pH curve that decreased as BSi increased, even in cases where post-depositional dissolution was not an issue, such as at Lake B503 on Banks Island. It is likely that when the transfer function was developed the BSi values from several lakes included in the regression were influenced by post-depositional

dissolution. We thus caution the use of a calibration equation based on sedimentary carbonates and BSi since diatom dissolution appears to be a larger problem in the Arctic than previously thought (Paull et al., 2017). The possibility of diatom dissolution should also be considered when interpreting longer sequences, particularly in hardwater lakes.

On Prince of Wales Island, Nunavut the vegetation composition underwent marked transitions during warm and cold periods. These changes were mainly observed in the proportion of Cyperaceae and Poaceae, which are indicative of warmer and colder conditions, respectively (Gajewski, 2002). In the last 100 years, *Salix* and *Betula* increased significantly at the expense of Cyperaceae and Poaceae. Mean July temperatures reconstructed from the pollen assemblages were consistent with other pollen-based studies from the central and western Arctic, particularly during the last 200 years, as well as reconstructions based on different proxies from across the Arctic. A long-term cooling trend was reconstructed between 1080 and 1915 CE, which likely represents the end of the MCA and transition to the sustained cold conditions of the LIA prior to modern warming. We demonstrated that pollen can record high and low frequency climate variability as long as the sampling resolution is fine enough and that there is no lag in the vegetation response to climate variability.

Despite chronological uncertainties, when sediment cores allow for a high-resolution pollen analysis they should be included in synthesis studies to enable a more complete spatial coverage when producing Arctic-wide paleoclimate syntheses. Their spatial representation across the Arctic would allow regional patterns to be distinguished from proxy-based biases. Furthermore, efforts should be made to produce high-resolution pollen-based reconstructions since vegetation changes can be directly associated with climate (Gajewski, 2015a, 2002).

5.2 Future Directions

Recent work on the Arctic climate of the last 2000 years based on existing proxy records (Linderholm et al., 2018; McKay & Kaufman, 2014; Nicolle et al., 2018; PAGES2k et al., 2017; Werner et al., 2018) has several limitations that prevent the development of robust analyses. In particular, the sparse proxy network biases reconstructions towards the North Atlantic region. This thesis provides new data for the central Canadian Arctic but there are still significant gaps in Siberia, Alaska and the CAA. While we acknowledge the difficulties associated with collecting and analyzing lake sediments, they remain the only archive with spatial representation across the Arctic and should be included in synthesis studies.

In order to obtain robust reconstructions from lake sediment archives multi-proxy studies should be performed where possible. We demonstrated that pollen is a reliable proxy for reconstructing both low and high frequency climate variability. To ensure success, researchers should obtain as many cores as possible during their field seasons since it is not uncommon for lakes to lack suitable proxies, as detailed in this thesis.

Obtaining a reliable chronology remains one of the most limiting factors when analyzing lake sediment archives. By quantifying the freshwater reservoir effect and developing methods of correcting radiocarbon dates, more reliable reconstructions could be obtained. Therefore, detailed studies of the freshwater reservoir effect across the Arctic are needed to understand how it varies both spatially and temporally.

There have been several circum-Arctic reconstructions using similar datasets of proxy records (Hanhijärvi et al., 2013; Kaufman et al., 2009; McKay & Kaufman, 2014; Nicolle et al., 2018; Overpeck et al., 1997; Shi et al., 2012; Werner et al., 2018), but they all reconstructed different amplitudes of change, particularly in warm periods. Large-scale reconstructions are significantly

affected by the methodology applied, proxies included, and calibration period (Christiansen & Ljungqvist, 2017; Esper et al., 2005). In cases where regression methods are applied between instrumental temperatures and proxies, the reconstructed amplitude is reduced and low-frequency trends may be underestimated (e.g. Kaufman et al., 2009). Selecting proxy records for a reconstruction is integral since it typically involves a trade-off between high-resolution, well-dated records and spatial coverage. This problem is enhanced in the Arctic where high-resolution records are regionally limited and there are chronological uncertainties in lower-resolution records. Further bias is introduced into circum-Arctic reconstructions via the geographical clustering of the current Arctic proxy network. When reconstruction models are calibrated to an instrumental period, the scaling period determines the amplitude of reconstructed temperatures. Scaling to a longer period can reduce the sensitivity of the reconstruction to high-frequency changes (Esper et al., 2005) but the difficulty of reconstructing temperatures that deviate from the range of the calibration interval can lead to the underestimation of low-frequency variability (Christiansen & Ljungqvist, 2017).

Although there is considerable work to be done resolving the methodological issues with reconstructions, error can be reduced by calibrating individual reconstructions into units of temperature rather than inputting them as raw or standardized proxy values. It is widely acknowledged that most proxies are influenced by factors other than temperature. Consequently, the raw proxy values likely do not represent the proper amplitude of change. Few records in the Arctic 2k proxy database (McKay & Kaufman, 2014) have been calibrated into units of temperature, so variations from the mean may not reflect solely changes in air temperatures.

This thesis provided suggestions for dealing with methodological problems associated with Arctic samples and developed new calibration samples to enable biogenic silica analysis. Although we determined several issues analyzing biogenic silica in the Arctic, the calibration samples may also

be used for non-Arctic samples since a range of biogenic silica concentration was captured. We caution the interpretation of biogenic silica as the sole proxy for climate or aquatic productivity since concentrations may be significantly affected by sedimentary characteristics. Furthermore, we demonstrated that pollen-based studies provide important information to help close the spatial gap in the proxy network across the Arctic, particularly in the Canadian Arctic and Alaska where modern calibration sets (Whitmore et al., 2005) have been developed to enable quantitative reconstructions of past temperatures.

References

Andres, H. J., & Peltier, W. R. (2016). Regional influences of natural external forcings on the transition from the Medieval Climate Anomaly to the Little Ice Age. *Journal of Climate*, *29*(16), 5779–5800.

Appleby, P. G., & Oldfield, F. (1978). The calculation of lead-210 dates assuming a constant rate of supply of unsupported 210Pb to the sediment. *Catena*, *5*(1), 1–8.

Ascough, P. L., Cook, G. T., Hastie, H., Dunbar, E., Church, M. J., Einarsson, Á., … Dugmore, A. J. (2011). An Icelandic freshwater radiocarbon reservoir effect: Implications for lacustrine 14C chronologies. *The Holocene*, *21*(7), 1073–1080.

Bednarski, J., England, J., Hodgson, D. A., & Koerner, R. M. (1989). Quaternary Geology of the Queen Elizabeth Islands. In *Quaternary Geology of Canada and Greenland* (pp. 443–478). Geological Society of America.

Bennett, K. D., & Willis, K. J. (2001). Pollen. In J. P. Smol, H. J. B. Birks, & W. M. Last (Eds.), *Tracking Environmental Change Using Lake Sediments. Volume 3: Terrestrial, Algal, and Siliceous Indicators* (pp. 5–32). Kluwer, Dordrecht, The Netherlands.

Berner, K. S., Koç, N., Godtliebsen, F., & Divine, D. (2011). Holocene climate variability of the Norwegian Atlantic Current during high and low solar insolation forcing. *Paleoceanography and Paleoclimatology*, *26*(2).

Bird, B. W., Abbott, M. B., Finney, B. P., & Kutchko, B. (2009). A 2000 year varve-based climate record from the central Brooks Range, Alaska. *Journal of Paleolimnology*, *41*(1), 25–41.

Birks, H. H., & Birks, H. J. B. (2000). Future uses of pollen analysis must include plant

macrofossils. *Journal of Biogeography*, *27*(1), 31–35.

Birks, H. H., & Birks, H. J. B. (2006). Multi-proxy studies in palaeolimnology. *Vegetation History and Archaeobotany*, *15*(4), 235–251.

Blaauw, M., & Christen, J. A. (2011). Flexible paleoclimate age-depth models using an autoregressive gamma process. *Bayesian Analysis*, *6*(3), 457–474.

Bond, G., Kromer, B., Beer, J., Muscheler, R., Evans, M. N., Showers, W., … Bonani, G. (2001). Persistent solar influence on North Atlantic climate during the Holocene. *Science*, *294*(5549), 2130–2136.

Bradley, R. S., Hughes, M. K., & Diaz, H. F. (2003). Climate in Medieval Time. *Science*, *302*(5644), 404–405.

Bradley, R. S., Wanner, H., & Diaz, H. F. (2016). The Medieval Quiet Period. *The Holocene*, *26*(6), 990–993. https://doi.org/10.1177/0959683615622552

Briffa, K. R., Shishov, V. V, Melvin, T. M., Vaganov, E. A., Grudd, H., Hantemirov, R. M., … Naurzbaev, M. M. (2008). Trends in recent temperature and radial tree growth spanning 2000 years across northwest Eurasia. *Philosophical Transactions of the Royal Society of London B: Biological Sciences*, *363*(1501), 2269–2282.

Briner, J. P., McKay, N. P., Axford, Y., Bennike, O., Bradley, R. S., de Vernal, A., … Gajewski, K. (2016). Holocene climate change in Arctic Canada and Greenland. *Quaternary Science Reviews*, *147*, 340–364.

Bronk Ramsey, C. (2009). Bayesian analysis of radiocarbon dates. *Radiocarbon*, *51*(1), 337–360.

CAVM, Walker, D. A., & Trahan, N. G. (2003). *Circumpolar Arctic Vegetation*. US Fish and

Wildlife Service.

Christen, J. A., & Perez, S. (2009). A new robust statistical model for radiocarbon data. *Radiocarbon*, *51*(3), 1047–1059.

Christiansen, B., & Ljungqvist, F. C. (2017). Challenges and perspectives for large-scale temperature reconstructions of the past two millennia. *Reviews of Geophysics*, *55*(1), 40–96.

Church, J. A., White, N. J., & Arblaster, J. M. (2005). Significant decadal-scale impact of volcanic eruptions on sea level and ocean heat content. *Nature*, *438*(7064), 74.

Clegg, B. F., Clarke, G. H., Chipman, M. L., Chou, M., Walker, I. R., Tinner, W., & Hu, F. S. (2010). Six millennia of summer temperature variation based on midge analysis of lake sediments from Alaska. *Quaternary Science Reviews*, *29*(23–24), 3308–3316. https://doi.org/10.1016/J.QUASCIREV.2010.08.001

Clegg, B. F., Kelly, R., Clarke, G. H., Walker, I. R., & Hu, F. S. (2011). Nonlinear response of summer temperature to Holocene insolation forcing in Alaska. *Proceedings of the National Academy of Sciences*, *108*(48), 19299–19304.

Conley, D. J. (1998). An interlaboratory comparison for the measurement of biogenic silica in sediments. *Marine Chemistry*, *63*(1–2), 39–48.

Conley, D. J., & Schelske, C. L. (2001). Biogenic silica. In J. P. Smol, H. J. B. Birks, & W. M. Last (Eds.), *Tracking Environmental Change Using Lake Sediments. Volume 3: Terrestrial, Algal, and Siliceous Indicators* (pp. 281–293). Kluwer, Dordrecht, The Netherlands.

Cook, E. R., Briffa, K. R., Meko, D. M., Graybill, D. A., & Funkhouser, G. (1995). The "segment length curse" in long tree-ring chronology development for palaeoclimatic studies. *The*

Holocene, *5*(2), 229–237. https://doi.org/10.1177/095968369500500211

Cook, T. L., Bradley, R. S., Stoner, J. S., & Francus, P. (2009). Five thousand years of sediment transfer in a high arctic watershed recorded in annually laminated sediments from Lower Murray Lake, Ellesmere Island, Nunavut, Canada. *Journal of Paleolimnology*, *41*(1), 77.

Courtney Mustaphi, C. J., & Gajewski, K. (2013). Holocene sediments from a coastal lake on northern Devon Island, Nunavut, Canada. *Canadian Journal of Earth Sciences*, *50*(5), 564–575.

Crowley, T. J., & Lowery, T. S. (2000). How warm was the medieval warm period? *AMBIO: A Journal of the Human Environment*, *29*(1), 51–54.

D'Andrea, W. J., Huang, Y., Fritz, S. C., & Anderson, N. J. (2011). Abrupt Holocene climate change as an important factor for human migration in West Greenland. *Proceedings of the National Academy of Sciences*, *108*(24), 9765–9769.

Dean, W. E. (1981). Carbonate minerals and organic matter in sediments of modern north temperate hard-water lakes.

Delcourt, H. R., & Delcourt, P. (1991). *Quaternary ecology: a paleoecological perspective*. Chapman & Hall.

DeMaster, D. J. (1981). The supply and accumulation of silica in the marine environment. *Geochimica et Cosmochimica Acta*, *45*(10), 1715–1732.

Diaz, H. F., Trigo, R., Hughes, M. K., Mann, M. E., Xoplaki, E., & Barriopedro, D. (2011). Spatial and Temporal Characteristics of Climate in Medieval Times Revisited. *Bulletin of the American Meteorological Society*, *92*(11), 1487–1500. https://doi.org/10.1175/BAMS-D-10-

05003.1

Divine, D., Isaksson, E., Martma, T., Meijer, H. A. J., Moore, J., Pohjola, V., … Godtliebsen, F. (2011). Thousand years of winter surface air temperature variations in Svalbard and northern Norway reconstructed from ice-core data. *Polar Research*, *30*(1), 7379.

Douglas, M. S. V, Smol, J. P., & Blake, W. (1994). Marked post-18th century environmental change in high-arctic ecosystems. *Science*, *266*(5184), 416–419.

Dranga, S. A., Hayles, S., & Gajewski, K. (2017). Synthesis of limnological data from lakes and ponds across Arctic and Boreal Canada. *Arctic Science*, *4*(2), 167–185.

Dyke, A. S., & Morris, T. F. (1988). Drumlin fields, dispersal trains, and ice streams in Arctic Canada. *Canadian Geographer/Le Géographe Canadien*, *32*(1), 86–90.

Edlund, S. A., & Alt, B. T. (1989). Regional congruence of vegetation and summer climate patterns in the Queen Elizabeth Islands, Northwest Territories, Canada. *Arctic*, 3–23.

Elmendorf, S. C., Henry, G. H. R., Hollister, R. D., Björk, R. G., Bjorkman, A. D., Callaghan, T. V, … Wookey, P. A. (2012). Global assessment of experimental climate warming on tundra vegetation: heterogeneity over space and time. *Ecology Letters*, *15*(2), 164–175. https://doi.org/10.1111/j.1461-0248.2011.01716.x

Environment and Climate Change Canada. (2018a). Monthly Data Report for 1947 - Eureka Airport. Retrieved from http://climate.weather.gc.ca/index_e.html

Environment and Climate Change Canada. (2018b). Monthly Data Report for 1947 - Resolute Bay. Retrieved from http://climate.weather.gc.ca/index_e.html

Environment and Climate Change Canada. (2018c). Monthly Data Report for 1955 - Sach's

Harbour. Retrieved from http://climate.weather.gc.ca/index_e.html

Esper, J., Cook, E. R., & Schweingruber, F. H. (2002). Low-frequency signals in long tree-ring chronologies for reconstructing past temperature variability. *Science*, *295*(5563), 2250–2253.

Esper, J., Frank, D. C., Wilson, R. J. S., & Briffa, K. R. (2005). Effect of scaling and regression on reconstructed temperature amplitude for the past millennium. *Geophysical Research Letters*, *32*(7).

Faegri, K., & Iversen, J. (1989). *Textbook of Pollen Analysis*. (K. Faegri, P. E. Kaland, & K. Krzywinski, Eds.) (4th ed.). John Wiley & Sons Ltd.

Finkelstein, S. A., Bunbury, J., Gajewski, K., Wolfe, A. P., Adams, J. K., & Devlin, J. E. (2014). Evaluating diatom-derived Holocene pH reconstructions for Arctic lakes using an expanded 171-lake training set. *Journal of Quaternary Science*, *29*(3), 249–260.

Finkenbinder, M. S., Abbott, M. B., Stoner, J. S., Ortiz, J. D., Finney, B. P., Dorfman, J. M., & Stansell, N. D. (2018). Millennial-scale variability in Holocene aquatic productivity from Burial Lake, Arctic Alaska. *Quaternary Science Reviews*, *187*, 220–234. https://doi.org/10.1016/J.QUASCIREV.2018.03.019

Fisher, D. A., Koerner, R. M., Bourgeois, J. C., Zielinski, G., Wake, C., Hammer, C. U., … Goto-Azuma, K. (1998). Penny ice cap cores, Baffin Island, Canada, and the Wisconsinan Foxe Dome connection: two states of Hudson Bay ice cover. *Science*, *279*(5351), 692–695.

Fisher, D. A., Koerner, R. M., Paterson, W. S. B., Dansgaard, W., Gundestrup, N., & Reeh, N. (1983). Effect of wind scouring on climatic records from ice-core oxygen-isotope profiles. *Nature*, *301*(5897), 205.

Flower, R. J. (1993). Diatom preservation: experiments and observations on dissolution and breakage in modern and fossil material. *Hydrobiologia*, *269*(1), 473–484.

Fortin, M.-C., & Gajewski, K. (2009). Assessing the use of sediment organic, carbonate and biogenic silica content as indicators of environmental conditions in Arctic lakes. *Polar Biology*, *32*(7), 985–998.

Fortin, M.-C., & Gajewski, K. (2010a). Holocene climate change and its effect on lake ecosystem production on Northern Victoria Island, Canadian Arctic. *Journal of Paleolimnology*, *43*(2), 219–234.

Fortin, M.-C., & Gajewski, K. (2010b). Postglacial environmental history of western Victoria Island, Canadian Arctic. *Quaternary Science Reviews*, *29*(17–18), 2099–2110.

Fritz, S. C., & Anderson, N. J. (2013). The relative influences of climate and catchment processes on Holocene lake development in glaciated regions. *Journal of Paleolimnology*, *49*(3), 349–362.

Fritz, S. C., Cumming, B. F., Gasse, F., & Laird, K. R. (2010). Diatoms as indicators of hydrologic and climatic change in saline lakes. In *The diatoms: applications for the environmental and Earth sciences* (pp. 186–208). Cambridge University Press.

Gajewski, K. (1995). Modern and Holocene Pollen Assemblages from Some Small Arctic Lakes on Somerset Island, NWT, Canada. *Quaternary Research*, *44*(02), 228–236. https://doi.org/10.1006/qres.1995.1067

Gajewski, K. (2002). Modern Pollen Assemblages in Lake Sediments from the Canadian Arctic. *Arctic, Antarctic, and Alpine Research*, *34*(1), 26–32. https://doi.org/10.2307/1552505

Gajewski, K. (2006). Essai: Is Arctic Palynology a “Blunt Instrument”? *Geographie Physique et Quaternaire*, *60*(2), 95–102.

Gajewski, K. (2015a). Impact of Holocene climate variability on Arctic vegetation. *Global and Planetary Change*, *133*, 272–287.

Gajewski, K. (2015b). Quantitative reconstruction of Holocene temperatures across the Canadian Arctic and Greenland. *Global and Planetary Change*, *128*, 14–23. https://doi.org/10.1016/j.gloplacha.2015.02.003

Gajewski, K., Garneau, M., & Bourgeois, J. C. (1995). Paleoenvironments of the Canadian High Arctic derived from pollen and plant macrofossils: problems and potentials. *Quaternary Science Reviews*, *14*(6), 609–629.

Gajewski, K., Mott, R. J., Ritchie, J. C., & Hadden, K. (2000). Holocene vegetation history of Banks Island, Northwest Territories, Canada. *Canadian Journal of Botany*, *78*(4), 430–436. https://doi.org/10.1139/b00-018

Garneau, M., & Alt, B. T. (2000). Environmental response to climate change in the Canadian high Arctic. *Geological Survey of Canada*, Bulletin 529.

Goosse, H., Crespin, E., Dubinkina, S., Loutre, M.-F., Mann, M. E., Renssen, H., … Shindell, D. (2012). The role of forcing and internal dynamics in explaining the “Medieval Climate Anomaly’’’.” *Climate Dynamics*, *39*(12), 2847–2866. https://doi.org/10.1007/s00382-012-1297-0

Goosse, H., & Renssen, H. (2006). Regional response of the climate system to solar forcing: The role of the ocean. *Space Science Review*, *125*(1–4), 227–235.

Gould, W. A., Raynolds, M., & Walker, D. A. (2003a). Vegetation, plant biomass, and net primary productivity patterns in the Canadian Arctic. *Journal of Geophysical Research: Atmospheres*, *108*(D2).

Gould, W. A., Walker, D. A., & Biesboer, D. (2003b). Combining research and education: bioclimatic zonation along a Canadian Arctic transect. *Arctic*, 45–54.

Graham, N. E., Ammann, C. M., Fleitmann, D., Cobb, K. M., & Luterbacher, J. (2011). Support for global climate reorganization during the "Medieval Climate Anomaly'''." *Climate Dynamics*, *37*(5), 1217–1245. https://doi.org/10.1007/s00382-010-0914-z

Grimm, E. C., Maher, L. J., & Nelson, D. M. (2009). The magnitude of error in conventional bulk-sediment radiocarbon dates from central North America. *Quaternary Research*, *72*(2), 301–308. https://doi.org/10.1016/J.YQRES.2009.05.006

Grootes, P. M., & Stuiver, M. (1997). Oxygen 18/16 variability in Greenland snow and ice with 10− 3-to 105-year time resolution. *Journal of Geophysical Research: Oceans*, *102*(C12), 26455–26470.

Grudd, H. (2008). Torneträsk tree-ring width and density AD 500–2004: a test of climatic sensitivity and a new 1500-year reconstruction of north Fennoscandian summers. *Climate Dynamics*, *31*(7–8), 843–857.

Håkanson, L., & Jansson, M. (1983). *Principles of lake sedimentology*. Springer-Verlag Berlin.

Hanhijärvi, S., Tingley, M. P., & Korhola, A. (2013). Pairwise comparisons to reconstruct mean temperature in the Arctic Atlantic Region over the last 2,000 years. *Climate Dynamics*, *41*(7–8), 2039–2060.

Harrison, J. C., Gilbert, C., Lynds, T., Ford, A., Thorsteinsson, R., Frisch, T., … Kerr, J. W. (2015). Geology, tectonic assemblage map of Alexandra Fiord, central Ellesmere and eastern Axel Heiberg islands, Nunavut. Natural Resources Canada.

Helama, S., Timonen, M., Holopainen, J., Ogurtsov, M. G., Mielikäinen, K., Eronen, M., … Meriläinen, J. (2009). Summer temperature variations in Lapland during the Medieval Warm Period and the Little Ice Age relative to natural instability of thermohaline circulation on multi-decadal and multi-centennial scales. *Journal of Quaternary Science*, *24*(5), 450–456.

Hill, G. B., & Henry, G. H. R. (2010). Responses of High Arctic wet sedge tundra to climate warming since 1980. *Global Change Biology*, *17*(1), 276–287. https://doi.org/10.1111/j.1365-2486.2010.02244.x

Hinzman, L. D., Bettez, N. D., Bolton, W. R., Chapin, F. S., Dyurgerov, M. B., Fastie, C. L., … Yoshikawa, K. (2005). Evidence and Implications of Recent Climate Change in Northern Alaska and Other Arctic Regions. *Climatic Change*, *72*(3), 251–298. https://doi.org/10.1007/s10584-005-5352-2

Hunt, B. G. (2006). The medieval warm period, the little ice age and simulated climatic variability. *Climate Dynamics*, *27*(7–8), 677–694.

Iwi, A. M., Hermanson, L., Haines, K., & Sutton, R. T. (2012). Mechanisms linking volcanic aerosols to the Atlantic meridional overturning circulation. *Journal of Climate*, *25*(8), 3039–3051.

Jankovská, V., & Komárek, J. (2000). Indicative value of Pediastrum and other coccal green algae in palaeoecology. *Folia Geobotanica*, *35*(1), 59–82.

Jones, P. D., Parker, D. E., Osborn, T. J., & Briffa, K. R. (2016). Global and Hemispheric Temperature Anomalies-Land and Marine Instrumental Records.

Joynt III, E. H., & Wolfe, A. P. (2001). Paleoenvironmental inference models from sediment diatom assemblages in Baffin Island lakes (Nunavut, Canada) and reconstruction of summer water temperature. *Canadian Journal of Fisheries and Aquatic Sciences*, *58*(6), 1222–1243. https://doi.org/10.1139/f01-071

Jungclaus, J. H., Lohmann, K., & Zanchettin, D. (2014). Enhanced 20th century heat transfer to the Arctic simulated in context of climate variations over last millennium. *Climate of the Past*, *10*, 2201–2213.

Kaufman, D. S. (2009). An overview of late Holocene climate and environmental change inferred from Arctic lake sediment. *Journal of Paleolimnology*, *41*(1), 1–6.

Kaufman, D. S., Schneider, D. P., McKay, N. P., Ammann, C. M., Bradley, R. S., Briffa, K. R., … Vinther, B. M. (2009). Recent Warming Reverses Long-Term Arctic Cooling. *Science*, *325*(5945), 1236–1239.

Kelts, K., & Hsü, K. J. (1978). Freshwater carbonate sedimentation. In L. A. (Ed.), *Lakes* (pp. 295–323). New York, NY: Springer.

Kerr, J. W. (1974). Geology of Bathurst Island Group and Byam Martin Island, Arctic Canada (Operation Bathurst Island). Department of Energy, Mines and Resources.

Komárek, J., & Jankovská, V. (2003). Review of the Green Algal Genus Pediastrum: Implication for Pollen-analytical Research. *Blumea*, *48*(2), 288.

Lamoureux, S. F., & Bradley, R. S. (1996). A late Holocene varved sediment record of

environmental change from northern Ellesmere Island, Canada. *Journal of Paleolimnology*, *16*(2), 239–255.

Larsen, D. J., Miller, G. H., Geirsdóttir, Á., & Thordarson, T. (2011). A 3000-year varved record of glacier activity and climate change from the proglacial lake Hvítárvatn, Iceland. *Quaternary Science Reviews*, *30*(19–20), 2715–2731.

Law, A. C., Anderson, N. J., & McGowan, S. (2015). Spatial and temporal variability of lake ontogeny in south-western Greenland. *Quaternary Science Reviews*, *126*, 1–16. https://doi.org/10.1016/J.QUASCIREV.2015.08.005

Lecavalier, B. S., Fisher, D. A., Milne, G. A., Vinther, B. M., Tarasov, L., Huybrechts, P., … Bourgeois, J. (2017). High Arctic Holocene temperature record from the Agassiz ice cap and Greenland ice sheet evolution. *Proceedings of the National Academy of Sciences*, *114*(23), 5952–5957. https://doi.org/10.1073/pnas.1616287114

Lim, D. S. S., Douglas, M. S. V, & Smol, J. P. (2001). Diatoms and their relationship to environmental variables from lakes and ponds on Bathurst Island, Nunavut, Canadian High Arctic. *Hydrobiologia*, *450*(1), 215–230. https://doi.org/10.1023/A:1017553112643

Linderholm, H. W., Nicolle, M., Francus, P., Gajewski, K., Helama, S., Korhola, A., … D'Andrea, W. J. (2018). Arctic hydroclimate variability during the last 2000 years. *Climate of the Past*, *14*(4), 473–514. https://doi.org/10.5194/cp-14-473-2018

Linge, H., Lauritzen, S.-E., Andersson, C., Hansen, J. K., Skoglund, R. Ø., & Sundqvist, H. S. (2009). Stable isotope records for the last 10000 years from Okshola cave (Fauske, northern Norway) and regional comparisons. *Climate of the Past*, *5*(4), 667–682.

Ljungqvist, F. C. (2010). A new reconstruction of temperature variability in the extra-tropical northern hemisphere during the last two millennia. *Geografiska Annaler: Series A, Physical Geography*, *92*(3), 339–351. https://doi.org/10.1111/j.1468-0459.2010.00399.x

Loso, M. G., Anderson, R. S., Anderson, S. P., & Reimer, P. J. (2006). A 1500-year record of temperature and glacial response inferred from varved Iceberg Lake, southcentral Alaska. *Quaternary Research*, *66*(1), 12–24.

Luoto, T. P., & Helama, S. (2010). Palaeoclimatological and palaeolimnological records from fossil midges and tree-rings: the role of the North Atlantic Oscillation in eastern Finland through the Medieval Climate Anomaly and Little Ice Age. *Quaternary Science Reviews*, *29*(17–18), 2411–2423. https://doi.org/10.1016/J.QUASCIREV.2010.06.015

MacDonald, G. M., Beukens, R. P., & Kieser, W. E. (1991). Radiocarbon dating of limnic sediments: a comparative analysis and discussion. *Ecology*, *72*(3), 1150–1155.

Mann, M. E., Zhang, Z., Rutherford, S., Bradley, R. S., Hughes, M. K., Shindell, D., … Ni, F. (2009). Global Signatures and Dynamical Origins of the Little Ice Age and Medieval Climate Anomaly. *Science*, *326*(5957), 1256–1260.

Martin, A. C., Jeffers, E. S., Petrokofsky, G., Myers-Smith, I., & Macias-Fauria, M. (2017). Shrub growth and expansion in the Arctic tundra: an assessment of controlling factors using an evidence-based approach. *Environmental Research Letters*, *12*(8), 85007.

Massa, C., Perren, B. B., Gauthier, E., Bichet, V., Petit, C., & Richard, H. (2012). A multiproxy evaluation of Holocene environmental change from Lake Igaliku, South Greenland. *Journal of Paleolimnology*, *48*(1), 241–258.

McKay, N. P., & Kaufman, D. S. (2014). An extended Arctic proxy temperature database for the past 2,000 years. *Scientific Data*, *1*, 140026.

McKay, N. P., Kaufman, D. S., & Michelutti, N. (2008). Biogenic silica concentration as a high-resolution, quantitative temperature proxy at Hallet Lake, south-central Alaska. *Geophysical Research Letters*, *35*(5).

Michelutti, N., Wolfe, A. P., Briner, J. P., & Miller, G. H. (2007). Climatically controlled chemical and biological development in Arctic lakes. *Journal of Geophysical Research: Biogeosciences*, *112*(G3).

Mignot, J., Khodri, M., Frankignoul, C., & Servonnat, J. (2011). Volcanic impact on the Atlantic Ocean over the last millennium. *Climate of the Past Discussions*, *7*, 2511–2554.

Miller, G. H., Brigham-Grette, J., Alley, R. B., Anderson, L., Bauch, H. A., Douglas, M. S. V, … Fitzpatrick, J. J. (2010). Temperature and precipitation history of the Arctic. *Quaternary Science Reviews*, *29*(15–16), 1679–1715.

Miller, G. H., Geirsdóttir, Á., Zhong, Y., Larsen, D. J., Otto-Bliesner, B. L., Holland, M. M., … Thordarson, T. (2012). Abrupt onset of the Little Ice Age triggered by volcanism and sustained by sea-ice/ocean feedbacks. *Geophysical Research Letters*, *39*(2). https://doi.org/10.1029/2011GL050168

Moore, J. J., Hughen, K. A., Miller, G. H., & Overpeck, J. T. (2001). Little Ice Age recorded in summer temperature reconstruction from vared sediments of Donard Lake, Baffin Island, Canada. *Journal of Paleolimnology*, *25*(4), 503–517.

Myers-Smith, I. H., Forbes, B. C., Wilmking, M., Hallinger, M., Lantz, T., Blok, D., … Lévesque,

E. (2011). Shrub expansion in tundra ecosystems: dynamics, impacts and research priorities. *Environmental Research Letters*, *6*(4), 45509.

Nicolle, M., Debret, M., Massei, N., Christophe, C., Divine, D., Werner, J. P., … Linderholm, H. W. (2018). Climate variability in the subarctic area for the last 2 millennia. *Climate of the Past*, *14*(1), 101.

Ortega, P., Lehner, F., Swingedouw, D., Masson-Delmotte, V., Raible, C. C., Casado, M., & Yiou, P. (2015). A model-tested North Atlantic Oscillation reconstruction for the past millennium. *Nature*, *523*(7558), 71.

Osborn, T. J., & Briffa, K. R. (2006). The spatial extent of 20th-century warmth in the context of the past 1200 years. *Science*, *311*(5762), 841–844.

Overpeck, J., Hughen, K., Hardy, D., Bradley, R., Case, R., Douglas, M., … Jennings, A. (1997). Arctic environmental change of the last four centuries. *Science*, *278*(5341), 1251–1256.

Overpeck, J., Webb, T., & Prentice, I. C. (1985). Quantitative interpretation of fossil pollen spectra: dissimilarity coefficients and the method of modern analogs. *Quaternary Research*, *23*(1), 87–108.

PAGES2k. (2013). Continental-scale temperature variability during the past two millennia. *Nature Geoscience*, *6*(5), 339.

PAGES2k, Emile-Geay, J., McKay, N. P., Kaufman, D. S., von Gunten, L., Wang, J., … Zinke, J. (2017). A global multiproxy database for temperature reconstructions of the Common Era. *Scientific Data*, *4*, 170088. Retrieved from http://dx.doi.org/10.1038/sdata.2017.88

Parsons, T. R. (1984). *A manual of chemical & biological methods for seawater analysis*. Elsevier.

Paull, T. M., Finkelstein, S. A., & Gajewski, K. (2017). Interactions between climate and landscape drive Holocene ecological change in a High Arctic lake on Somerset Island, Nunavut, Canada. *Arctic Science*, *3*(1), 17–38.

Peros, M., & Gajewski, K. (2009). Pollen-based reconstructions of late Holocene climate from the central and western Canadian Arctic. *Journal of Paleolimnology*, *41*(1), 161–175. https://doi.org/10.1007/s10933-008-9256-9

Philippsen, B. (2013). The freshwater reservoir effect in radiocarbon dating. *Heritage Science*, *1*(1), 24. https://doi.org/10.1186/2050-7445-1-24

Podritske, B., & Gajewski, K. (2007). Diatom community response to multiple scales of Holocene climate variability in a small lake on Victoria Island, NWT, Canada. *Quaternary Science Reviews*, *26*(25–28), 3179–3196.

Porinchu, D. F., MacDonald, G. M., & Rolland, N. (2009). A 2000 year midge-based paleotemperature reconstruction from the Canadian Arctic archipelago. *Journal of Paleolimnology*, *41*(1), 177–188.

Post, E., Forchhammer, M. C., Bret-Harte, M. S., Callaghan, T. V, Christensen, T. R., Elberling, B., … Aastrup, P. (2009). Ecological Dynamics Across the Arctic Associated with Recent Climate Change. *Science*, *325*(5946), 1355–1358.

Reimer, P. J., Bard, E., Bayliss, A., Beck, J. W., Blackwell, P. G., Ramsey, C. B., … van der Plicht, J. (2013). IntCal13 and Marine13 Radiocarbon Age Calibration Curves 0–50,000 Years cal BP. *Radiocarbon*, *55*(4), 1869–1887. https://doi.org/DOI: 10.2458/azu_js_rc.55.16947

Ritchie, J. C. (1987). *Post-glacial vegetation of Canada*. New York, NY: Cambridge University

Press.

Rolland, N., Larocque, I., Francus, P., Pienitz, R., & Laperrière, L. (2009). Evidence for a warmer period during the 12th and 13th centuries AD from chironomid assemblages in Southampton Island, Nunavut, Canada. *Quaternary Research*, *72*(01), 27–37. https://doi.org/10.1016/j.yqres.2009.03.001

Rouillard, A., Michelutti, N., Rosén, P., Douglas, M. S. V., & Smol, J. P. (2012). Using paleolimnology to track Holocene climate fluctuations and aquatic ontogeny in poorly buffered High Arctic lakes. *Palaeogeography, Palaeoclimatology, Palaeoecology*, *321–322*, 1–15. https://doi.org/10.1016/J.PALAEO.2012.01.011

Ryves, D. B., Battarbee, R. W., Juggins, S., Fritz, S. C., & Anderson, N. J. (2006). Physical and chemical predictors of diatom dissolution in freshwater and saline lake sediments in North America and West Greenland. *Limnology and Oceanography*, *51*(3), 1355–1368.

Sawada, M. (2006). An open source implementation of the Modern Analog Technique (MAT) within the R computing environment. *Computers & Geosciences*, *32*(6), 818–833. https://doi.org/10.1016/J.CAGEO.2005.10.008

Schleussner, C.-F., & Feulner, G. (2013). A volcanically triggered regime shift in the subpolar North Atlantic Ocean as a possible origin of the Little Ice Age. *Climate of the Past*, *9*(3), 1321–1330.

Schurer, A. P., Hegerl, G. C., Mann, M. E., Tett, S. F. B., & Phipps, S. J. (2013). Separating forced from chaotic climate variability over the past millennium. *Journal of Climate*, *26*(18), 6954–6973.

Schurer, A. P., Tett, S. F. B., & Hegerl, G. C. (2014). Small influence of solar variability on climate over the past millennium. *Nature Geoscience*, *7*(2), 104–108.

Schwager, M. (2000). Ice core analysis on the spatial and temporal variability of temperature and precipitation during the late Holocene in North Greenland. *Rep. Polar Res*, *362*, 1–136.

Sejrup, H. P., Haflidason, H., & Andrews, J. T. (2011). A Holocene North Atlantic SST record and regional climate variability. *Quaternary Science Reviews*, *30*(21–22), 3181–3195. https://doi.org/10.1016/J.QUASCIREV.2011.07.025

Servonnat, J., Yiou, P., Khodri, M., Swingedouw, D., & Denvil, S. (2010). Influence of solar variability, CO 2 and orbital forcing between 1000 and 1850 AD in the IPSLCM4 model. *Climate of the Past*, *6*(4), 445–460.

Shi, F., Yang, B., Ljungqvist, F. C., & Yang, F. (2012). Multi-proxy reconstruction of Arctic summer temperatures over the past 1400 years. *Climate Research*, *54*(2), 113–128.

Shindell, D. T., Schmidt, G. A., Mann, M. E., Rind, D., & Waple, A. (2001). Solar forcing of regional climate change during the Maunder Minimum. *Science*, *294*(5549), 2149–2152.

Sicre, M., Hall, I. R., Mignot, J., Khodri, M., Ezat, U., Truong, M., … Knudsen, K. (2011). Sea surface temperature variability in the subpolar Atlantic over the last two millennia. *Paleoceanography*, *26*(4).

Sigl, M., Winstrup, M., McConnell, J. R., Welten, K. C., Plunkett, G., Ludlow, F., … Woodruff, T. E. (2015). Timing and climate forcing of volcanic eruptions for the past 2,500 years. *Nature*, *523*, 543–549.

Smol, J. P., Wolfe, A. P., Birks, H. J. B., Douglas, M. S. V, Jones, V. J., Korhola, A., …

Antoniades, D. (2005). Climate-driven regime shifts in the biological communities of arctic lakes. *Proceedings of the National Academy of Sciences*, *102*(12), 4397–4402.

Snyder, J. A., Miller, G. H., Werner, A., Jull, A. J. T., & Stafford, T. W. (1994). AMS-radiocarbon dating of organic-poor lake sediment, an example from Linnévatnet, Spitsbergen, Svalbard. *The Holocene*, *4*(4), 413–421. https://doi.org/10.1177/095968369400400409

Spielhagen, R. F., Werner, K., Sørensen, S. A., Zamelczyk, K., Kandiano, E., Budeus, G., … Hald, M. (2011). Enhanced Modern Heat Transfer to the Arctic by Warm Atlantic Water. *Science*, *331*(6016), 450–453.

Stenchikov, G., Delworth, T. L., Ramaswamy, V., Stouffer, R. J., Wittenberg, A., & Zeng, F. (2009). Volcanic signals in oceans. *Journal of Geophysical Research: Atmospheres*, *114*, D16104.

Tape, K., Sturm, M., & Racine, C. (2006). The evidence for shrub expansion in Northern Alaska and the Pan-Arctic. *Global Change Biology*, *12*(4), 686–702. https://doi.org/10.1111/j.1365-2486.2006.01128.x

Thomas, E. K., & Briner, J. P. (2009). Climate of the past millennium inferred from varved proglacial lake sediments on northeast Baffin Island, Arctic Canada. *Journal of Paleolimnology*, *41*(1), 209–224.

Thompson, R., Battarbee, R. W., O'sullivan, P. E., & Oldfield, F. (1975). Magnetic susceptibility of lake sediments. *Limnology and Oceanography*, *20*(5), 687–698.

Tingley, M. P., & Huybers, P. (2013). Recent temperature extremes at high northern latitudes unprecedented in the past 600 years. *Nature*, *496*, 201.

Trouet, V., Esper, J., Graham, N. E., Baker, A., Scourse, J. D., & Frank, D. C. (2009). Persistent positive North Atlantic Oscillation mode dominated the medieval climate anomaly. *Science*, *324*(5923), 78–80.

Viau, A. E., & Gajewski, K. (2009). Reconstructing millennial-scale, regional paleoclimates of boreal Canada during the Holocene. *Journal of Climate*, *22*(2), 316–330.

Viau, A. E., Ladd, M., & Gajewski, K. (2012). The climate of North America during the past 2000 years reconstructed from pollen data. *Global and Planetary Change*, *84*, 75–83.

Vieira, L. E. A., Solanki, S. K., Krivova, N. A., & Usoskin, I. (2011). Evolution of the solar irradiance during the Holocene. *Astronomy & Astrophysics*, *531*, A6.

Vincent, J.-S. (1989). Quaternary Geology of the Northern Canadian Interior Plains. In R. J. Fulton (Ed.), *Quaternary geology of Canada and Greenland. Geological Survey of Canada* (pp. 100–137).

Vinther, B. M., Clausen, H. B., Fisher, D. A., Koerner, R. M., Johnsen, S. J., Andersen, K. K., … Svensson, A. M. (2008). Synchronizing ice cores from the Renland and Agassiz ice caps to the Greenland Ice Core Chronology. *Journal of Geophysical Research: Atmospheres*, *113*(D8).

Vinther, B. M., Clausen, H. B., Johnsen, S. J., Rasmussen, S. O., Andersen, K. K., Buchardt, S. L., … Steffensen, J. P. (2006). A synchronized dating of three Greenland ice cores throughout the Holocene. *Journal of Geophysical Research: Atmospheres*, *111*(D13).

Vinther, B. M., Jones, P. D., Briffa, K. R., Clausen, H. B., Andersen, K. K., Dahl-Jensen, D., & Johnsen, S. J. (2010). Climatic signals in multiple highly resolved stable isotope records from

Greenland. *Quaternary Science Reviews*, *29*(3–4), 522–538.

Walker, D. A., Gould, W. A., Maier, H. A., & Raynolds, M. K. (2002). The Circumpolar Arctic Vegetation Map: AVHRR-derived base maps, environmental controls, and integrated mapping procedures. *International Journal of Remote Sensing*, *23*(21), 4551–4570.

Wanner, H., Beer, J., Bütikofer, J., Crowley, T. J., Cubasch, U., Flückiger, J., … Kaplan, J. O. (2008). Mid-to Late Holocene climate change: an overview. *Quaternary Science Reviews*, *27*(19–20), 1791–1828.

Werner, J. P., Divine, D. V, Ljungqvist, F. C., Nilsen, T., & Francus, P. (2018). Spatio-temporal variability of Arctic summer temperatures over the past 2 millennia. *Climate of the Past*, *14*(4), 527.

Wheeler, J. C., Hoffman, P. F., Card, K. D., Davidson, A., Sandford, B. V., Okulitch, A. ., & Roest, W. R. (1997). Geological map of Canada. Ottawa, Ont.: Geological Survey of Canada.

Whitmore, J., Gajewski, K., Sawada, M., Williams, J. W., Shuman, B., Bartlein, P. J., … Brubaker, L. (2005). Modern pollen data from North America and Greenland for multi-scale paleoenvironmental applications. *Quaternary Science Reviews*, *24*(16–17), 1828–1848. https://doi.org/10.1016/J.QUASCIREV.2005.03.005

Wiles, G. C., D'Arrigo, R. D., Barclay, D., Wilson, R. S., Jarvis, S. K., Vargo, L., & Frank, D. (2014). Surface air temperature variability reconstructed with tree rings for the Gulf of Alaska over the past 1200 years. *The Holocene*, *24*(2), 198–208.

Williams, J. W., & Shuman, B. (2008). Obtaining accurate and precise environmental reconstructions from the modern analog technique and North American surface pollen

dataset. *Quaternary Science Reviews*, *27*(7–8), 669–687.

Wolfe, A. P. (2002). Climate modulates the acidity of Arctic lakes on millennial time scales. *Geology*, *30*(3), 215–218.

Xing, P., Chen, X., Luo, Y., Nie, S., Zhao, Z., Huang, J., & Wang, S. (2016). The Extratropical Northern Hemisphere Temperature Reconstruction during the Last Millennium Based on a Novel Method. *PLOS ONE*, *11*(1), e0146776.

Zabenskie, S., & Gajewski, K. (2007). Post-glacial climatic change on boothia peninsula, Nunavut, Canada. *Quaternary Research*, *68*(2), 261–270.

Zabenskie, S., Peros, M., & Gajewski, K. (2006). The use of heavy-liquid in the separation of pollen from Arctic lake sediments. *Can. Assoc. Palynologists*, *29*, 5–7.

Zhong, Y., Miller, G. H., Otto-Bliesner, B. L., Holland, M. M., Bailey, D. A., Schneider, D. P., & Geirsdottir, A. (2011). Centennial-scale climate change from decadally-paced explosive volcanism: a coupled sea ice-ocean mechanism. *Climate Dynamics*, *37*(11–12), 2373–2387.

Zhou, A., He, Y., Wu, D., Zhang, X., Zhang, C., Liu, Z., & Yu, J. (2015). Changes in the Radiocarbon Reservoir Age in Lake Xingyun, Southwestern China during the Holocene. *PLOS ONE*, *10*(3), e0121532.